TECHNISCHE UNIVERSITÄT MÜNCHEN

Lehrstuhl für Physiologie

Regulation of Glucagon Secretion

Veronika Leiss

Vollständiger Abdruck der von der Fakultät Wissenschaftszentrum Weihenstephan für Ernährung, Landnutzung und Umwelt der Technischen Universität München zur Erlangung des akademischen Grades eines

Doktors der Naturwissenschaften

genehmigten Dissertation.

Vorsitzender: Univ.-Prof. Dr. R. Schopf

Prüfer der Dissertation: 1. Univ.-Prof. Dr. H. H. D. Meyer

2. Univ.-Prof. Dr. F. Hofmann

Die Dissertation wurde am 05.08.2008 bei der Technischen Universität München eingereicht und durch die Fakultät Wissenschaftszentrum Weihenstephan für Ernährung, Landnutzung und Umwelt am 14.10.2008 angenommen.

I.   Chapter

II. Abstract

The islets of Langerhans in the endocrine pancreas act as glucose sensors, adjusting hormone output to the prevailing blood glucose level. The mainly released hormones are the functional antagonists insulin and glucagon. Insulin-secreting B-cells are active at hyperglycaemia, whereas glucagon is secreted from A-cells during hypoglycaemia. Glucagon induces hepatic glucose output by stimulating glycogenolysis and gluconeogenesis. The molecular mechanisms whereby glucose modulates the A-cell stimulus secretion coupling remain to be elucidated. It is generally accepted that activation of calcium channels, an influx of calcium ions and thus an increase of the intracellular calcium concentration result in the hormone release. However, not only calcium channels but also sodium channels are supposed to be involved in the excitatory machinery, because A-cells express tetrodotoxin (TTX) sensitive sodium channels. In this study the sodium channel isoform $Na_V1.7$ was detected in A-cells of Langerhans islets. By using the Cre-loxP site-specific recombination system, A-cell specific $Na_V1.7$ knockout ($Na_V1.7^{Acko}$) mice were generated. It was tested whether this conditional deletion of $Na_V1.7$ would effect glucagon secretion *in vitro* and *in vivo*. Indeed, glucagon release was disturbed at high glucose conditions in analyzed $Na_V1.7^{Acko}$ mice.

An additional approach within this study was addressed on the regulation of glucagon release by the A-cell expressed Iα isoform of the cGMP dependent protein kinase type I (cGKI). The analysis of established and recently generated cGKI deficient mice, which lack islet cGKI revealed disturbed glucagon-releasing properties. Similar to $Na_V1.7^{Acko}$ mice, deletion of A-cell cGKIα increased rather than decreased glucagon secretion at high glucose conditions. Additionally, A-cell triggered hormone release was also deregulated in an opposite unphysiological direction at basal glucose conditions compared to controls. Furthermore, an improved glucose challenge increased fasting blood glucose and serum glucagon levels emphasize the functional importance of cGKI *in vivo*.

Together, the results of the present study indicate that both $Na_V1.7$ and cGKI act as negative regulators of glucagon release mainly at high glucose conditions.

III. Abbreviations

[c]	concentration	FCS	fetal calf serum
$[Ca^{2+}]_i$	intracellular calcium concentration	Fig.	figure
ADP	adenosine-5'-diphosphate	FITC	fluoreszeinisothiocyanate
AMP	adenosine-5'-monophosphate	floxed	loxP flanked
ANP	atrial natriuretic peptide	g	grams or relative centrifugal force
AP	alkaline phosphatase	GABA	gamma aminobutyric acid
ATP	adenosine-5'-triphosphate	GLUT	glucose transporter
β-actin	beta smooth muscle actin	GMP	guanosine-5'-monophosphate
β-gal	β-galactosidase	h	hour
BNP	brain natriuretic peptide	HBSS	Hanks balanced salt solution
bp	base pairs	HCl	hydrochloride acid
C	Celsius	HCl_{conc}	concentrated hydrochloride acid
Ca^{2+}	calcium ion	HEPES	4-(2-hydroxyethyl)-1-piperazineethanesulfonicacis
cAMP	cyclic adenosine-3', 5'-monophosphate	HPRT	hypoxanthine-guanine-phosphoriboxyl-transferase
cDNA	copy DNA	HRP	horseradish peroxidase
cGK	cGMP-dependent protein kinase		
cGKI	cGMP-dependent protein kinase type I	I	current
cGKII	cGMP-dependent protein kinase type II	i.p.	intra peritoneal
cGKIα	cGMP-dependent protein kinase type Iα isoform	I_{max}	maximum current
cGKIβ	cGMP dependent protein kinase G type Iβ isoform	iNOS	inducible NOS
cGMP	cyclic guanosine-3', 5'-monophosphate	IP_3	inositol-1,4,5-triphosphate
Cl^-	chloride ion	IP_3K	inositol-1,4,5-triphosphate kinase
CNG	cyclic nucleotide-gated ion channel	IRAG	inositol 1,4,5 tri-phosphate receptor associated cGMP-kinase substrate
CNP	C-type natriuretic peptide cyclization	IRS	insulin receptor signaling
Cre	recombination		
CsOH	caesium hydroxide	ITT	insulin tolerance test
ctr	control	Iα	cGKIα
CY3	carbocyanine 3	Iβ	cGKIβ
DAB	diaminobenzidine	K^+	potassium ion
ddH_2O	double distilled water	K_{ATP} channel	ATP sensitive potassium channel
dl	deciliter	KBHS	Krebs buffered HEPES solution
DMSO	dimethylsulfoxide	kDa	kilo Dalton
DNA	deoxyribonucleic acid	ko	knockout
dNTP	deoxynucleotide triphosphate	l	liter
DRG	dorsal root ganglia	loxP	locus of X-over of P1
e.g.	for example	M	moles per liter
EDTA	ethylenediaminetetraacid	MetOH	methanol
eNOS/NOS3	endothelial NO synthase	mg	milligram
ES	embryonic stemcells	$MgCl_2$	magnesium chloride
EtOH	ethanol	min	minute

ml	milliliters	pM	picomoles per liter
mM	millimoles per liter	*prkg*	cGK gene locus
mV	millivolt	PVDF	polyvinyliden dufluoride
MW	molecular weight	RNA	ribonucleic acid
Na$^+$	sodium ion	RT	room temperature
NaOH	sodium hydroxide	RT	reverse transcriptase
Na$_V$	voltage dependent sodium channel	s	second
Na$_V$1.7^{Acko}	conditional knockout of Na$_V$1.7 in A-cells	SDS	sodium dodecyl sulfate
NGS	normal goat serum	sGC	soluble guanylyl cyclase
nNOS/NOS2	neuronal NO synthase	SM22alpha	smooth muscle specific protein 22 kDa
NO	nitric oxide	TBE	Tris-borate-EDTA-buffer
NOS	nitric oxide synthase	TBS	Tris-buffered saline
NP	natriuretic peptide	TBS-T	Tris-Tween-buffered saline
NRP	natriuretic receptor peptide	TEMED	N,N,N',N'-tetramethylethyylenediamine
oGTT	oral glucose tolerance test	tg	transgene
PBS	phosphate buffered saline	TRIS	2-amino-2-hydroxymethyl-1,3-propanediol
PCR	polymerase chain reaction	TTX	tetrodotoxin
PDE	phosphodiesterase	U	units
PEPD	paroxysmal extreme pain disorder	µm	micrometer
PFA	paraformaldehyde	µM	micromoles per liter
pGC	particulate guanylyl cyclase	V	voltage
PK	proteinase K	X-Gal	5-Bromo-4-chloro-3-indolyl b-D-galactosidase

IV. Index

V. Figure Legends

Figure Legends

1 Introduction

1.1 *Physiology of the islets of Langerhans*

The endocrine cells of the pancreas are organized in the islets of Langerhans. In general, they constitute approximately 1 to 2% of the mass of the entire pancreas and are distributed all over the organ. Although the islets present only a small part of the pancreas, they are groups of highly specialized cells that are of critical importance for the metabolism of nutrients and energy homeostasis of the whole body. There are about one million islets in a healthy human pancreas. An individual islet consists of five distinct types of electrically excitable cells, namely A-cells, B-cells, D-cells, E-cells, and F-cells (Broglio et al., 2003; Elayat et al., 1995). The last two cell types are found in negligible amounts (1-5%) that secrete grehlin and pancreatic polypeptide respectively (Herrera, 2002; Wierup et al., 2002). D-cells produce somatostatin, an inhibitory hormone that suppresses the release of insulin and glucagon (Schuit et al., 1989). B-cells, 80% of Langerhans islets, act as glucose sensors by adjusting insulin output to the prevailing blood glucose levels. Insulin is critically important for the promotion of glucose storage and the prevention of glycogen breakdown (MacDonald et al., 2005). The counterregulatory hormone of insulin is glucagon, secreted from A-cells, which constitute about 15 to 20% of islet cells. To increase blood glucose, glucagon promotes hepatic glucose output by stimulating glycogenolysis and gluconeogenesis and by decreasing glycogenesis and glycolysis in a concerted fashion via multiple mechanisms (Gromada et al., 2007).

1.2 *Diabetes mellitus*

As mentioned above, under physiological conditions the glucose homeostasis is mainly regulated by the peptide hormones insulin and glucagon. This high-sensitive regulatory mechanism is able to keep the blood glucose level in a physiological balance. The imbalance of pancreatic hormone secretion can lead to diabetes mellitus. Diabetes is described as a metabolic disorder leading to a chronically hyperglycemia that is characterized by an increased blood glucose level. In general, two different types of diabetes mellitus are distinguished: (1), type-1 diabetes, which is an autoimmune disease that results in the dysfunction and finally deletion of insulin secreting B-cells. Therefore, quality of life and long-term survival of patients with type-1 diabetes mellitus can only be assured by continuous insulin therapy. (2), type-2 diabetes is characterized by insulin resistance of target organs and/or impaired insulin secretion. In industrial countries especially type-2 diabetes became a widespread disease caused by increasing rates of obesity and changes in lifestyle, such as an imbalanced nutrition and the less active course of life. In the diabetic state, insulin levels are inadequately low, which often is accompanied by increased glucagon levels that further exacerbate the hyperglycemia (Unger, 1971).

1.3   Mechanism of glucagon secretion

The 29 amino acid polypeptide glucagon is released during hypoglycemia and stimulates hepatic glucose synthesis and output by binding directly to glucagon receptors in the membrane of liver cells. The exact mechanisms coupling low blood glucose levels to glucagon secretion are still unknown, however, it is proposed that low blood glucose directly acts on A-cells to increase intracellular calcium concentrations $[Ca^{2+}]_i$, and stimulates fusion of glucagon-containing granules with the membrane leading to hormone release (MacDonald et al., 2007). This increase of $[Ca^{2+}]_i$ is induced by electrical excitation and an influx of Ca^{2+} ions through voltage gated calcium channels (Barg et al., 2000; Leung et al., 2006). In addition to voltage-gated Ca^{2+} channels, tetrodotoxin (TTX) sensitive voltage-gated sodium channels are also supposed to play a major role for glucagon secretion (Barg et al., 2000; Gopel et al., 2000b; Gromada et al., 2007) (Fig. 1).
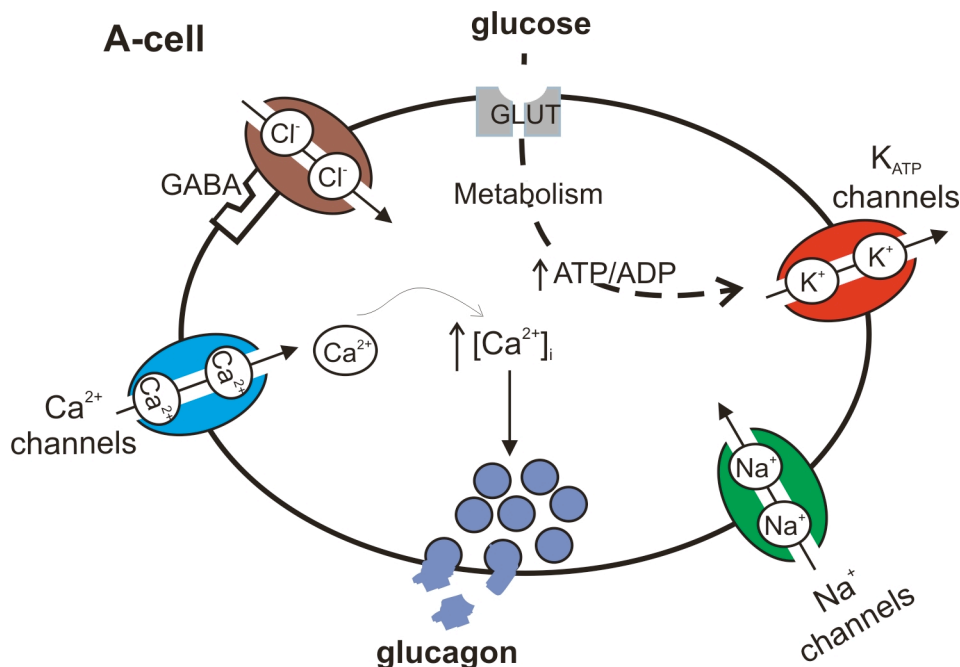
Fig. 1: Mechanism of glucagon secretion. Glucose uptake and metabolism lead to changes in the ATP/ADP ratio (dotted lines) and the closure of ATP-sensitive K^+-channels (K_{ATP}-channel) (red). Activation of voltage gated Ca^{2+}-channels (blue), and influx of Ca^{2+} results in an increase of $[Ca^{2+}]_i$ and glucagon secretion. Sodium channels (Na^+-channels; green colored pores) are assumed to play an important role for action potential generation. Furthermore, A-cells express also gamma-aminobutyric acid ($GABA_A$) receptors for neuronal input (e.g. gamma-aminobutyric acid (GABA)) on their plasma membrane. Activation of GABA receptors leads to an inward Cl^- current that induces inhibition of cellular activity by hyperpolarization; Ca^{2+} - calcium; Na^+ - sodium; Cl^- - chloride; $[Ca^{2+}]_i$ – intracellular calcium concentration (adapted from Gromada et al., 2007).

As indicated, glucagon release is a complex process that involves activation/deactivation of many signalling components. In addition, A-cell activity is under control of neuronal inputs and hormonal influences (Ahren, 2000). For example, adrenaline stimulates glucagon secretion via binding to α_1- and β-adrenoceptors (Vieira et al., 2004). Besides adrenaline, insulin and somatostatin secreted from neighbouring B- and D-cells act as well on pancreatic A-cells. Both hormones have inhibitory

effects on glucagon release, thus paracrine signalling is also an important regulatory mechanism for glucagon secretion by binding directly to receptors on the membrane of A-cells (Gromada et al., 2007). Furthermore, insulin-secreting vesicles contain γ-aminobutyric acid (GABA) which acts as another inhibitor of glucagon release via binding to the respective A-cell receptors (Rorsman et al., 1989). This induces an inward chloride (Cl^-) current that causes cell inhibition by hyperpolarization (Cherubini et al., 1991), and thus, prevents depolarization and glucagon secretion.

1.4 Voltage-gated sodium channels

Electrical signals control the contraction of muscles, the secretion of hormones, processing of information in the brain, and output from the brain to peripheral tissues (Catterall et al., 2007). In excitable cells, electrical signals influence the intracellular metabolism and signaling transduction, gene expression, and protein synthesis and degradation (Catterall, 2000). The electrical signal transduction is maintained by members of the ion channel superfamily, a set of more than 140 structurally related pore-forming proteins (Yu and Catterall, 2004). The first member characterized were the voltage-gated sodium channels, which mainly generate electrical signals required for action potential generation and conduction in excitable cells such as nerves, muscles and endocrine cells. These channels are responsible for an influx of positively charged sodium ions and trigger the raising phase of the action potentials. In mammalian tissues, the functional unit of sodium channels is formed by one principal α-subunit and one or two auxiliary β-subunits (Catterall, 2000). The α-subunit contains the voltage-sensing and pore-forming elements. Furthermore, it is composed of four homologous domains (I-IV), each containing six hydrophobic transmembrane α-helices (S1-S6) (Fig. 2). The pore loops are located between every fifth and sixth transmembrane segment. In addition, the voltage sensor located in the S4 segment is responsible for the voltage-dependent sensitivity. It contains positively charged amino acid residues at every third position followed by two hydrophobic residues. The pore opens in response to voltage by a conformational change. Moreover, the short intracellular loop connecting transmembrane segment III and IV serves as the inactivation gate by folding into the channel structure and blocking the pore from the inside during sustained depolarization of the membrane (Catterall et al., 2007; Catterall et al., 2005). At present, nine voltage-gated sodium channel α-subunits have been functionally identified. Nine different genes encode these isoforms ($Na_V1.1$ to $Na_V1.9$). Six of them ($Na_V1.1$ to $Na_V1.4$, $Na_V1.6$, and $Na_V1.7$) are TTX sensitive. In general, the nomenclature of each individual sodium channel includes the chemical symbol of the main permeating ion (Na) and the principal physiological regulator (V for voltage) indicated as a subscript (Na_V). The number following the subscript displays the gene subfamily (Na_V1), the subsequent number reflects the specific channel isoform (e.g., $Na_V1.7$).
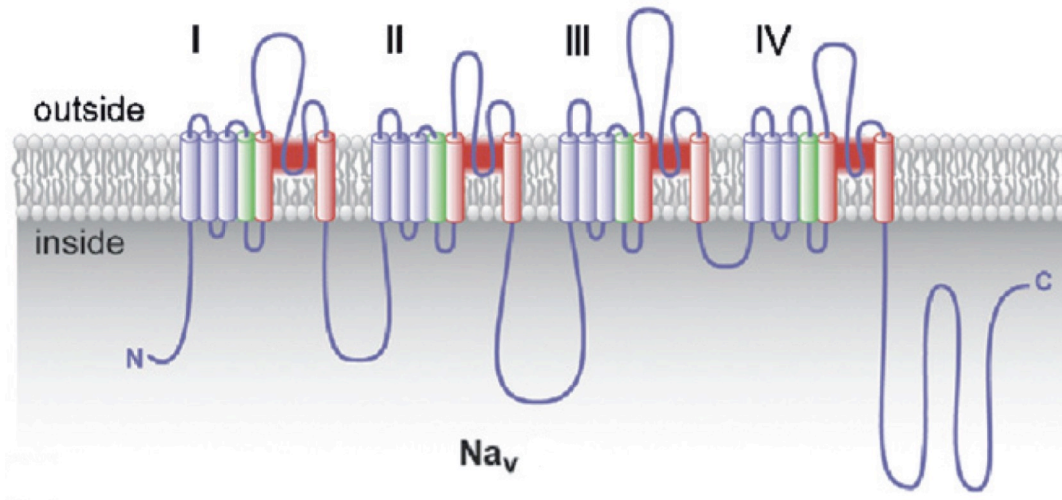
Fig. 2: Structure of voltage-gated sodium channels. The ion channel is illustrated as a transmembrane folding diagram in which cylinders represent the transmembrane α-helices. The green colored cylinders show the voltage sensors in the S4 segment. Blue colored are the transmembrane segments S1 to S3. Red represents the pore forming segments S5 and S6. Na_V – voltage-gated sodium channel (adapted from Catterall et al., 2007**)**

The Na_V1.7 isoform is mainly expressed in spinal sensory neurons (i.e. dorsal root ganglia (DRG)), and in high levels in nociceptive DRG neurons (Djouhri et al., 2003; Felts et al., 1997; Sangameswaran et al., 1997). In humans, mutations of Na_V1.7 were identified in two distinct clinical syndromes associated with severe pain: The inherited erythromelalgia and the paroxysmal extreme pain disorder (PEPD) (Waxman, 2007). In patients suffering from erythmelalgia single amino acid mutations in Na_V1.7 cause the syndrome. These mutations lead to a shift of the channel activation resulting in earlier activation of the channel, causing a decrease of the channel deactivation rate. Thus, the open status of the channel is prolonged, and, therefore, the response to small depolarizing stimuli is enhanced, which normally does not lead to channel activation (Cummins et al., 2004; Waxman, 2006; Yang et al., 2004). In PEPD patients the mutation of the sodium channel isoform causes an impairment of channel inactivation leading to a prominent persisting current. This promotes prolongation of action potentials and results in permanent firing in response to stimuli like cold and stretching (Fertleman et al., 2006; Fertleman et al., 2007). In contrast to the two mutations metioned above, a third mutation in the amino acid sequence of Na_V1.7 is involved in channelopathy-associated insensitivity to pain. Here, a truncation of the sodium channel leads to degradation of Na_V1.7 proteins. Affected patients are insensitive to any type of pain (Cox et al., 2006).

1.5 Sodium channels in pancreatic islets

Sodium channels are detectable in pancreatic A-, B-, and D-cells, respectively (Leung et al., 2005). Experiments on isolated islets showed that the sodium channels differ in their electrophysiological properties. The half-maximal inactivation values measured by steady-state inactivation for A, B-, and D-cells are -47 mV, -100 mV, and -28 mV, respectively (Gopel et al., 1999; Kanno et al., 2002; Leung et al., 2005). For that reason, the individual properties of pancreatic sodium channels are often used to distinguish the different islet cell types.

In glucagon-secreting A-cells, sodium channels play an important role for action potential generation (Gopel et al., 1999). Those expressed in murine glucagon-secreting A-cells are activated at potentials around -30 mV (Barg et al., 2000; Gopel et al., 2000b; Vignali et al., 2006). The islet sodium channels are TTX sensitive. TTX inhibits glucagon release in isolated mouse islets to an extent similar to that observed in the presence of a maximally inhibitory concentration of glucose (Gopel et al., 2000b; Gromada et al., 2004). Previous experiments revealed that the molecular basis for the TTX-sensitive sodium channels expressed in pancreatic islets are $Na_V1.3$ and $Na_V1.7$ (Vignali et al., 2006), but their precise role for glucagon secretion remained unknown (Gopel et al., 2000b; Gromada et al., 2007).

1.6 Conventional and conditional mutagenesis of genes in mice

Specific gene deletion in mice can be achieved at least by two different gene knockout strategies. (1.) The gene of interest can be deactivated by a genetic manipulation that becomes manifested in the germ line, and, therefore, leads to a functional deletion of the gene in every cell (conventional knockout). (2.) The gene of interest can be manipulated in a tissue specific manner (conditional knockout), which often is accomplished by the use of a genetic tool, the Cyclization Recombination locus of X-over of P1 (Cre-loxP) system (Nagy, 2000).

In conventional knockouts a functionally important part of a gene is deleted by homologous recombination in embryonic stem (ES) cells. The manipulated ES cells are inserted in the germ line. In the progeny the mutation can become manifested in all tissues that lack the gene. In case of deleting functional important genes, their deletion can lead to reduced life expectancy of affected animals or to their death during embryogenesis. To analyze the specific function of cGKI *in vivo* a conventional knockout mouse line was generated (Pfeifer et al., 1998). In these mice a homologous domain of the cGKIα and Iβ isoform coding for the kinase and ATP-binding domain was deleted. Due to the importance of endogenous cGKI activity for many physiological processes, the cGKI mutants lacking the kinase show a reduced life expectancy caused by their multiple and severe phenotypes. 50% of the mice die during the first 5 to 6 weeks after birth. For example, the chronic inactivation of cGKI leads to hypertrophy of the gastric fundus and pylorus, severe disturbances of the gastrointestinal motility, and relaxation of visceral smooth muscle cells (Pfeifer

et al., 1998). In addition, platelet and immune functions are disturbed and the animals develop a severe anemia (Foller et al., 2008; Massberg et al., 1999; Ny et al., 2000; Persson et al., 2000; Pfeifer et al., 1998; Werner et al., 2005).

In the case of the $Na_V1.7$ isoform, those conventional knockout mice die shortly after birth, apparently because of a failure to feed (Nassar et al., 2004). Thus, deleting $Na_V1.7$ in all sensory and sympathetic neurons causes a lethal prenatal phenotype.

Because of the often severe and complex phenotypes, it is difficult to investigate the proper role of a gene in specific physiological processes. An additional factor complicating the analysis is caused by the fact that the deletion of a gene in the whole organism can result in defects of very different organs, which can mask and/or affect other processes making it difficult to distinguish between primary and secondary effects. To avoid these disadvantages the conditional gene deletion approach by the use of Cre-loxP system can be applied.

5' ATAACTTCGTATAATGTATGCTATACGAAGTTAT 3'
3' TATTGAAGCATATTACATACGATATGCTTCAATA 5'
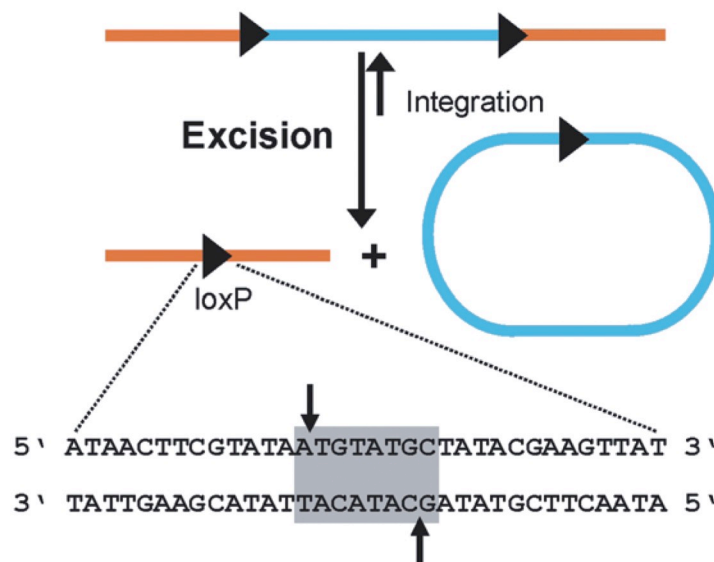
Fig. 3: Cre-loxP mediated excision and ligation of DNA. The loxP recognition site consists of a 34 bp sequence. The grey colored sequence marks the spacer sequence containing the phosphodiester bounds cleaved by the Cre-enzyme (indicated by the black arrows), flanked by two palindromic sequences. The orientation of the two loxP sites in the same direction leads to an excision of the flanked DNA segment (Lukowski et al., 2005).

The Cre-recombinase (cyclization recombination) is a site-specific DNA recombinase derived from the P1 bacteriophage with a molecular weight of 38 kDa. The enzyme catalyzes the recombination of DNA between specific sites in a DNA molecule. Those specific sites recognized by the Cre-recombinase are the loxP (locus of X-over of P1) consensus sequences. The double stranded DNA is cut at both loxP sites by Cre and then recombined to produce one remaining consensus sequence. For two loxP sites on one chromosome orientated in the same direction a deletion of the intermediate DNA sequence is caused (Fig. 3) (Nagy, 2000).

During the 80th to 90th it became obvious that the Cre-loxP system works in eukaryotic cells (Sauer and Henderson, 1988) and is an ideal tool to delete specific genes of interest in transgenic mice (Lakso et al., 1992; Orban et al., 1992). Particularly in mouse genetics the Cre-mediated excision of DNA segments was used to generate tissue or cell-specific inactivations of selected genes. By homologous recombination the loxP sequences were inserted in the embryonic stem cells into intronic gene sequences flanking an essential exon. This "floxed" version of the gene should not be influenced by the insertion of the loxP sites since the introns are excised during gene expression.

To generate mice with the conditional gene deletion the "floxed" target mouse is crossed to a Cre transgenic mouse strain expressing the enzyme under the control of a tissue-specific promotor (Fig. 4).
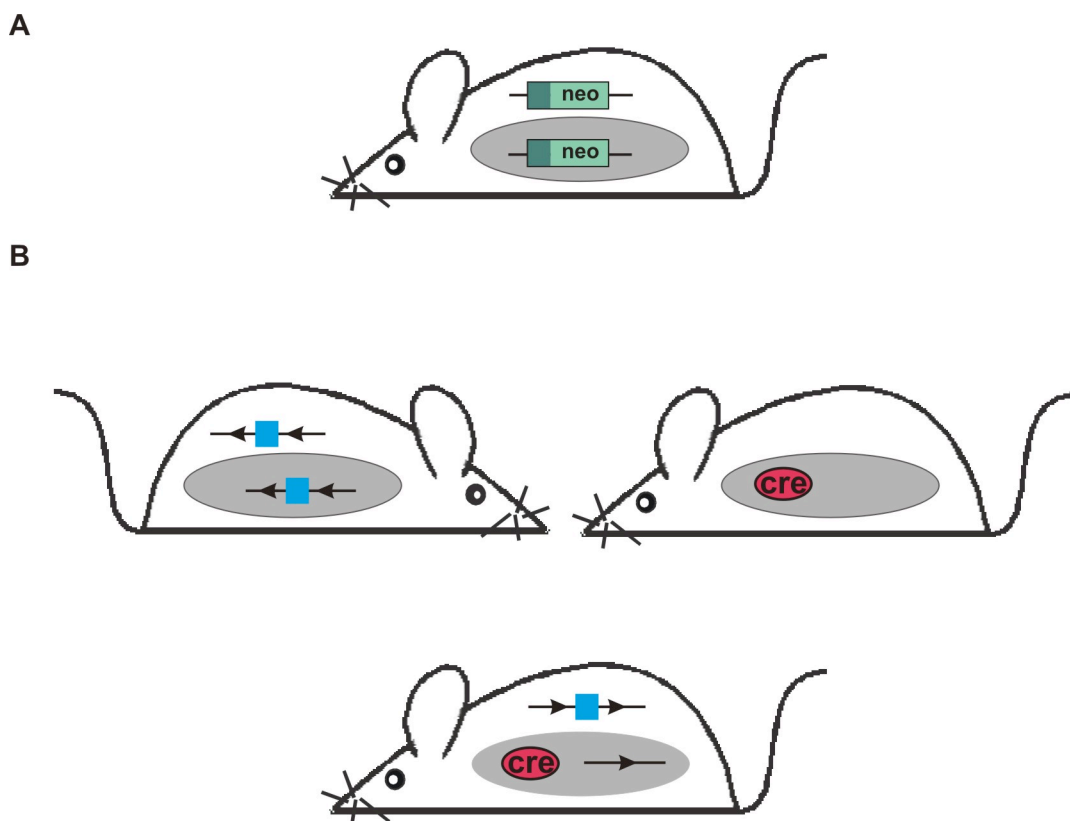
Fig. 4: Conventional and conditional deletion of genes in mice. (A) Permanent (conventional) deletion of a gene in mice. In all tissues and organs an essential exon (green rectangle) of the gene is deleted using a neomycin (neo) resistance cassette. The deletion is already manifested in the germ line. (B) Tissue specific (conditional) deletion of a gene. A target mouse with a floxed gene is crossed with a mouse expressing Cre-recombinase under control of a tissue-specific promotor (e.g. the glucagon promotor controlling Cre expression specifically in A-cells).

In the offspring, a Cre-mediated knockout is manifested in all cell types where the recombinase was or is still active. The time point of gene deletion depends on the activity of the tissue-specific promotor controlling the expression of the Cre-protein. One advantage of tissue-specific in comparison to conventional knockouts such as the $Na_V1.7$ deficient mice is a bypass of the prenatal lethality that limits the analysis of the gene knockout in the adult mouse. Furthermore, the

mutant phenotypes developed in Cre-mediated knockouts are reduced to the Cre-expressing cell types, and interfering peripheral effects can mainly be excluded.

Within this study mice carrying the floxed Na$_V$1.7 gene (Nassar et al., 2004) were crossed with transgenic mice expressing the Cre-recombinase under the control of the glucagon promotor (Herrera, 2000). In pancreatic islets, the expression of the glucagon promotor is A-cell specific, and, therefore, Na$_V$1.7 is only deleted in glucagon-secreting A-cells of the islets of Langerhans.

1.7 The cGKIα and cGKIβ rescue mice

As mentioned above, conventional cGKI knockout mice have a reduced life expectancy, and, therefore, are inappropriate for long term *in vivo* investigations. Recently, a new mouse line was generated, expressing the Iα or Iβ isoform specifically in smooth muscle (Weber et al., 2007). Therefore, the cGKIα and cGKIβ coding sequences were placed under the control of the smooth muscle specific promotor SM22alpha. The so-called, cGKIα and cGKIβ rescue mice were generated by crossing animals that express either the Iα or Iβ isoform under control of SM22alpha promotor on a cGKI deficient background. In rescue animals, the expression level of the respective isoforms in smooth muscle was comparable to the endogenous cGKI levels of wild type mice. In all non-smooth muscle cells analyzed neither isoform was detectable. Consequently, the authors concluded that the cGKIα and cGKIβ rescue mice display a GKI knockout system for non-smooth muscle cells. The rescues have an ameliorated state of health and longer life expectancy rates as compared to conventional cGKI knockout mice (Weber et al., 2007). Therefore, for investigating the specific role of cGKI in non-smooth muscle cells, such as the endocrine pancreas, these animals are ideal model systems.

1.8 The NO/NP-cGMP-cGMP dependent protein kinase type I signaling pathway

Gaseous nitric oxide (NO) is an important messenger molecule involved in many physiological and pathophysiological processes within the mammalian body (Wink et al., 2000). The signaling molecule is synthesized by the conversion of L-arginine and oxygen to L-citrulline by the nitric oxide synthase (NOS) enzymes (Krumenacker et al., 2004). So far, three different isoforms have been described. The inducible (iNOS/NOS-2) NO synthase is independent of cellular Ca^{2+} concentrations, whereas the constitutively expressed neuronal isoform nNOS/NOS-1 and the endothelial isoform eNOS/NOS-3 are Ca^{2+}-calmodulin dependent (Nathan and Xie, 1994). iNOS plays an important role in the immune, and cardiovascular system (Rastaldo et al., 2007; Tripathi et al., 2007). nNOS is mainly involved in neuronal cell communication, and eNOS is generally participating in vasodilatation (Chanrion et al., 2007; Green et al., 2004). The highly reactive radical NO diffuses into cells and interacts with soluble guanylyl cyclases (sGC), which generate

the second messenger cyclic guanosine-3',5'-monophosphate (cGMP). NO binds to the prosthetic heme group, and, thus, activates the enzyme to synthesize cGMP by converting guanosine-5'-triphosphate (GTP) to cGMP (Koesling et al., 2004). This ubiquitous second messenger cGMP is involved in many cellular processes like regulating ion channel conductance, cell apoptosis, neurotransmission, and relaxation of (vascular) smooth muscle tissues. It mainly acts by activating cGMP-dependent protein kinases (cGKs). The cGMP synthesis is not only catalyzed by sGCs but also by particular guanylyl cyclases (pGC). The GCs differ in their cellular localization and activation by different ligands. The particular guanylyl cyclases (pGCs) are localized in the cellular membrane and are specific receptors for natriuretic peptides (NPs), like atrial (ANP), brain (BNP), and C-type (CNP) natriuretic peptides (Garbers and Lowe, 1994). The soluble guanylyl cyclases (sGCs) are mainly found in the cytosol. After synthesis, the second messenger cGMP can be degraded by phosphodiesterases (PDEs). The PDEs comprise a group of enzymes, which mediate the hydrolysis of cyclic nucleotides such as cyclic adenosine-3',5'-monophosphate (Campbell et al.) and/or cGMP to adenosine-5'-monophosphate (AMP) and/or guanosine-5'-monophosphate (GMP), respectively. In insulin secretion the PDE 3B is mainly involved in the exocytotic machinery by hydrolyzing cAMP in pancreatic B-cells (Parker et al., 1995; Walz et al., 2007). One of the most important PDE isoforms for cGMP degradation is the PDE 5, which plays an important role e.g. in the regulation of the vascular tone. Its specific inhibitor sildenafil is therapeutically relevant in the clinical treatment of erectile dysfunction and pulmonal hypertension (Rybalkin et al., 2003).
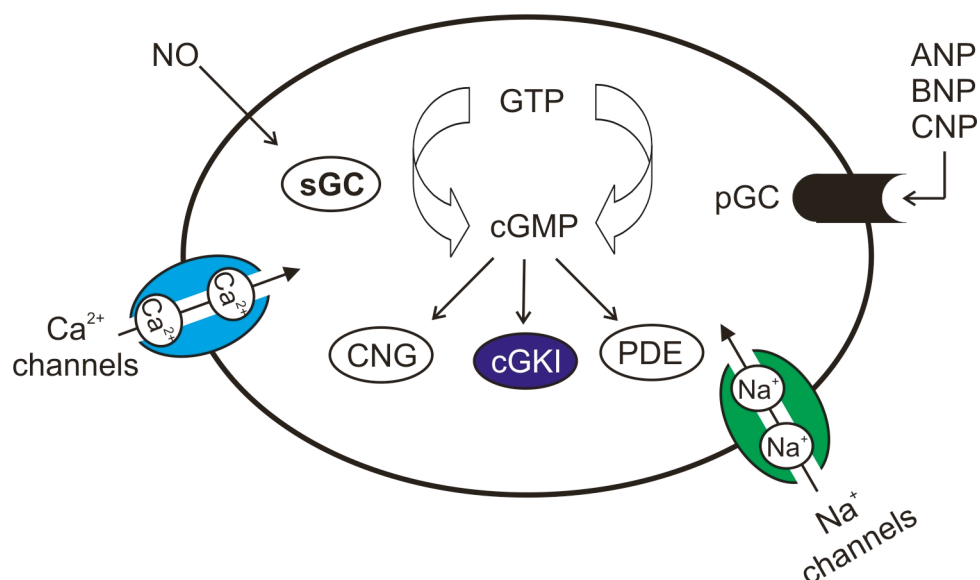
Fig. 5: cGMP signaling within a cell. cGMP is synthesized by soluble or particular guanylyl cyclases, respectively. The second messenger activates cGMP-dependent protein kinase type I (cGKI), binds to cGMP-dependent cation channels (CNG), and activates or inhibits phosphodiesterases (PDE) leading to hydrolyzation of cGMP or cAMP, respectively. sGC – soluble guanylyl cyclases; pGC – particular guanylyl cyclases;

The effectiveness of cGMP depends on several mechanisms within a cell. As already mentioned, cGMP synthesis is regulated via the guanylyl cyclases, whereas its breakdown is mainly controlled by the PDEs. However, cGMP does not only activate PDEs within a cell. The second messenger

also binds to and activates directly cyclic nucleotide-gated cation channels, for example in the visual system (Kaupp and Seifert, 2002). However, the main effectors in many cell types are presumably the cGMP-dependent protein kinases. The cGMP-dependent signaling pathways are summarized in figure 5.

1.9 General properties of the cGKs

The cGMP-dependent protein kinases belong to the serine-threonine family of protein kinases and are important receptors for cGMP. In mammals two different genes encoding for three different kinases have been identified. The *prkg1* gene codes for the genetic information of the two cGK isoforms type Iα (cGKIα) and type Iβ (cGKIβ), whereas the *prkg2* gene encodes the cGK type II enzyme (Hofmann, 2005). The cGKIα and cGKIβ isoforms differ only in their individual NH$_2$-terminal ends that are produced by alternatively used exons (Fig. 6).
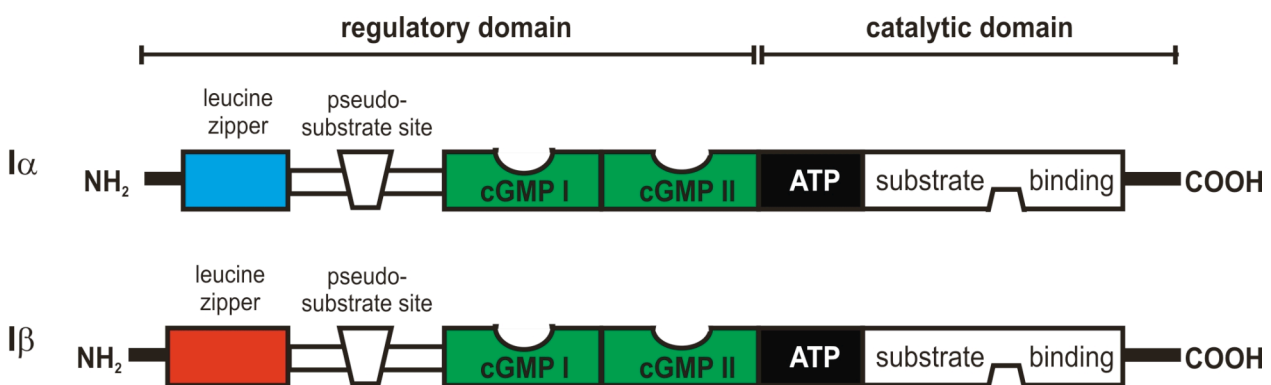
Fig. 6: Structure of cGMP-dependent protein kinase type I isoforms encoded by the *prkg1* gene. cGKIα and cGKIβ only differ in their individual NH$_2$-terminal ends (blue and red triangle). For further information, see text; (according to Kleppisch, 1999).

Both types of cGKs are composed of three functional domains:

(1) The NH$_2$-terminal isoleucine/leucinezipper region mediates the homodimerization of identical cGK monomers. Their specific amino termini mediate the interaction with partner proteins via the zipper region and target the kinases to their subcellular localization. The NH$_2$-terminus functions also as an autoinhibitory/pseudosubstrate site by binding to the catalytic center during the absence of cGMP, and, thereby, inactivates the enzyme.

(2) The catalytic domain catalyzes the γ-phosphate transfer of ATP to serine and/or threonine residues of the substrate proteins. This kinase domain harbors the adenosine-5'-triphosphate (ATP) and substrate binding sites.

(3) The regulatory domain contains two tandem non-identical cGMP binding pockets with low and high affinity to cGMP. Binding of cGMP to the regulatory domain induces a

conformational change that releases the inhibition of the catalytic core of the N-terminus and allows the phosphoryation of target substrates.

In contrast to the structural similarities, the cGKs differ in their tissue distribution, cellular localization, and their specific functions. cGKII is anchored at the plasma membrane and mainly expressed in several brain nuclei, intestinal mucosa, kidney, adrenal cortex, chondrocytes, and lung (de Vente et al., 2001; el-Husseini et al., 1995; Lohmann et al., 1997; Werner et al., 2004). The cGKIα and cGKIβ isoforms are soluble enzymes using their different NH_2 termini for their interactions with other proteins within a cell. The Iα isozyme is expressed in lung, heart, dorsal root ganglia, and cerebellum (Feil et al., 2005b; Geiselhoringer et al., 2004; Keilbach et al., 1992). Both isoforms are detectable in smooth muscle, including uterus, vessels, intestine, and trachea (Keilbach et al., 1992; Landgraf et al., 1992), whereas the Iβ isozyme is found in platelets, hippocampal neurons, and olfactory bulb neurons (Gambaryan et al., 2004; Kleppisch et al., 1999).

1.10 NO and its role in pancreatic islets of Langerhans

NO is considered as a ubiquitous messenger molecule in many different organ systems, and it is also produced in the islets of Langerhans (Alm et al., 1999; Lajoix et al., 2001; Schmidt et al., 1992). The function of NO in pancreatic islets in general is discussed controversially (Panagiotidis et al., 1992; Schmidt et al., 1992). The expression patterns of eNOS and iNOS have been investigated in detail in murine and rat A- and B-cells (Alm et al., 1999; Henningsson et al., 2000; Lajoix et al., 2001). Both, inducible and constitutive NOS isoforms are expressed in glucagon-, and insulin-secreting cells, respectively (Salehi et al., 2008). NO derived from iNOS is supposed to be mainly involved in mechanisms responsible for B-cell destruction (Corbett et al., 1993; Sandler et al., 1991), and is implicated in the dysfunction of B-cells in insulin-dependent type-1 diabetes mellitus (Eizirik and Pavlovic, 1997). In contrast, eNOS is mainly expressed in pancreatic B-cells, and in part associated with insulin granules, but the exact function of eNOS derived NO is still debated (Akesson et al., 1996; Henningsson et al., 2000; Henningsson et al., 2002). On the one hand, NO synthesized by eNOS was found to be a strong negative modulator of glucose-stimulated insulin release (Campbell et al., 2007; Henningsson et al., 2002). Thus, the application of various NOS inhibitors resulted in an increase of insulin secretion (Henningsson et al., 2002). On the other hand, long-term inhibition of NOS had no influence on insulin secretion in freely fed animals, but enhanced insulin release in 24 h fasted mice (Henningsson et al., 2000). In addition, it was suggested that NO positively stimulates glucagon release, which was efficiently inhibited by unspecific NOS inhibitors (Akesson et al., 1996). In contrast, findings by others implicate a chronically suppression of NOS leads to an increased glucagon secretion rate at basal (7 mM) and high (20 mM) glucose conditions (Henningsson et al., 2000). As mentioned above, NO can stimulate the generation of the second messenger cGMP by activating sGCs (Koesling et al., 2004). The current knowledge concerning the involvement of cGMP on glucagon secretion is very

limited. Some evidence comes from a study on a mouse clonal A-cell line showing that elevation of cGMP levels stimulated glucagon release (Mori et al., 2001). Furthermore, it could be demonstrated that chronic inhibition of NOS affected the intra-islet cGMP levels (Henningsson et al., 2000; Mori et al., 2001), but the exact mechanisms underlying those effects are unknown. In addition, an effector protein present in islets mediating putative effects of the second messenger cGMP has not been identified.

1.11 Aim of the work

In the present study the functional role of both the sodium channel $Na_V1.7$ and the cGMP-dependent protein kinase type I (cGKI) on glucagon secretion were examined in different transgenic mouse models lacking the respective protein of interest in pancreatic islet cells of Langerhans. In general, glucagon release is an important physiological process but the exact mechanisms regulating the hormone secretion are incompletely understood. Previous experiments revealed the importance of sodium channels contributing to the glucagon release (Gopel et al., 2000b; MacDonald et al., 2007), which was corroborated by the finding that the mRNA transcript for the sodium channel isoform $Na_V1.7$ is expressed in pancreatic islets (Vignali et al., 2006). However, the islet specific expression pattern as well as the direct involvement of this sodium channel isoform on glucagon secretion were not determined. To further elucidate the islet cell specific distribution of $Na_V1.7$ and its role on e.g. glucagon secretion and glucose homeostasis a conditional $Na_V1.7$ deletion in pancreatic A-cells was generated. In these mutants, *in vitro* glucagon secretion experiments of isolated islets and insulin/glucose challenges *in vivo* were planed to directly test the putative effect of the $Na_V1.7$ inactivation on A-cell activity. In addition, the use of $Na_V1.7$ specific antibodies should help to characterize the islet-cell specific localization of the sodium channel isoform in control versus conditional $Na_V1.7$ knockout mice.

The role of the signaling molecule NO on islet hormone release is currently discussed very controversial (Campbell et al., 2007; Mori et al., 2001; Salehi et al., 2008). In many cell types the intracellular second messengers of NO is cGMP, which in turn can activate cGKI (Hofmann et al., 2000). Indeed, only few experiments using artifical cell culture systems indicated that islet cGMP and/or cGKI might be involved in glucagon secretion (Henningsson et al., 2000; Mori et al., 2001). Due to the fact that conventional cGKI knockout mice have a reduced life expectancy, and, additionally, severe phenotypes those animals are inappropriate for long-term *in vivo* or tissue-specific loss of function studies. However, the recently generated cGKIα and cGKIβ rescue mice (Weber et al., 2007) expressing the respective cGKI isoform only in smooth muscle, allow the analysis of non smooth-muscle cells that lack cGKI *in vivo* in relatively healthy animals. The expression pattern of cGKI in pancreatic islets of Langerhans was verified by analyzing established and new gene-targeted cGKI mouse models (e.g. cGKI$^{-/-}$, cGKIα and cGKIβ rescue mice) in

comparison to control animals. Furthermore, the recently generated rescue animals should help to elucidate putative functional roles of the NO/cGMP/cGKI signaling pathway in islets.
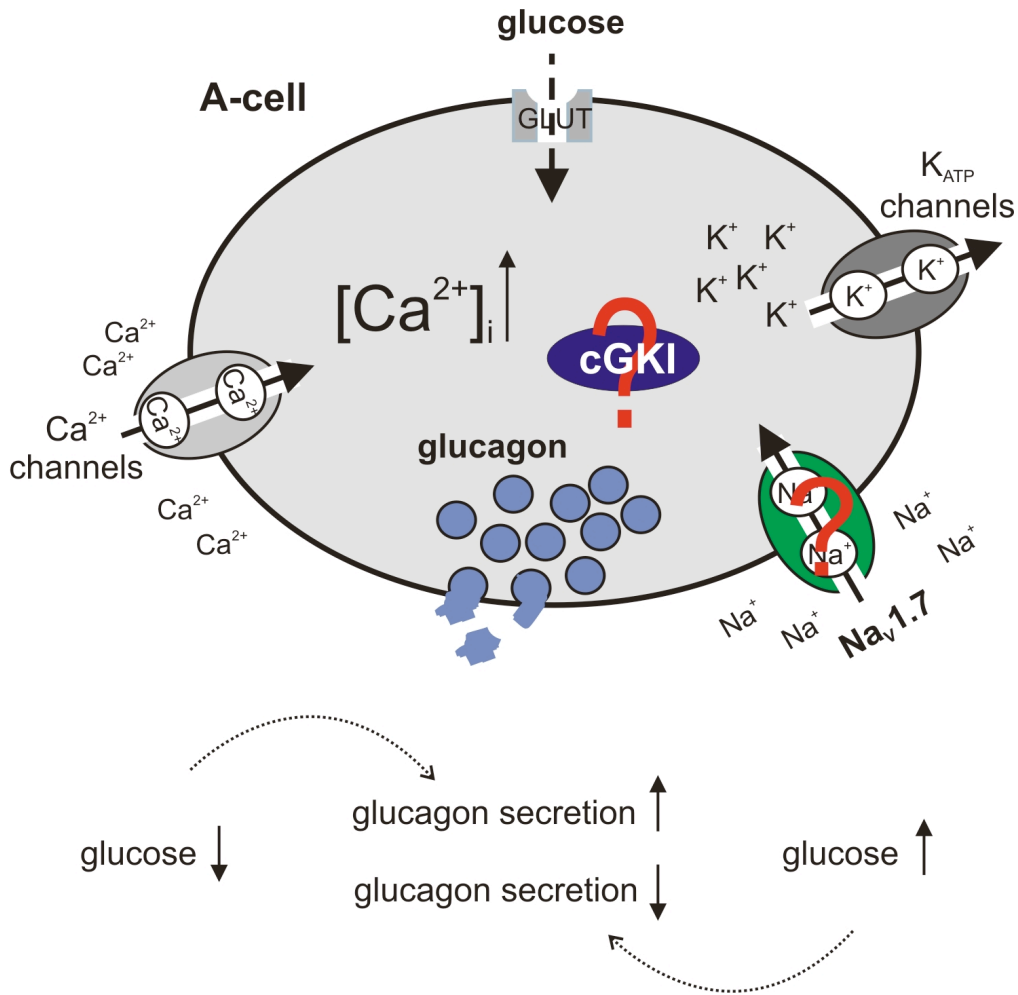
Fig. 7: Schematic illustration summarizing aim of the work. Glucagon is released from pancreatic A-cells. Low glucose conditions lead to low activity of K_{ATP} channels to keep the membrane potential sufficiently negative to prevent voltage-dependent inactivation of voltage-gated ion channels. Activation of Ca^{2+}-channels and an increase of $[Ca^{2+}]_i$, which triggers hormone secretion. At high glucose conditions glucagon secretion is inhibited. The expression and the role of $Na_V1.7$ and cGKI in the regulatory mechanisms of glucagon release were investigated in the present study. K_{ATP} channel – ATP-sensitive potassium channel; Ca^{2+}-channel - calcium channel; $[Ca^{2+}]_i$ – intracellular calcium concentration; GLUT – glucose transporter; Na^+ – sodium ion;

2 Materials and Methods

If not mentioned otherwise, all chemicals were purchased from Invitrogen (Karlsruhe), Sigma (Schnelldorf), Roche (Penzberg), Roth (Karlsruhe), Millipore (Schwalbach), and Vector Laboratories (Loerrach). All primers used in this work were synthesized by Eurofins MWG Operon (Ebersberg). Commercial primary and secondary antibodies were purchased from Santa Cruz Biotechnology (Heidelberg), DAKO (Hamburg), Abcam (Cambridge), and Millipore (Heidelberg).

2.1 Transgenic mouse lines

For experiments, inbred mice on C57BL/6 or 129Sv backgrounds with or without specific genetic modifications were used.

2.1.1 Floxed Na$_V$1.7 knockout mice

Mice carrying the loxP-flanked exons 14 and 15 coding for the main part of domain II of the sodium channel subtype Na$_V$1.7 were described previously (Nassar et al., 2004). These mice were a gift from Prof. Dr. J. Wood (University College London, London, Great Britain).

2.1.2 Gluc-Cre recombinase mice

The transgenic Gluc-Cre animals express the Cre recombinase under the control of the glucagon promotor. The generation and characterization of this mouse line was described previously (Herrera, 2000). These animals were a gift from Prof. Dr. M. Herrera (University of Geneva Medical School, Geneva, Switzerland).

2.1.3 Rosa26 β-gal Cre reporter mice

The Rosa26 β-gal Cre reporter (R26R) mice were obtained from the Jackson Laboratory (Bar Harbor, ME). The generation and general characterization of the mice was described elsewhere (Soriano, 1999). In brief, for the analysis of recombination efficiency of the Cre recombinase under the control of the glucagon promoter animals carrying the Rosa26 β-gal allele, were crossed to heterozygous Gluc-Cre mice (see Materials and Methods 2.1.2). In R26R animals, LacZ is not expressed until an intervening STOP sequence is specifically excised by Cre. Cre recognizes and binds to two loxP sites flanking the STOP sequence. In the Gluc-Cre; R26R animals LacZ was expressed in cells and/or tissues expressing active Cre recombinase under the control of the glucagon promotor.

2.1.4 A-cell specific Na$_V$1.7 knockout mice

To generate A-cell specific Na$_V$1.7-deficient mice, the Na$_V$1.7$^{+/L2}$ mouse carrying one floxed (L2) allele and one wild-type (+) allele was crossed to a heterozygous Gluc-Cre$^{+/tg}$ mouse. The resulting Na$_V$1.7$^{+/L2}$; Gluc-Cre$^{+/tg}$ offsprings were mated to Na$_V$1.7$^{L2/L2}$ mice homozygous for the L2 allele. In the offspring of this breeding, A-cell specific knockouts (Na$_V$1.7^{Acko}) (genotype: Na$_V$1.7$^{L2/L2}$; GlucCre$^{+/tg}$) and control animals (genotype: Na$_V$1.7$^{+/L2}$; Gluc-Cre$^{+/tg}$) were obtained for experiments.

2.1.5 Conventional cGKI deficient mice

The generation and characterization of the cGMP-dependent kinase I deficient mice (cGKI$^{-/-}$) was described earlier (Pfeifer et al., 1998). Mice lacking the cGKI protein have a reduced lifespan. About 50% of the animals die before adulthood.

2.1.6 cGKIα and cGKIβ rescue mice

The generation and characterization of the cGKIα and cGKIβ rescue animals was described earlier (Weber et al., 2007). The mice express either the Iα or Iβ isoform of cGKI under the control of the endogenous smooth muscle promoter SM22α. Thus, in all non-SMCs these mice are deficient for cGKI. In comparison to cGKI$^{-/-}$ mice the rescue animals have an increased life expectancy and normal SMC functions. Therefore, the *in vivo* experiments included in this work were performed in cGKIα rescue mice and their littermate controls.

2.2 Analysis of experimental animals

2.2.1 Genotyping

2.2.1.1 Tail tip biopsy

Reagents

Proteinase K (PK) 50 mg/ml

10 x Taq DNA Polymerase buffer (Promega)

PK working solution:

	50 µl	[c]
PK (50 mg/ml)	1 µl	1 µg/µl
10 x Taq DNA Polymerase buffer	5 µl	1 x
MgCl$_2$	3 µl	1.6 mM
ddH$_2$O	41 µl	-

Protocol

For genotyping 2 mm of mouse-tail tip biopsy material from 10-14 day old animals was used. Tips were incubated over night at 55°C in 50 µl proteinase K (PK) working solution containing 1 µg/µl PK. The next day, samples were heated at 95°C for 15 min to inactivate remaining PK activity. Then, samples were centrifuged at 18,000 rpm for 1 min and stored at -20°C until genotyping by PCR was carried out.

2.2.1.2 Polymerase chain reaction

Reagents

10 x Taq DNA Polymerase buffer (Promega)

1.25 mM dNTPs:

	Stock	200 µl	[c]
dATP	100 µM	2.5 µl	1.25 µM
dCTP	100 µM	2.5 µl	1.25 µM
dGTP	100 µM	2.5 µl	1.25 µM
dTTP	100 µM	2.5 µl	1.25 µM

add 190 µl ddH$_2$O

Taq DNA Polymerase (Promega) 5 U/µl

Protocol

By the polymease chain reaction (PCR) DNA is amplified *in vitro*. One key component of the PCR is the DNA polymerase. Here, a thermostable DNA polymerase isolated from the gram-negative Thermus aquaticus (Promega) was used (Taq DNA polymerase). Additionally, several other components are necessary: template DNA, large quantities of the four deoxynucleotide triphosphates (dNTPs), and an excess of primer. The PCR itself is characterized by a series of 25 to 35 repeated temperature changes, called cycles. Each cycle includes three different temperatures: (1) Denaturation – this step is carried out at 94°C. The double stranded DNA helix is separated in two single DNA strands. (2) Annealing – during this step the primers bind to their complementary template DNA sequences. The step is usually performed at 50°C to 65°C, which depends e.g. on the sequences of the primer pairs. (3) Elongation – the Taq DNA polymerase adds nucleotides to the primers and synthesizes a complementary strand of the template DNA at 72°C. During each cycle each template DNA is duplicated once. The sequence of interest is flanked by a primer pair, and, therefore, amplified.

Standard PCR reaction mixture:

	Stock	25 µl
PCR buffer	10x	2.50 µl
dNTPs	1.25 µM	4 µl
Taq DNA Polymerase	5 U/µl	0.25 U/µl
Primer A	10 µM	1. 5 µl
Primer B	10 µM	1.5 µl
Primer C	10 µM	1.5 µl
ddH$_2$O	-	14.75 µl
DNA	-	2 µl

A so-called master mix for all samples of one reaction was prepared, containing the PCR buffer, ddH$_2$O, dNTPs, and specific primer pairs. Next, all components were mixed well. Finally, the Taq DNA polymerase was added to the master mix and 24 µl of the mixture were distributed into the reaction tubes. Finally, 2 µl of tail tip DNA were added. The PCR was carried out in a Biometra Thermocycler with the following protocol:

	Temperature	Time	Repeats
Initial denaturation	94°C	5 min	-
Denaturation	94°C	15 sec	x25 - 30
Annealing	55°C	30 sec	
Elongation	72°C	30 sec	
Final elongation	72°C	5 min	∞

These standard conditions were varied depending on the size of the amplicons and the primer pairs used.

2.2.2 Reverse transcription PCR (RT-PCR)

Reagents

RNAse free DNAse (Roche) 10 U/µl

Reverse Transcriptase (Invitrogen) 20 U/µl

10 x RT-PCR buffer:

	Stock	5.0 ml	[c]
KCl	1 M	2.5 ml	500 mM
Tris-Cl pH 8.0	1 M	500 µl	100 mM
MgCl$_2$	1 M	750 µl	15 mM

add ddH$_2$O to 5.0 ml

10 x RT-PCR buffer with dNTPs:

	Stock	5.0 ml	[c]
KCl	1 M	2.5 ml	500 mM
Tris-Cl pH 8.0	1 M	500 µl	100 mM
MgCl$_2$	1 M	750 µl	15 mM
dNTPS	100 mM	each 100 µl	2 mM

add ddH$_2$O to 5.0 ml

A-Taq DNA Polymerase (Promega) 5 U/µl

Protocol

Before starting the RT-PCR reaction of the RNA extracts a genomic DNA digestions step was performed (for RNA isolation please consult Materials and Methods chapter 2.6.1). Therefore, 1 U/µl RNase free DNase was added to the isolated RNA and incubated at 37°C for 30 min. Next, the DNA digestion was stopped by heating the samples at 80°C for 4 min. Then, the RT-PCR was carried out.

The Reverse Transcriptase (RT) is a RNA-dependent DNA polymerase, thus it is an enzyme able to transcribe single stranded mRNA into single stranded copy DNA (cDNA). As DNA polymerase, the RT needs a small piece of DNA, called primer, to start the transcription. For every RT-PCR reaction specific primer pairs for the mRNA of interest, as well as a housekeeping standard primer pair specific for hypoxanthine-guanine phosphoribosyltransferase (HRPT) were added to the RT-PCR reaction.

RT-PCRs were performed to analyze the Gluc-Cre mediated recombination of the floxed Na$_V$1.7 gene in pancreatic islets and dorsal root ganglia (DRGs). In addition, RT-PCR reactions were used to analyze the expression of possible components of the NO/NPs/cGMP/cGKI signaling pathway expressed in pancreatic islets. For positive controls, RNA extracts from primary vascular smooth muscle cells (VSMCs) or the duodenum were analyzed.

Standard RT-PCR reaction mixture:

	stock	45 µl
RT-PCR buffer with dNTPs	10 x	5.5 µl
Primer A	25 µM	0.5 µl
Primer B	25 µM	0.5 µl
Primer HPRT A	12.5 µM	0.5 µl
Primer HPRT B	12.5 µM	0.5 µl
DEPC-H$_2$O	-	27.5-35 µl
RNA	0.1 µg/µl	2.5-10 µl

In detail, the master mix, containing the components listed above, was prepared on ice. Depending on the tissue, 2.5 – 10 µg RNA were included to the master mix. The mixture was put into a Biometra Thermocycler and heated to 80°C for 5 min. After slowly cooling the samples (0.7°C/s) to 50°C, 1 U/µl RT was added, and all reagents were incubated for an additional 20 min at 50°C. After 20 min reverse mRNA transcription into cDNA the reaction was finished by the addition of 0.5 U/µl Taq-DNA polymerase and a standard (RT-)PCR amplification protocol was started.

Standard RT-PCR amplification protocol:

	temperature	time	repeats
denaturation	94°C	15 sec	
annealing	58°C	30 sec	x35 - 38
elongation	72°C	30 sec	

These standard conditions were varied depending on the size of the amplicons and the primer pairs used. For amplicons smaller than 500 bp the elongation step was skipped. In general, a semi-quantitative protocol was performed. Therefore, 10 µl were collected five times in three cycle intervals during the last 15 cycles of the (RT-)PCR.

2.2.3 Agarose gel electrophoresis

Reagents

SeaKem LE Agarose (Biozym)

Ethidium bromide solution (10 mg/ml)

Bromphenol blue:

	10 ml	[c]
bromphenol blue	0.5 g	50 mg/ml

add ddH$_2$O to 10 ml.

Xylencyanol FF:

	10 ml	[c]
Xylencyanol FF	0.5 g	50 mg

add ddH$_2$O to 10 ml

10 x TBE gel buffer:

	MW [g/mol]	1 l	[c]
Tris-Cl	121.14	107.78	0.9 M
$Na_2EDTA \cdot 2H_2O$	372.24	7.44 g	20 mM
Boric acid	61.83	55.0 g	0.9 M

add ddH_2O to 1 l

6 x DNA loading dye:

	stock	100 ml	[c]
Ficoll type 400	-	18 g	18%
EDTA, pH 8.0	0.5 M	24 ml	0.12 M
10 x TBE	10 x	60 ml	6 x
Bromphenol blue	50 mg/dl	3 ml	0.15%
Xylencyanol FF	50 mg/dl	3 ml	0.15%

add ddH_2O to 100 ml

DNA electrophoresis standard:

	6 ml
1 kb DNA ladder (1 µg/µl)	100 µl
6 x DNA loading dye	1 ml
10 x TE buffer	0.6 ml

add ddH_2O to 6 ml

Protocol

Agarose gel electrophoresis is a method to separate negatively charged DNA molecules by their size. In general, larger DNA molecules move slower than smaller DNA fragments through an agarose matrix in an electrical field. The fragments can be visualized with UV light within the 2% agarose gel by the fluorescent dye ethidium bromide, which intercalates into DNA. For the determination of the size of the amplicons a 1 kb DNA ladder of mixed DNA fragments of known size is used as an electrophoresis standard. For the determination of the size of the separated DNA fragments in samples they were compared to their relative position to the standard.

The agarose was dissolved in 1 x TBE buffer in a microwave, cooled down, and ethidium bromide was added (final concentration 20 mg/ml). Before the PCR products were loaded the samples were diluted in 6 x loading dye. Then, the electrophoresis was carried out at 150 V for about 30 min.

2.3 Electrophysiological measurements

Reagents

Intracellular solution:

	MW [g/mol]	Stock	100 ml	[c]
CsCl	168.36	-	2.1 g	125 mM
MgCl$_2$	203.3	0.1 M	1 ml	1 mM
EGTA	380.35	-	0.38 g	10 mM
Mg$_2$ATP	507.2	-	0.15 g	3 mM
HEPES	238.31	-	0.238 g	10 mM

Add H$_2$O to 100 ml. Adjust pH to 7.2 with CsOH

Extracellular solution:

	MW [g/mol]	Stock	100 ml	[c]
NaCl	58.44	1 M	11.8 ml	118 mM
Tetraethyl-ammoniumchloride	165.7	-	0.32 g	20 mM
KCl	74.56	1 M	0.56 ml	5.6 mM
BaCl$_2$/CaCl$_2$	244.28/110.01	0.1 M	2.6 ml	2.6 mM
MgCl$_2$	203.3	0.1 M	1.2 ml	1.2 mM
HEPES	238.31	-	0.119 g	5 mM
Glucose Monohydrate	198.17	-	0.099 g	5 mM

Add H$_2$O to 100 ml. Adjust pH to 7.5 with NaOH

Protocol

To study the electrical properties of sodium channels in pancreatic islets whole cell measurements on intact islets were performed. Therefore, pancreatic islets were isolated and cultured over night as described (2.4). The next day, sodium currents were recorded at room temperature by whole cell patch clamp experiments. The measurements were carried out using an EPC-9 patch-clamp amplifier (HEKA Electronics) and Pulse software. The patch pipettes were pulled from borosilicate glass with a resistance of 2.5 – 3.5 MΩ when filled with the intracellular solution. The islets were fixed with a holding pipette in the measuring chamber. The holding potential was -70 mV, and steady state inactivation was measured by a conventional two-pulse protocol was conducted in which a 50 ms test depolarization to 0 mV was preceded by a 10 ms conditioning pulse (V_{pre}) to voltages between -180 mV to 30 mV in 10 mV steps. Data for steady state inactivation were fitted by a Boltzmann equation:

$I/I_{max} = (1-A)/\{1+\exp[(V_{pre} – V_{0.5})/k]\} + A,$

where I/I_{max} is the relationship between the current amplitudes (I) and the maximum current amplitude at the most negative V_{pre} (I_{max}), A is the saturated level of I/I_{max}, $V_{0.5}$ is the potential at which I/I_{max} is half-maximal, and k represents the slope factor. The electrophysiological data were analyzed with Origin6.1.

2.4 Isolation of pancreatic islets

Reagents

1 x Hanks Buffered Salt Solution (HBSS) (Sigma):

	MW [g/mol]	1 l	[c]
HBSS	-	9 g	1 x
NaHCO$_3$	84.01	0.35 g	4 mM

Add ddH$_2$O to 1 l

Collagenase:

	Stock	2 ml	[c]
Collagenase	19 U/ml	200 µl	1.9 U/ml

Add 1 x HBSS to 2 ml

Islet culture medium:

	10 ml	[c]
RPMI-1640 5 mM glucose (Gibco)	10 ml	-
Penicillin/Streptavidin (Gibco)	130 µl	1.3%
Fetal calve serum (Gibco)	500 µl	5%

Protocol

Preparation of islets was performed as previously described (Barg et al., 2000; Schulla et al., 2003; Vignali et al., 2006). In brief, mice were sacrificed by cervical dislocation. By a transversal incision the abdominal wall was opened with scissors. The ampulla of Vater (papilla Vateri) and the bile duct (ductus choledochus) were dissected by the use of blunt forceps. Next, by surgical clamps the papilla vateri was occluded, and 2 ml collagenase (1.9 U/ml) were injected through the bile duct using an injection with a 27-gauge needle. The collagenase digestion solution enters the pancreas retrograde via the ductus pancreaticus. The semi-digested pancreas was transferred to a reaction tube and promptly put on ice. Next, a digestion step followed for 10 to 12 min at 37°C, depending on the age of the mice. By the addition of 10 ml ice cold 1 x HBSS the digestion was stopped. An intensive shaking step separated the islets from the exocrine pancreas. Several subsequent washing steps were performed to loose the exocrine tissue from the islets. Finally, the isolated islets were transferred to 2 ml islet culture medium and cultured over night at 37°C and 5% CO$_2$.

For analysis performed on single islet cells, islets were cultured in 24 well plates, each well containing a plastic cover slip to facilitate adhesion of the islet cells. To disperse pancreatic islets into single islet cells a 1 ml pipette was used to induce physical stress.

2.5   RNA and protein purification

Reagents

1 x PBS, pH 7.4:

	MW [g/mol]	1 l	[c]
NaCl	58.44	8. 00g	135 mM
KCl	74.56	0.20 g	3 mM
$Na_2HPO_4 \bullet 2H_2O$	177.99	1.44 g	8 mM
KH_2PO_4	136.09	0.24 g	2 mM

Dissolve in 0.8 l H_2O and adjust pH to 7.4 with HCl. Add ddH_2O to 1 l

Protocol

Islets were isolated, cultured as described (2.4), and washed the following day 3 times in 1 x PBS. Next, the tissue was transferred to a (RNase-free) reaction tube, followed by a short and gently centrifugation step (30 seconds at 2,000 xg). The supernatant was discarded, and islets were shock frozen on liquid nitrogen, then stored at -80°C until further usage. Control organs (e.g. duodenum) were dissected, washed in ice cold 1 x PBS and stored also at -80°C.

2.5.1 Extraction of RNA

Reagents

PeqGold RNA pure (PeqLab)

75% EtOH-Diethylpyrocarbonate (DEPC)-H_2O

DEPC-H_2O

Trichlormethane

100% isopropanol

Protocol

Islets pooled from 5 animals were homogenized in 500 µl PeqGOLD reagent each. Next, 0.2 volumes trichlormethane were added to each homogenate. After incubation for 5 min at RT, the sample was centrifuged at 13,000 rpm for 5 min. The upper aqueous phase accounting for 300 µl was transferred to a new RNase free reaction tube, and 0.7 volumes isopropanol were added to precipitate the RNA. Precipitation was expanded at 4°C over night, followed by a centrifugation

step at 18.000 xg at 4°C. Next, two subsequent washing and centrifugation steps with 800 µl 75% EtOH-DEPC-H$_2$O were applied to loose residual isopropanol washed samples. After drying the RNA pellets for about 10 min at RT, they were dissolved in 50 µl DEPC-H$_2$O. The amount of RNA was quantified by standard UV photometry, and then stored at -20°C until RT-PCR was carried out.

2.5.2 Extraction of protein

Reagents

1 x PBS

SDS lysis buffer:

	Stock	10 ml	[c]
Tris-Cl, pH 8.3	1 M	210 µl	21 mM
Sodium Dodecyl Sulfate (SDS)	10%	670 µl	0.67%
2-mercaptoethanol	14.2 M	170 µl	238 mM
Phenylmethylsulphonylfluoride (PMSF)	100 mM	20 µl	0.2 mM

Add ddH$_2$O to 10 ml

Protocol

In general, the frozen islets (see chapter 2.4) were lysed by the addition of 50 µl SDS lysis buffer. Then, the lysates were heated at 95°C for 10 min, centrifuged at 18.000 xg for 5 min, and the supernatants were transferred to a new reaction tube. The proteins were stored at -20°C until Western blot was performed. Protein lysates from heart and stomach were a gift from Dr. Robert Lukowski (Pharmakologie und Toxikologie, TU München), and were used as positive and/or negative control protein for the Western blot analysis.

2.6 Western blot analysis

Reagents

For 8% separating gels

6 x SDS sample buffer

4 x Tris-Cl-SDS, pH 6.8:

	MW [g/mol]	50 ml	[c]
Tris-Cl	121.14	3.02 g	0.5 M
SDS	288.38	0.2 g	3.5 mM

Ad 50 ml ddH$_2$O and adjust pH to 6.8 pH

4 x Tris-Cl-SDS, pH 8.8:

	MW [g/mol]	100 ml	[c]
Tris-Cl	121.14	18.2 g	1.5 M
SDS	288.38	0.4 g	7 mM

Ad 100 ml ddH$_2$O and adjust pH to 8.8 pH

Separating gel:

4 x Tris-Cl pH 8.8	3.75 ml
30% Acrylamide / 0.8% Bisacrylamide	4 ml
ddH$_2$O	7.25 ml
30% ammonium persulfate (APS)	50 µl
N,N,N',N'-tetramethylethylenediamine (TEMED)	10 µl

Stacking gel:

4 x Tris-Cl pH 6.8	1.25 ml
30% Acrylamide / 0.8% Bisacrylamide	0.65 ml
ddH$_2$O	3.05 ml
30% APS	12.5 µl
TEMED	5 µl

10 x SDS electrophoresis buffer:

	MW [g/mol]	1 l	[c]
Tris-Cl	121.14	30.2 g	0.24 M
Glycerol	92.1	144.0 g	1.5 M
SDS	288.38	10.0 g	35 mM

Ad 1 l ddH$_2$O

For 13% Tricine gels

Gel buffer, pH 8.4:

	MW [g/mol]	100 ml	[c]
Tris-Cl	121.14	36.33 g	3 M
SDS	288.38	0.3 g	0.3%

Dissolve in 80 ml ddH$_2$O by adjusting pH to 8.4 with HCl$_{conc.}$
Add ddH$_2$O to 100 ml

Separating gel:

	13%
24.25% acrylamide / 0.75% bisacrylamide solution	8 ml
Gel buffer	5 ml
Glycerol	2 g
ddH$_2$O	3.4 ml
30% APS	30 µl
TEMED	15 µl

Stacking gel:

24.25% acrylamide / 0.75% bisacrylamide solution	1 ml
Gel buffer	1.55 ml
ddH$_2$O	3.7 ml
30% APS	12 µl
TEMED	20 µl

10 x Anode buffer, pH 8.9:

	MW [g/mol]	500 ml	[c]
Tris-Cl	121.14	12.11 g	2 M

Dissolve in 450 ml ddH$_2$O by adjusting pH to 8.9 with HCl$_{conc}$
Add ddH$_2$O to 500 ml

10 x Cathode buffer, pH 8.25:

	MW [g/mol]	500 ml	[c]
Tris-Cl	121.14	60.6 g	1 M
Tricine	179.2	89.6 g	1 M
SDS	288.38	5 g	1%

Dissolve in 450 ml ddH$_2$O by adjusting pH to 8.25 with HCl$_{conc}$
Add ddH$_2$O to 500 ml

Anode transfer buffer I, pH 10.4

	MW [g/mol]	1 l	[c]
Tris-Cl	121.14	36.3 g	0.3 M
Methanol	100 %	200 ml	20%

Dissolve Tris-Cl in 0.8 l ddH$_2$O and adjust pH to 10.4 with HCl$_{conc}$.
Ad 0.2 l Methanol.

Anode transfer buffer II, pH 10.4:

	MW [g/mol]	1 l	[c]
Tris-Cl	121.14	3.03 g	20 mM
Methanol	100%	200 ml	20%

Dissolve Tris-Cl in 0.8 l ddH$_2$O and adjust pH to 10.4 with HCl$_{conc.}$
Ad 0.2 l Methanol.

Cathode transfer buffer, pH 7.6:

	MW [g/mol]	1 l	[c]
Tris-Cl	121.14	3.03 g	20 mM
6-aminocapoic acid	131.18	5.2 g	40 mM
Methanol	100%	200 ml	20%

Dissolve Tris-Cl in 0.8 l ddH$_2$O and adjust pH to 7.6.
Ad 0.2 l methanol

10 x TBS, pH 8.2:

	MW [g/mol]	1 l	[c]
Tris-Cl	121.14	6.05	50 mM
NaCl	58.44	43.8 g	750 mM

Dissolve Tris-Cl in 0.8 l ddH$_2$O and adjust pH to 8.2.
Ad 0.2 l methanol

1 x TBS-T (0.1% Tween):

10 x TBS	100 ml
Tween20	1 ml

Add ddH$_2$O to 1 l

1 x TBS-T blocking solution (5% milk powder):

1 x TBS-T	50 ml
Milk powder	2.5 g

1 x TBS-T washing solution (1.5% milk powder):

1 x TBS-T	100 ml
Milk powder	1.5 g

Protocol

By Western blot analysis a specific protein can be detected in a given sample of tissue homogenate or extract. Denatured proteins are separated by their molecular size by gel electrophoreses, and, afterwards, transferred to a nitrocellulose or polyvinyliden difluoride (PVDF) membrane. The immobilized proteins of interest are probed using specific antibodies. This method was performed to analyze the tissue specific expression pattern of cGKI and other components of the NO/NPs/cGMP/cGKI signaling cascade in pancreatic islets.

In general, 20 µl of isolated islet protein were loaded on an 8 % SDS polyacrylamide gel or a 13% tricine gel without prior quantification. For positive controls 10 µg protein extracts from heart and stomach tissues were used. All organ samples were diluted to a final concentration of 1-2 µg/µl in 6 x SDS sample buffer. The probes were denatured at 95°C for 5 min, loaded on the gel, and separated by their molecular weight by gel electrophoresis. Afterwards, proteins were transferred to a PVDF membrane using a semi-dry transfer chamber. An electric current for electroelution was used to move negatively charged proteins via the electric field from the gel onto the surface of the PVDF membrane. The proteins moved from within the gel onto the membrane by maintaining the size-dependent separation (organization) they had acquired within the gel during electrophoresis. The gel and the membrane were submerged between filter papers, saturated with conducting transfer buffers during the blotting procedure. The configuration of the blotting chamber was as follows: (1) anode plate; (2) 4 x filter papers saturated with anode transfer buffer I; (3) 4 x filter papers saturated with anode transfer buffer II; (4) PVDF membrane soaked in 100% methanol and saturated with anode transfer buffer II; (5) protein gel, (6) 8 x filter papers saturated with cathode transfer buffer; and (7) cathode plate. The transfer was performed for 1 h at 60 mA.

Unspecific binding sites for the antibodies on the membrane surface were blocked with 1 x TBS-T blocking solution for 1 h, followed by 3 washing steps, each for 10 min in 1 x TBS-T. Defined pieces of the membrane were incubated with specific primary antibodies over night at 4°C. After rinsing the membrane to remove unspecific and unbound primary antibodies three times in 1 x TBS-T washing solution for 10 min, the membranes were incubated with the specific secondary antibodies (diluted 1:2000 in TBS-T washing solution) for 1 h at RT. The secondary antibodies were linked to horseradish peroxidase, which is important for the luminescence reaction during detection, followed by three more washing steps in 1 x TBS-T (each for 10 min). The detection was performed with the enhanced chemiluminescent method, based on the peroxidase-catalyzed oxidation of luminol. Before, 1 ml of a 1:1 mixture of detection reagent A and B was used for each membrane. By exposure of the membrane to an appropriate chemiluminescent sensitive film, each protein antigen was visualized by a specific band. The molecular weights of the proteins were identified by comparing the protein bands with standards containing proteins of known size.

2.7 Histological methods

2.7.1 Paraffin sectioning of pancreatic mouse tissue

Reagents

1 x PBS, pH 7.4

Cellfix:

	Stock	100 ml	[c]
Formaldehyde	37%	5.4 ml	2%
Glutaraldehyde	25%	0.4 ml	0.2%

Add 1 x PBS, pH 7.4 to 100 ml

Paraformaldehyde solution:

	MW [g/mol]	100 ml	[c]
PFA	100%	4 g	4%

Dissolve in 1 x PBS at 60°C

Formaldehyde solution:

	Stock	100 ml	[c]
Fromaldehyde	37%	10 ml	3.7%

Add 1 x PBS, pH 7.4 to 100 ml.

Paraplast embedding medium

EtOH (50%, 60%, 70%, 80%, 90%, 95% in ddH$_2$O, and 100%)

EtOH – Toluol 1:1

Toluol

Protocol

Experimental animals were sacrificed by cervical dislocation and the abdominal wall was opened with scissors. The pancreas was dissected via the papilla of vateri. Therefore, surgical clamps disconnected the papilla vateri, and 2 ml cellfix, formaldehyde or PFA were injected through the bile duct into the pancreas. The fixed tissue was removed with scissors and transferred to a reaction tube. The pancreas was incubated in the same fixative for an additional 1 h (cellfix and formaldehyde) or 3 h (PFA) at RT. After 3 washing steps in 1 x PBS, each for 1 h at RT, the tissue was dehydrated successively in an alcohol series with increasing concentrations of EtOH (50%, 60%, 70%, 80%, 90%, 95%) at RT. If not mentioned otherwise the respective incubation steps were 1 h. The dehydration was completed by in 100% EtOH (3 x 20 min), 30 min incubation in

EtOH (100%): Toluol 1:1, and 100% Toluol (3 x 20 min). The tissue was passed through 3 changes of molten paraffin (60°C) in a tissue-processing cassette for at least 1 h each. Finally, the material was embedded in molten paraffin on an embedding system that combines cassettes and rings. The paraffin blocks were stored at RT until further usage.

To perform histological analysis, the pancreas was cut in serial sections of 8 μm thickness. The sections were transferred to a clean water bath with distilled water, and mounted on poly-L-lysine coated slides. Before further processing the sections were allowed to dry at 37°C over night in an upright position in order to facilitate adhesion between sections and the charged glass surface.

For immunohistochemistry stainings (2.7.3) the slides were deparaffinized in Toluol for 2 x 5 min, and then rehydrated in a descending series of alcohol (100%, 90%, 70%, and 50%) for 5 min, respectively. Finally, sections were washed with 1x PBS.

2.7.2 β–D-galactoside (X-Gal) staining

Reagents

X-Gal (5-Bromo-4-chloro-3-indolyl β–D-galactoside) 40 mg/ml in 100% dimethyl sulfoxide (DMSO)

X-Gal staining solution:

	MW [g/mol]	250 ml	[c]
Potassium hexacyanoferrate (III)	329.26	0.42 g	2.5 mM
Potassium hexacyanoferrate (Schmidt et al.) trihydrate	422.39	1.07 g	2.5 mM
MgCl$_2$ (1M)	203.30	1.0 ml	2.0 mM

Add X-Gal (1 mg/ml) to staining solution

Protocol

For analyzing the recombination efficiency of the Gluc-Cre transgene, the Gluc-Cre mice were crossed with the R26R Cre reporter mouse strain. The Cre-mediated recombination pattern was visualized by a β-galactosidase staining. Therefore, islets were isolated as described before (2.4) and fixed for 1 h in cellfix after over night culture. After 3 washing steps in 1 x PBS isolated islets were incubated in X-Gal staining solution over night at RT. The next day tissues were passed through 3 changes of 1 x PBS to intense the blue staining and remove residual X-Gal staining solution. Finally, whole mount digital pictures were taken.

To examine the recombination pattern statistically whole islets were dispersed into single cells and cultured over night on plastic cover slips in a 24-well plate. The next day, fixation in cellfix, washing and incubation steps were performed as described above. Then, the number of all cells and the

number of X-gal positively stained cells were counted. Finally, the ratio of blue stained cells to the whole number of cells was calculated.

2.7.3 Immunohistochemistry

Reagents

1 x PBS, pH 7.4

Permeabilization solution:

	250 ml	[c]
Triton-X 100	0.75 ml	0.3%

Add 1 x PBS pH 7.4 to 250 ml

Peroxidase blocking solution:

	stock	10 ml	[c]
Methanol	100%	2 ml	20%
H_2O_2	30%	1 ml	3%

Add 1 x PBS pH 7.4 to 10 ml

Antigen retrieval solution:

	1 l	[c]
Tri-sodium citrate • $2H_2O$	2.94 g	10 mM

Add ddH$_2$O to 1 l. Adjust pH to 6.0 with HCl$_{conc}$

Serum-PBS blocking solution:

	50 ml	[c]
Normal goat serum (NGS)	750 µl	1.5%

Add 1 x PBS pH 7.4 to 50 ml

Biotinylated secondary antibody 1:200 in Serum-PBS blocking solution

ABC solutions

Vectastain alkaline phosphatase (ABC-AP) standard kit

Vectastain peroxidase (ABC-Peroxidase) elite standard kit:

	10 ml
Reagent A (Avidin DH)	100 µl
Reagent B (Biotinylated enzyme)	100 µl

Add 1 x PBS pH 7.4 to 10 ml. Incubate 30 min before use in the dark.

Vectastain alkaline phosphatase and peroxidase (elite) standard kits contain reagent A and B.

3,3'-diaminobenzidine tetrahydrochloride (DAB) stock solution:

	50 ml	[c]
DAB	50 mg	0.1%

Add 1 x PBS pH 7.4 to 50 ml

DAB staining solution:

	Stock	10 ml	[c]
DAB	0.1%	5 ml	0.05%
H_2O_2	30%	10 µl	0.03%

Add 1 x PBS pH 7.4 to 10 ml

Tris-Cl pH 8.0:

	MW [g/mol]	250 ml	[c]
Tris-Cl	121.14	3.03 g	100 mM

Add ddH$_2$O to 250 ml. Adjust pH to 8.0 with HCl$_{conc}$

Alkaline phosphatase substrate III:

	5 ml
Vector Blue Substrate solution reagent 1	100 µl
Vector Blue Substrate solution reagent 2	100 µl
Vector Blue Substrate solution reagent 3	100 µl

Add 100 mM Tris-HCl to 5 ml

Fluorescence-labeled secondary antibodies (see Appendix)

Aquatex mounting medium (VWR)

Permafluor mounting medium (Beckmann Coulter)

Protocol

Immunohistochemistry refers to the process of localizing proteins in cells of tissue sections by the use of antibodies that bind specific antigens in the cells. To examine the expression pattern of different proteins in islets, an indirect method was used. Antigen-antibody complexes were detected by biotinylated secondary antibodies, which were bound to alkaline phosphatase or peroxidase-coupled-avidin-complexes. Since the two enzymes can catalyze a color-producing reaction by the addition of respective substrates the complexes can be visualized. In detail, fixed paraffin embedded slices were deparaffinized, rehydrated as described before (2.7.1), and then washed in 1 x PBS. After that, slices were incubated in permeabilization solution for 30 min. Additionally, for the detection of cGKI, antibody-binding sites (epitopes) were unmasked by an

additional incubation step in antigen retrieval solution for 15 min., followed by a heating step at maximal power in a microwave for 2 min. Then, slices were allowed to cool down for another 15 min in the solution. To remove the antigen retrieval solution completely, slices were passed through 3 changes of 1 x PBS and surrounded with a fat pen. For peroxidase performed staining, unspecific peroxidase binding sites were blocked with peroxidase blocking solution for 10 min, followed by 3 washing steps in 1 x PBS. To block unspecific antibody binding sites, slices were incubated in serum PBS blocking solution for 1 h, before the diluted primary antibodies were applied (for dilutions of primary antibodies please see Appendix page 78). Slices were incubated over night in primary antibody solution. The next day, an additional incubation step in primary antibody dilutions followed for 1 h at RT. After removal of the primary antibody solutions, slices were passed through 3 changes of serum PBS blocking solution before biotinylated secondary antibodies were added for 1 h at RT (for dilutions of secondary antibodies please see Appendix page 79). During this incubation step, the Avidin-biotinylated-enzyme-complex (ABC) solutions were prepared and preincubated 30 min in the dark. After three more washing steps in 1 x PBS, the peroxidase or alkaline phosphatase ABC working solutions were applied for additional 30 min incubation in the dark. The slices were passed through 3 changes of 1 x PBS before the visualization of the antigen-antibody complexes was carried out. For that purpose, the DAB staining solution or alkaline phosphatase substrate III for peroxidase or alkaline phosphatase were added respectively. Brown (DAB) or blue (alkaline phosphatase substrate III) staining was finished after 5 to 40 min depending on the antigen, and stopped by a final washing step in 1 x PBS. Finally, slices were mounted in Aquatex mounting medium.

For co-localization experiments secondary antibodies labeled with fluorescent dyes were applied. Therefore, pancreatic tissue sections were processed as described (see above) followed by an over night incubation in the first primary antibody dilution (for primary antibody dilutions please note Appendix page 78). The next day, the primary antibody was removed and the sections were passed through 3 changes of 1 x PBS. Again, unspecific binding sites were blocked with serum-PBS blocking solution for 1 h at RT. Then, the second primary antibody was added and incubated over night at 4°C. Next, sections were passed through 3 changes of 1 x PBS, then incubated with the fluorescent labeled secondary antibodies for 1 h at RT in the dark. The secondary fluorescent antibodies were diluted in 1 x PBS as listed in the Appendix. The secondary antibodies were discarded, sections washed 3 times in 1 x PBS, and mounted with Permafluor to shield and intensify the fluorescence. Finally, sections were kept at 4°C until digital pictures were taken with a confocal laser scanning microscope (LSM 510, Zeiss).

2.8 Experiments on glucose homeostasis

2.8.1 *In vivo* experiments

Reagents

Aprotinin (Roche):

	MW [g/mol]	50 ml	[c]
Aprotinin	6500	0.5 mg	10 µM

Dissolve in 50 ml ddH$_2$O

Aprotinin working solution (1 µM)

Glucose solution:

	MW [g/mol]	20 ml	[c]
D-glucose	180.2	4 g	200 mM

Ad 20 ml ddH$_2$O.

Insulin:

	Stock	10 ml	[c]
Insulin	100 U/ml	4 µl	40 U/ml

Ad 10 ml sterile 0.9% NaCl.

Protocol

The *in vivo* glucose homeostasis was investigated by glucose and insulin challenges. Before the particular *in vivo* experiments were performed, the animals were fasted over night. Therefore, the mice were put into bedding free clean cages with a drinking possibility. After 12 h fasting, and during glucose and insulin tolerance tests blood glucose levels were measured with an Ascensia Elite Sensor (Bayer). Each mouse received a definite dose of insulin or glucose in relation to its body weight. For the determination of serum insulin and glucagon levels blood samples were taken by tail bleeding at different time points during the tolerance tests. The blood samples were collected in reaction tubes, 1 µl aprotinin was added, and put on ice until clotting.

To extract the blood serum from blood plasma, samples were centrifuged at 2,000 xg for 10 min at 4°C. The sera were transferred to new reaction tubes, and stored at -20°C until the samples were analyzed using the Mouse endocrine Lincoplex kit (Millipore).

2.8.1.1 Glucose tolerance test

To determine the glucose clearance from the blood glucose tolerance tests were carried out. After 12 h fasting, each mouse received 2 mg glucose per g body weight by oral or intra peritoneal (i.p.) application. Blood glucose levels were measured 5, 15, 30, 60, and 120 minutes after the application, and blood samples were taken as described before (2.8.1).

2.8.1.2 Insulin tolerance test

The insulin tolerance test (ITT) provides information on the functionality of the insulin receptor is working. Insulin was administered i.p. and the fall in plasma glucose was recorded for the determination of the dynamic insulin sensitivity. Mice received 0.5 mU insulin per g body weight. Blood sugar levels were determined 30, 60, 90, 120, and 180 minutes after application, and blood samples were taken simultaneously.

2.8.2 Determination of serum insulin, leptin, and glucagon

Reagents

Mouse endocrine Lincoplex kit (Millipore)

Protocol

The principle of the Mouse Endocrine Lincoplex kit is based on fluorescent coded beads. Each bead carries a specific fluorescent-labeled antibody on its surface. The antibody binds to its specific antigen in the serum. In a second incubation step streptavidin-phycoerithrin labeled reporter tags bind also on the surface of the beads. Next, the samples were analyzed by two lasers. One of them detects the quantity of the bound endocrine; the other one recognizes which endocrine is measured. The respective concentrations are determined in relation to defined standard curves. The whole procedure was performed as described in the handbook enclosed to the Lincoplex kit. The 96-well plates were analyzed in a Bioplex machine at the Helmholtz Zentrum für Molekulare Immunologie, München. The data were analyzed in Microsoft Excel, and significances were determined by t-tests.

2.8.3 Hormone secretion experiments

Reagents

Krebs buffered HEPES solution (KBHS):

	MW [g/mol]	stock	100 ml	[c]
NaCl	58.44	1 M	12 ml	120 mM
KCl	74.56	1 M	0.47 ml	4.7 mM
$CaCl_2$	110.01	0.1 M	2.5 ml	2.5 mM
KH_2PO_4	136.09	0.1 M	1 ml	1 mM
$MgSO_4$	120.4	0.1 M	1.2 ml	1.2 mM
HEPES	238.31		0.238 g	10 mM
$NaHCO_3$	84.01		0.168 g	20 mM
D-glucose • H_2O	198.17		0.396 g	20 mM

Ad ddH_2O to 100 ml and 0.5 mg/ml BSA and adjust pH to 7.45 with NaOH.

Acid alcohol: EtOH H_2O HCl 52:17:1

Protocol

To analyze the glucagon released from pancreatic A-cells hormone secretion experiments on isolated islets were performed. For that purpose, islets were isolated and cultured as described before (2.4). The next day, islets were passed through three changes of 5 mM glucose in KBHS to remove residues of fetal calve serum supplemented to the islet culture medium. Batches of 20 isolated islets were incubated for 1 h in 200 µl 1 mM glucose/KBHS at 37°C and 5% CO_2. Next, islets were allowed to sediment, then the supernatant containing the hormones released under this low (unphyiological) conditions was collected in new reaction tubes and stored at -20°C until further usage. The islets were incubated in a second step in unphysiological (1 mM), basal (6 mM), or high (20 mM) glucose concentrations added to the KBHS for 30 min at 37°C and 5% CO_2. Again, islets were allowed to sediment, and the supernatant was transferred to new reaction tubes for storage at -20°C until analysis of the samples by Radioimmunoassays was performed. Finally, 200 µl ice-cold acid alcohol were added to the islets for the extraction of glucagon from the islets, thus allowing the determination of the mean glucagon content. Islets were as well stored at -20°C until further analysis.

2.8.4 Radioimmunoassay for glucagon

To determine the glucagon secreted from islets during hormone secretion experiments radioimmunoassays for glucagon were carried out. In general, for the determination of mean total glucagon contents in the batches of 20 islets, islets in acid alcohol were centrifuged, and

supernatants were diluted 1:50 in KBHS. Supernatants, collected during the hormone secretion experiments (at 1, 6, and 20 mM glucose) and those for determination of whole glucagon content were diluted 1:4 in KBHS solution and incubated with 100 µl glucagon antibody over night at 4°C. The next day 100 µl radioactive labeled glucagon was added to the reaction tubes and incubated over night at 4°C. Next, a precipitating reagent was added to precipitate complexes of glucagon and the respective antibody. The complexes were sedimented by centrifugation for 20 min at 2,000 xg, and the supernatant was discarded. The remaining radioactivity in the air-dried pellet was measured in a gamma counter, and glucagon concentrations calculated in comparison to definite standards delivered within the RIA kit (Linco). Data were analyzed in Microsoft Exel, and significances were determined by t-tests.

3 Results

3.1 Recombination analysis of the Gluc-Cre mice

To analyze the recombination efficiency and pattern of the Gluc-Cre mouse line (Herrera, 2000), transgenic animals were crossed to a Cre reporter mouse line that carries the ROSA26 β-gal allele (Soriano, 1999). In the offspring, the expression of active Cre mediates the excision of a floxed polyadenylation sequence. This intervening DNA sequence inhibits the expression of LacZ in the absence of Cre. Accordingly, the activity of Cre correlates with the expression of LacZ, which can be demonstrated by X-Gal staining for β-gal activity. Figure 8A shows X-gal stainings of isolated pancreatic islets from Gluc-Cre; Rosa26 β-gal reporter mice. The blue staining was restricted to a subset of cells that localized to the mantle of the islets. In comparison to glucagon and insulin specific stainings of islets (Fig. 8B), only the glucagon positive cells in the islet periphery corresponded to the blue stained cells (Fig. 8A). These data indicated that Cre expressed under the control of the glucagon promotor was indeed only active in glucagon secreting A-cells.
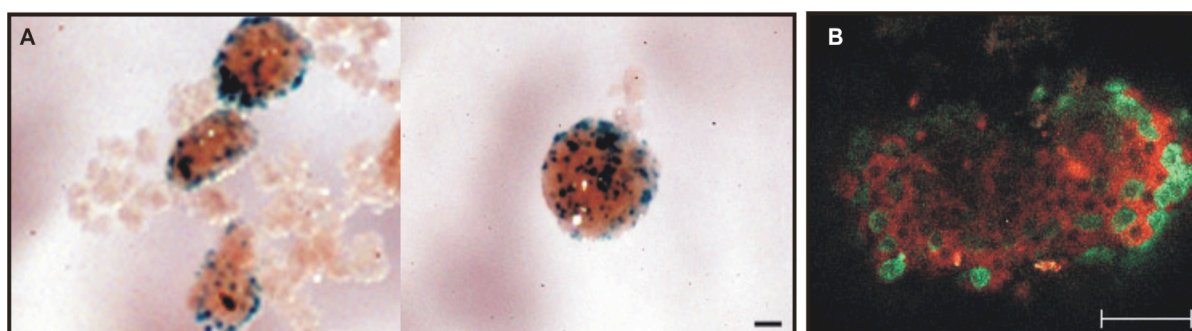

Fig. 8: Gluc-Cre is highly effective in pancreatic A-cells. (A) X-gal staining of whole pancreatic islets from Gluc-Cre; ROSA26 β-gal reporter mice. Blue cells indicate Cre-mediated recombination that was only detectable in the islet periphery. (B) Immunofluorescence analysis of whole pancreatic islet using specific antibodies to detect insulin (red) – and glucagon (green), respectively. Scale bars, 50 μm.

To define the recombination efficiency a statistical analysis of X-gal stained cells compared to total islet cells was performed (Fig. 9). Therefore, whole islets were dispersed into individual cells and counted. In total, 172 ± 23 cells were isolated per islet. A small fraction of 27 ± 4 cells was X-gal positive (n=8). Hence, 15.7% of dispersed islet cells were stained blue. Indeed, it is assumed that 15 to 20% of murine islet cells are glucagon-producing A-cells (Baetens et al., 1979).

Thus, the X-gal stainings of islets correspond well with the recombination efficiency and the number of A-cells, and makes the Gluc-Cre mouse line an ideal genetic tool to delete specific genes in pancreatic A-cells, and to analyze the outcome of the cell-specific loss of function of the gene of interest.
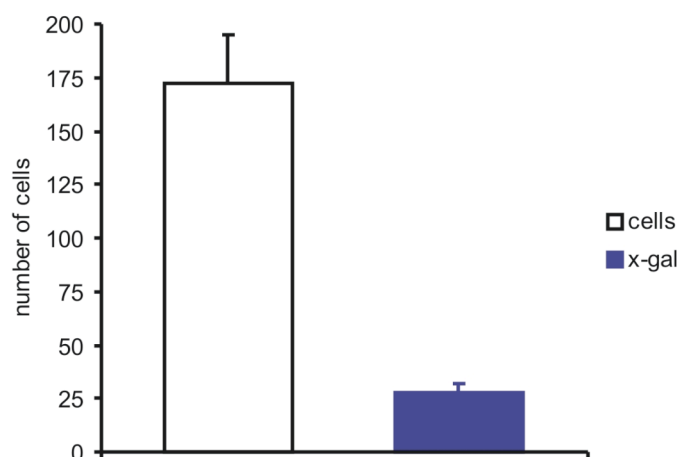
Fig. 9: Statistical analysis of the recombination efficiency of Gluc-Cre; ROSA26 β-gal reporter mice. 27 ± 4 cells of 172 ± 23 cells showed the typical blue staining indicating β-gal activity analyzed from 8 different islets.

3.2 Expression of Na$_V$1.7 in A-cells of Langerhans

In pancreatic islets the expression of Na$_V$1.3 and Na$_V$1.7 sodium channels have been shown (Vignali et al., 2006). Previous single-cell RT-PCR analysis suggested that Na$_V$1.7 is the dominant isoform in pancreatic islets (Vignali et al., 2006).
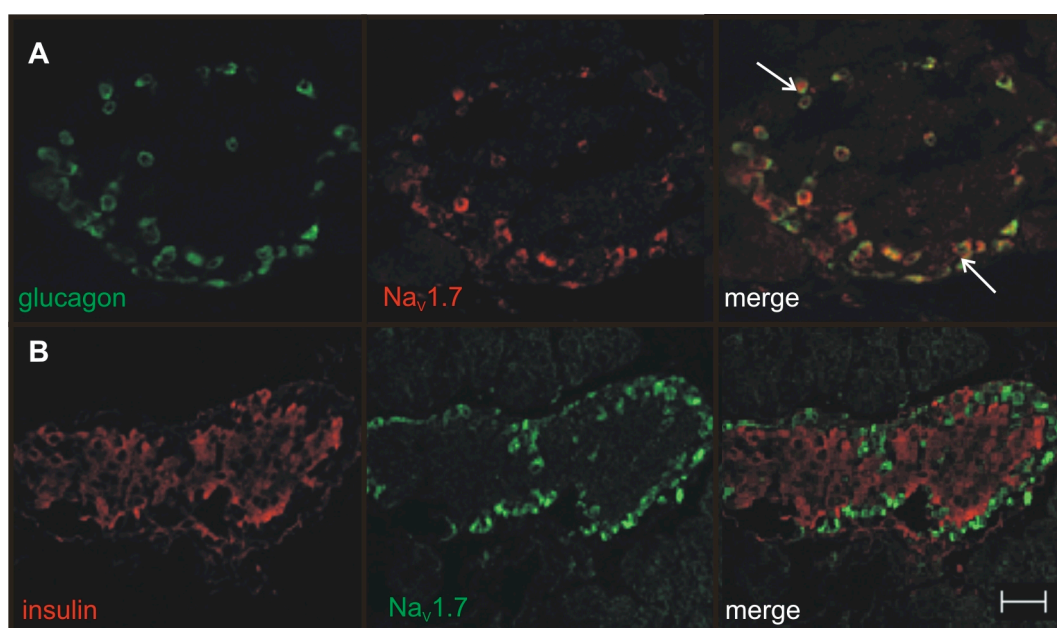

Fig. 10: Expression analysis of Na$_V$1.7 in pancreatic islets. (A) Primary antibody complexes with glucagon and Na$_V$1.7 protein were detected by using FITC-coupled (green) and Cy3-labeled (red) secondary antibodies, respectively. Merged picture shows yellow cells, indicating the co-localization of Na$_V$1.7 and glucagon in the mantle of the islet. (B) Insulin (red) was stained with Cy-3 labeled secondary antibodies. Na$_V$1.7 was detected with FITC-labeled secondary antibodies. No co-localization of Na$_V$1.7 with insulin was detectable (merge). Scale bar, 20 µm.

To analyze in more detail the expression pattern of Na$_V$1.7 immunohistochemical analysis were performed. Figure 10 shows that the expression of Na$_V$1.7 is restricted to a small part of the

pancreatic islets mainly localized in cells of the mantle (Fig. 10A, 10B middle). Further, immunofluorescence experiments using Na$_V$1.7 and glucagon specific antibodies showed clear co-localization of the sodium channel and glucagon (Fig. 10A merge), whereas no co-localization of Na$_V$1.7 was detectable with cells stained positively for insulin (Fig. 10B merge).

The histological data indicates that Na$_V$1.7 is mainly expressed in A-cells of pancreatic islets.

3.2.1 Conditional deletion of Na$_V$1.7 in A-cells of Langerhans

The function of Na$_V$1.7 in A-cells in general and its contribution to the release of glucagon is unknown. To get an idea of its specific role in A-cells, Na$_V$1.7 was conditionally deleted in glucagon-secreting cells. Therefore, floxed Na$_V$1.7 mice were crossed to the Gluc-Cre mouse line. In heterozygous and homozygous offsprings, Cre mediated the excision of the loxP-flanked exons 14 and 15 encoding the part of domain II, which is the essential pore forming alpha subunit (please consult chapter 1.3) (Nassar et al., 2004), of the Na$_V$1.7 gene resulting in the A-cell specific Na$_V$1.7 knockout (Na$_V$1.7^{Acko}). Two different strategies were used to analyze the successful deletion of Na$_V$1.7 in A-cells. First, RT-PCRs were performed with specific primers, which should demonstrate the excision of exons 14 and 15 on mRNA level. Second, immunohistochemical analysis with Na$_V$1.7 specific antibodies were carried out to verify the knockout of Na$_V$1.7 on protein level.

For RT-PCR analysis mRNA was isolated from islets of control (genotype: Gluc-Cre$^{+/tg}$; Na$_V$1.7$^{+/L2}$) and knockout (genotype: Gluc-Cre$^{+/tg}$; Na$_V$1.7$^{L2/L2}$) animals. Different primer pairs were used, which specifically bind to the Na$_V$1.7 mRNA in the vicinity and/or within the floxed Na$_V$1.7 exons (Fig. 11). As expected, no PCR product was detectable in islets of the A-cell specific Na$_V$1.7 knockout mice by using the primer pair B that binds within the deleted exons (Fig. 11B). Surprisingly, no amplicon (expected length: 273 bp) of the Na$_V$1.7 mRNA was detectable by the use of primer pair C (Fig. 11C) flanking the excision locus. Similar results were found in knockout animals using primer pair D (expected length: 285 bp) (Fig. 11D). In contrast, in islets isolated from control animals, as well as in dorsal root ganglia (DRGs) extracted from A-cell specific Na$_V$1.7 mice, which were used as a positive control for the expression of Na$_V$1.7, the predicted amplicons had the correct size (398bp; 686 bp; 698 bp) (Fig. 11B, 11C, 11D). Furthermore, HPRT amplification worked in control and knockout islets. These results show that Na$_V$1.7 mRNA is already intrinsically degraded in knockout islets. The deletion of Na$_V$1.7 is A-cell specific, since DRG of A-cell specific Na$_V$1.7 knockout mice still express the Na$_V$1.7 mRNA. Above all, Na$_V$1.7 is only expressed in A-cells, because in knockout islets no amplicons were detectable.
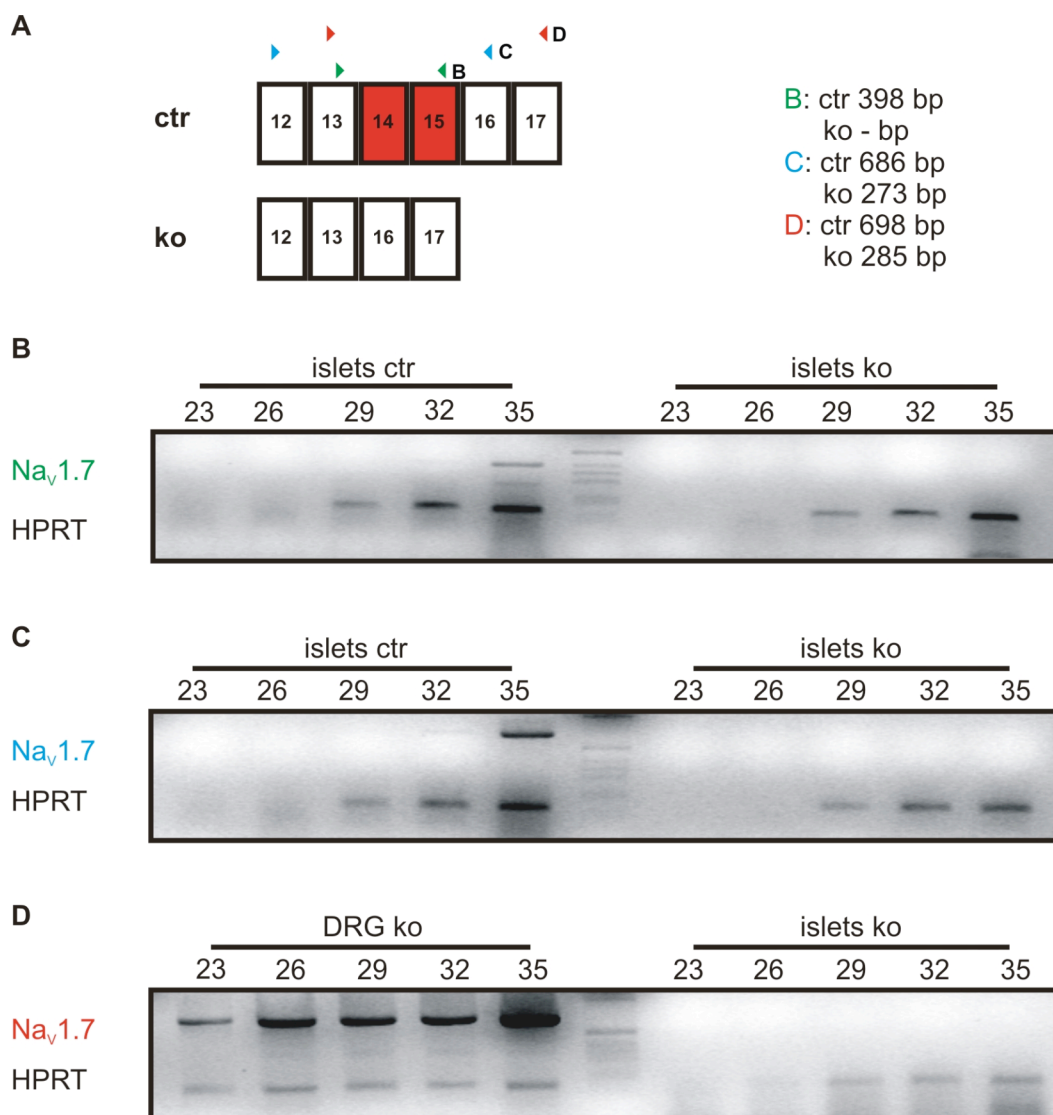
Fig. 11: Semi-quantitative RT-PCR analysis with Na$_V$1.7 specific primer pairs in wt and Na$_V$1.7^{Acko} in DRGs and islets. (A) Primer strategy for the detection of control and recombinant Na$_V$1.7 mRNA. (B) PCR products amplified with primer pair B resulting in a 398 bp amplicon only in control islets. (C) PCR product amplified with primer pair C resulting in a 686 bp amplicon only in control islets. The predicted recombinant 273 bp amplicon in the Na$_V$1.7^{Acko} islets was not detectable (see text for further explanation). (D) PCR product amplified with primer pair D resulting in a 696 bp amplicon only in DRGs isolated from Na$_V$1.7^{Acko} mice. No recombination is detectable in DRG indicating the specificity of the Na$_V$1.7^{Acko} mice. HPRT was co-amplified in every PCR reaction as an internal standard.

Although, RT-PCR analysis showed the complete loss of Na$_V$1.7 in Na$_V$1.7^{Acko} A-cells, the most important criteria of a functional gene deletion is the ablation of the protein itself within the tissue of interest. In line with the RT-PCR results, immunohistochemistry analysis using Na$_V$1.7 specific antibodies revealed a positive staining of control islet cells, whereas Na$_V$1.7^{Acko} islet cells were completely unstained (Fig. 12).
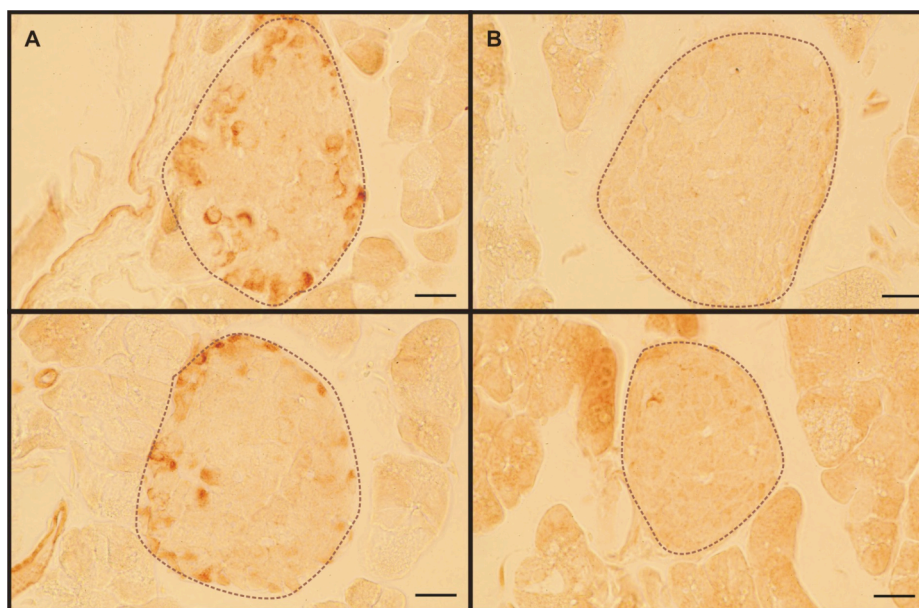
Fig. 12: Immunohistochemical analysis of $Na_V1.7$ in pancreatic islets. (A) The $Na_V1.7$ protein was detectable in control islet cells only in the mantle of the islets by detection of $Na_V1.7$ with specific $Na_V1.7$ antibodies. (B) No positive staining of $Na_V1.7$ was detectable in islets of $Na_V1.7^{Acko}$ mice. For better illustration a white line was introduced to indicate the islets perimeter. Scale bars, 20 μm.

These data prove that islet $Na_V1.7$ is indeed expressed exclusively in A-cells and that the functional expression of $Na_V1.7$ protein was completely abolished in the $Na_V1.7^{Acko}$ mice.

3.2.2 Electrophysiological experiments of sodium channels in control and $Na_V1.7^{Acko}$ islet cells

Two types of TTX-sensitive sodium channels were characterized in islet cells by their different voltage dependency. In B-cells the voltage-dependent sodium current is only exhibited at hyperpolarized holding potentials (Gopel et al., 2004; Leung et al., 2005; MacDonald et al., 2007; Vignali et al., 2006). In contrast, A-cells express a prominent TTX-sensitive sodium current, which is activated and measurable at physiological membrane potentials in intact islets (Barg et al., 2000; Gopel et al., 1999; Leung et al., 2005; MacDonald et al., 2007).

The voltage dependence of a given current can be determined by a steady-state inactivation protocol. Increasing parts of the current are inactivated by a step-wise increase of a prepulse followed by a consistent test pulse. The voltage at which 50% of the current are inactivated by the prepulse is called $V_{0.5}$. A differentiation of the sodium currents by their typical inactivation pattern (Fig. 13C) revealed both, the residual as well as the early inactivating sodium current in control islets. 43% of the cells had the detectable early inactivating sodium current with a mean value of $V_{0.5}$ at -111 mV. Thus, sodium channels most likely expressed in B-cells. The residual current ($V_{0.5}$ = -43 mV) was measured in 23% of the control cells. Therefore supposed to be expressed in A-cells (Fig. 13C). In contrast to control cells, in $Na_V1.7^{Acko}$ cells only the early inactivating sodium current was detectable, with a mean value of $V_{0.5}$ at -111 mV (Fig. 13D). Compared to control cells

the amount of $Na_V1.7^{Acko}$ cells expressing the early inactivating current was unchanged (38%), whereas the number of cells with residual current decreased to 8% (Fig. 13B). Furthermore, in control islets, the majority of cells had a sodium current (81%), whereas in $Na_V1.7^{Acko}$ islets the majority (54%) of cells lacked a sodium current (Fig. 13A). These results support the notion, that $Na_V1.7$ is especially expressed in islet A-cells and can be deleted in $Na_V1.7^{Acko}$ mice.

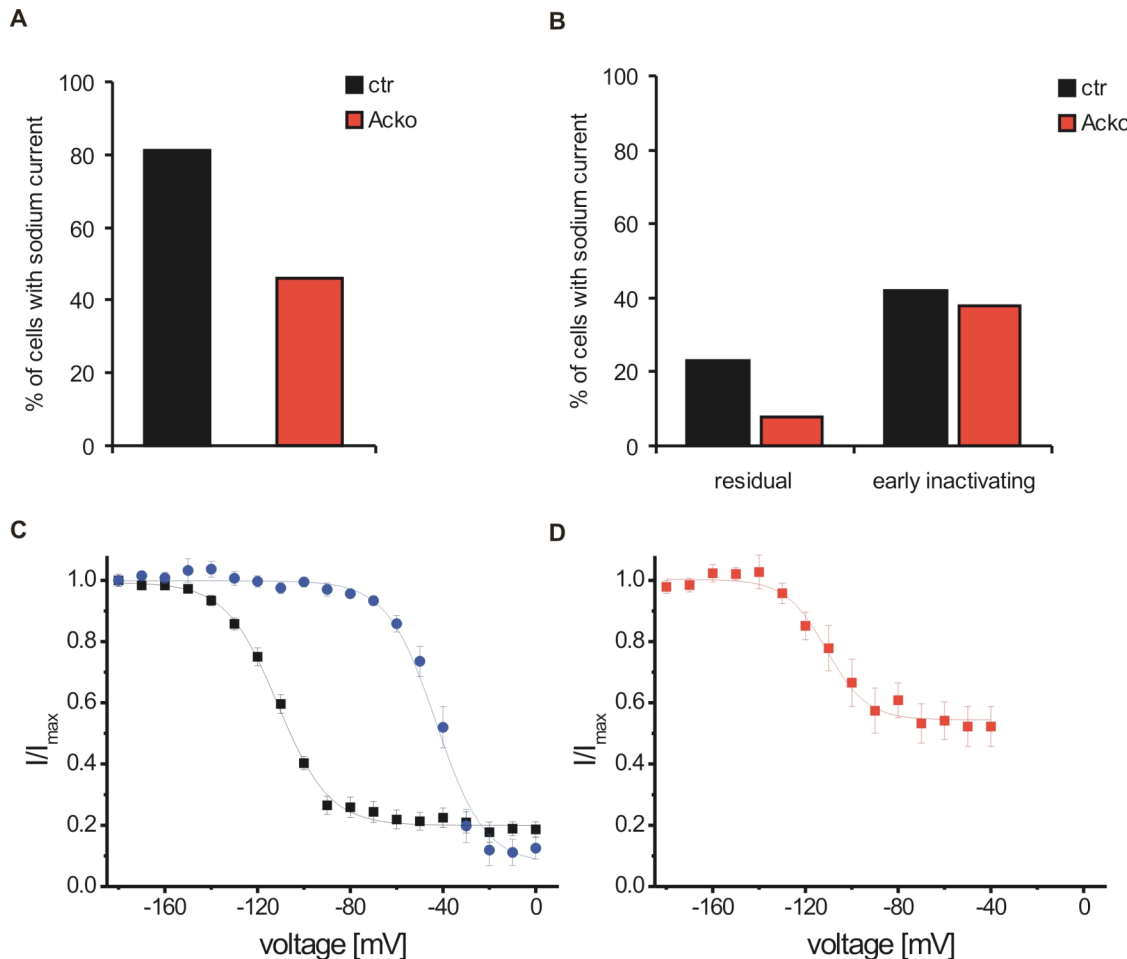**Fig. 13: Statistical analysis and steady-state inactivation of sodium currents in whole islets of control and $Na_V1.7^{Acko}$ islet cells.** (A) In $Na_V1.7^{Acko}$ (ko) islets (n=13) significantly less islets had a detectable sodium current compared to control (ctr) islets (n=31); (B) Statistical distribution of residual and early inactivating sodium currents in control (ctr) and $Na_V1.7^{Acko}$ (Acko) islets. (C) Steady-state inactivation was measured in control islets. Early inactivating (■) (n = 15) and the residual (•) (n = 7) sodium currents were detected with $V_{0.5}$ = -111 mV and $V_{0.5}$ = -43 mV. (D) Steady-state inactivation was measured in $Na_V1.7^{Acko}$ islets. Only the early inactivating (■) (n = 9) current was detectable with $V_{0.5}$ = -111 mV. Please note, no residual current was detectable in $Na_V1.7^{Acko}$ cells. Results are means ± S.E.M. The data was fitted by the Boltzmann equation. The continuous curve represents the averaged Boltzmann fit.

The primary characterization of $Na_V1.7$ in pancreatic islets revealed the expression of this sodium channel subtype mainly in pancreatic A-cells, whereas $Na_V1.7$ knockout islets failed to express the respective channel specifically in A-cells.

3.2.3 Glucagon secretion in $Na_V1.7^{Acko}$ islets

To analyze the role of the $Na_V1.7$ isoform on glucagon secretion hormone secretion experiments were performed. Isolated islets from control and knockout animals were exposed to low (1 mM) and high (20 mM) glucose concentrations (Fig. 14).

Under low glucose conditions, control as well as knockout islets released glucagon to the same amount (ctr 4.20 ± 0.7 pg/islet/h (n=5); ko 4.27 ± 0.7 pg/islet/h (n=7)). As expected, the exposure to high glucose conditions reduced the glucagon release of control islets (ctr 1.29 ± 0.3 pg/islet/h (n=5)). In contrast, in isolated $Na_V1.7^{Acko}$ islets the glucose-induced inhibition of glucagon release was abolished. In particular, the glucagon release was unchanged and comparable to the release rates at low glucose conditions ($Na_V1.7^{Acko}$ 4.85 ± 0.4 pg/islet/h (n=7)).
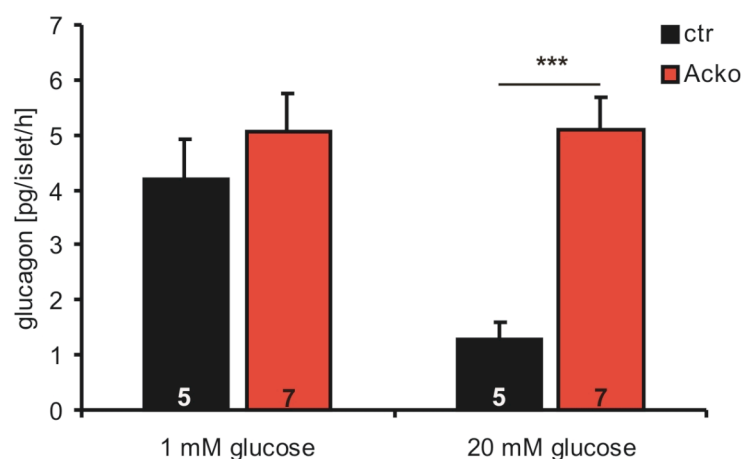

Fig. 14: Glucagon secretion of isolated islets of control and $Na_V1.7^{Acko}$ islets. Islets of control (ctr; black) and $Na_V1.7^{Acko}$ (Acko; red) were exposed to low (1 mM) or high (20 mM) glucose for 1 h. Glucagon secretion was reduced to 30% in control islets in high glucose conditions (20 mM), whereas $Na_V1.7^{Acko}$ islets were not able to downregulate glucagon release. Data was pooled from islets of 5 control and 7 $Na_V1.7$ knockouts (***; p < 0.001).

Thus, the *in vitro* hormone secretion experiments demonstrated that the specific deletion of $Na_V1.7$ in pancreatic A-cells had a functional consequence for the glucagon release at high glucose concentrations *in vivo*. The collected data suggests that the $Na_V1.7$ is perhaps an inhibitor of glucagon release.

3.2.4 Glucose homeostasis in $Na_V1.7^{Acko}$ mice

To investigate, whether the *in vitro* recognized deregulation of glucagon secretion of islets lacking $Na_V1.7$ in pancreatic A-cells had any consequences *in vivo*, the fasting blood glucose levels were determined in control and $Na_V1.7^{Acko}$ mice (Fig. 15A). In addition, an oral glucose tolerance test was performed to test the glucose clearance from the blood (Fig. 15B). Compared to control animals, in $Na_V1.7^{Acko}$ mice neither their fasting blood glucose levels (ctr 63.3 ± 2.5 mg/dl; $Na_V1.7^{Acko}$ 64 ± 1.5 mg/dl) nor their glucose clearance during glucose challenge showed any

differences. As in control animals, glucose treatment increased blood glucose levels in $Na_V1.7^{Acko}$ mice to a maximum value detectable 15 minutes after oral application (ctr 213.3 ± 8.8 mg/dl (n=4); $Na_V1.7^{Acko}$ 208.2 ± 7.0 mg/dl (n=5)). Both genotypes were able to counter-regulate their blood sugar levels within 120 minutes in a similar manner (ctr 115.3 ± 4.6 (n=4); $Na_V1.7^{Acko}$ 130.0 ± 5.0 mg/dl (n=5)).
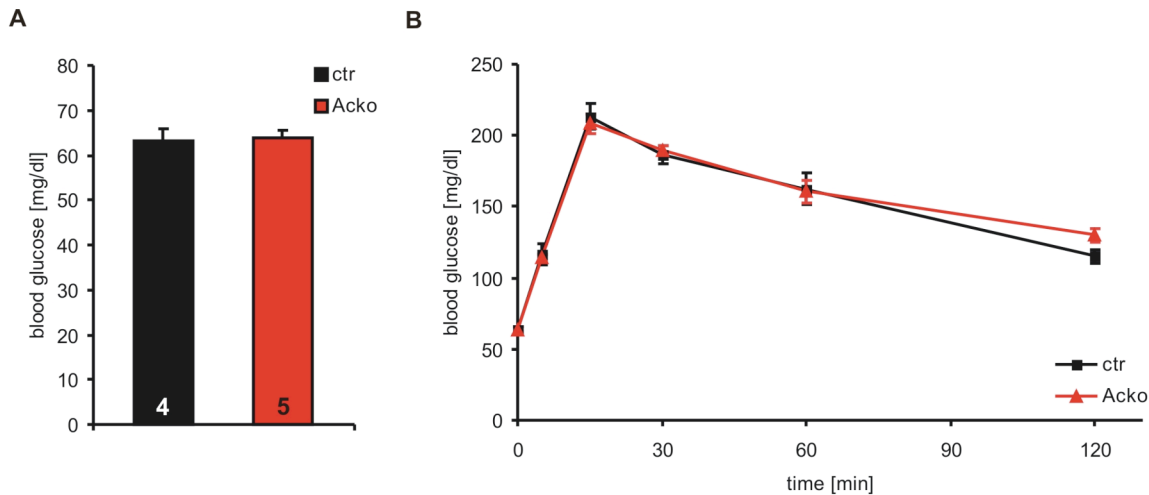

Fig. 15: Glucose homeostasis in $Na_V1.7^{Acko}$ versus control mice. (A) Basal blood glucose levels determined from 15-20 week old $Na_V1.7^{Acko}$ (Acko) and control (ctr) mice. (B) Time courses of blood glucose levels during oral glucose tolerance test in $Na_V1.7^{Acko}$ (Acko) (n=5) and control (ctr) (n=4) mice.

These data suggest that after exogenous glucose treatment glucose handling is normal in $Na_V1.7^{Acko}$ mice.

3.3   Expression of cGKI in pancreatic islets of Langerhans

The cGKI belongs to the serine/threonine kinases and is involved in many physiological processes (Hofmann, 2005). Immunoblot analysis revealed the expression of cGKI in pancreatic islets of control mice (genotype: cGKI$^{+/L1}$). In contrast in cGKI$^{-/-}$, cGKIα (genotype: SM22$^{+/Iα}$; cGKI$^{-/-}$), and cGKIβ (genotype: SM22$^{+/Iβ}$; cGKI$^{-/-}$) rescue animals no cGKI protein was detectable (Fig 16).
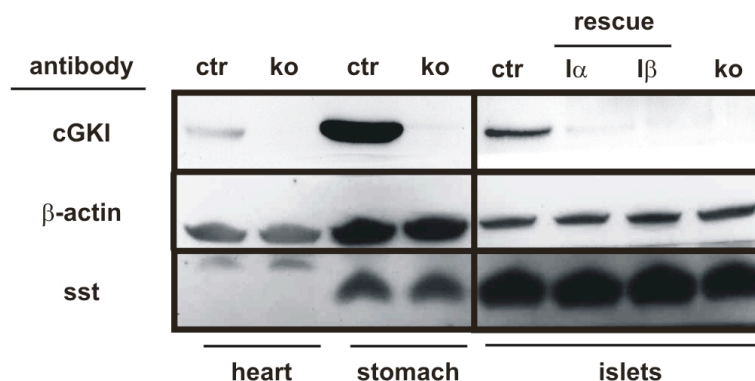

Fig. 16: Immunoblot analysis of cGKI expression in islets of Langerhans. The cGKI prtoein was expressed in islets of control (ctr) animals, but not in cGKI$^{-/-}$ (ko), cGKIα (Iα), and cGKIβ (Iβ) rescue mice. As positive and negative controls

for the endogenous expression of cGKI, protein lysates from control (ctr) and cGKI$^{-/-}$ (ko) stomach and heart are shown. Equal loading of the gel within the corresponding lysates was demonstrated by detecting β-actin., the somatostatin (sst) protein was detected as a marker of pancreatic islets by the use of specific antibodies.

Immunohistochemical analysis support the finding that cGKI was expressed in pancreatic islets of control mice. As indicated in figure 17, cGKI was mainly detectable in a subset of cells, which localized to the mantle of the islet. The expression pattern implicated that cGKI was expressed in A- and/or D-cells, respectively. Furthermore, in the exocrine pancreas small vessels containing smooth muscle cells were positively stained for cGKI in control, cGKIα and cGKIβ mice, but remained unstained in conventional cGKI$^{-/-}$ animals (Fig. 17 black arrows). Importantly, islets of conventional cGKI knockouts, as well as islets of cGKIα and cGKIβ rescue mice were not stained for cGKI (Fig. 17), thus, lacked the cGKI protein.
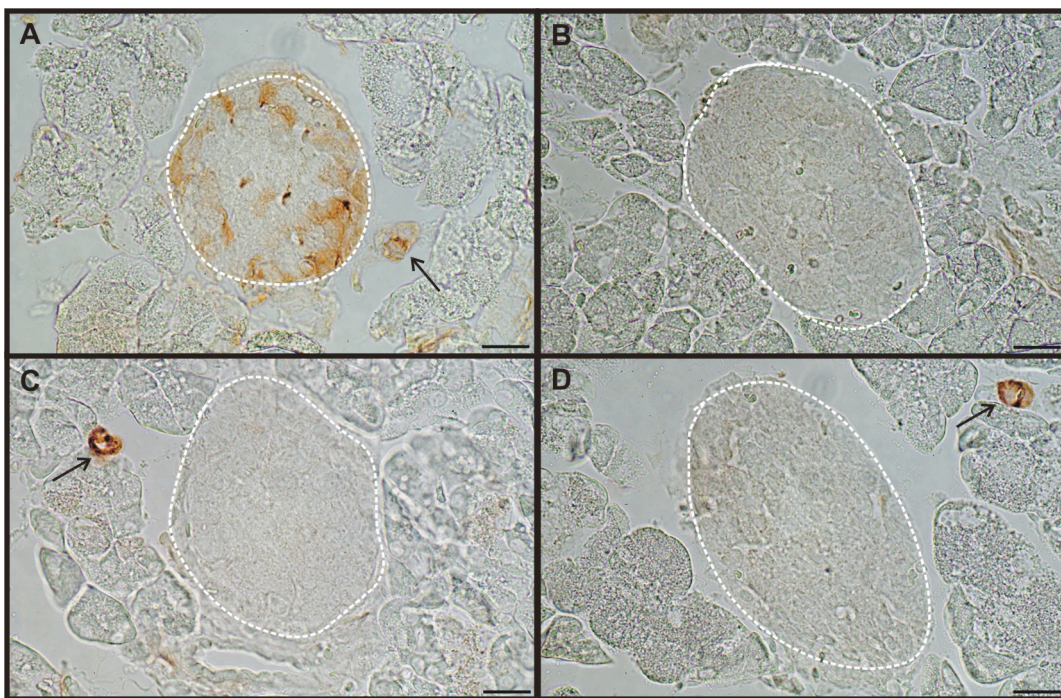

Fig. 17: Immunohistochemical analysis of cGKI expression in pancreatic tissue sections. The cGKI protein was detectable in islets of control (A) animals, whereas islets of cGKI$^{-/-}$ (B), cGKIα (C) and cGKIβ (D) rescue animals remained unstained. As indicated (black arrow), small blood vessels showed expression of cGKI in control, cGKIα, and cGKIβ mice (A and C+D). In the exocrine pancreas no cGKI expression was detectable in all four genotypes analyzed. For better illustration a white line was introduced to indicate the islets perimeter. Scale bars, 20 µm.

To define which islet cell type(s) (A-, B-, and/or D-cells) express(es) the cGKI protein, immunohistochemical double stainings were performed on pancreatic islets. Successive staining of the B-cell specific marker insulin, and cGKI by the use of specific antibodies revealed no co-expression of the two proteins in the same cell type of control animals indicating that cGKI is not expressed in pancreatic B-cells (Fig. 18A). Additionally, the insulin expression pattern of cGKI deficient islets in cGKI$^{-/-}$, cGKIα, and cGKIβ rescue islets was not different from control islets (Fig. 18B-D).
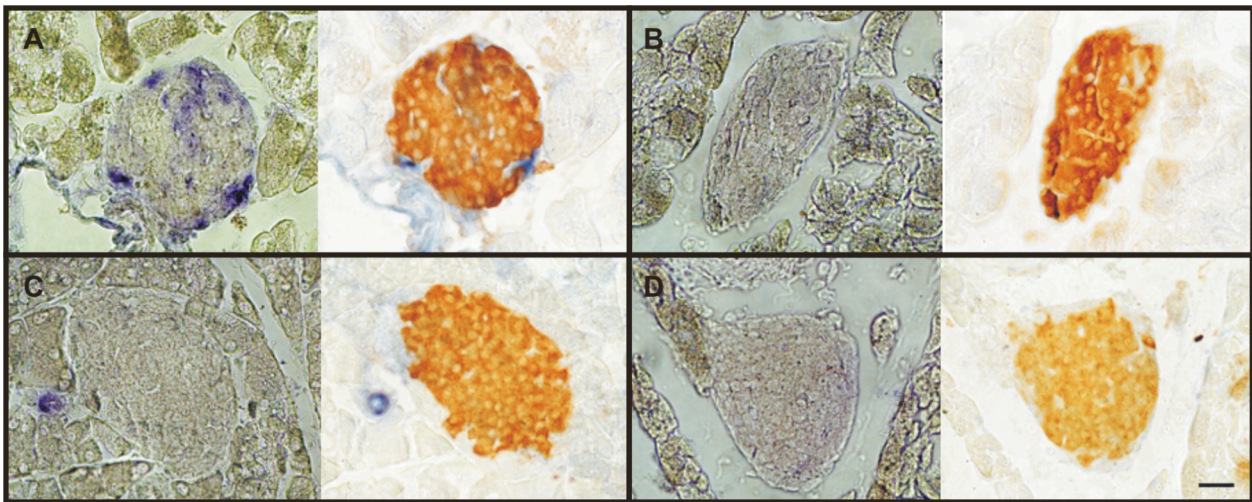
Fig. 18: Immunohistochemical analysis of successive stainings for cGKI and insulin protein in pancreatic islets of Langerhans. Blue staining indicates expression of cGKI (left part of all pictures). Brown staining demonstrates the expression of insulin (right part of all pictures) in control (A), cGKI$^{-/-}$ (B), and cGKIα (C) and cGKIβ (D) rescue mice. Scale bar 20 μm.

A minority of somatostatin stained D-cells showed co-localization with the cGKI protein. However, most somatostatin positive cells were not cGKI positive. As mentioned for insulin, somatostatin expression was not altered in the cGKI deficient islets (Fig. 19). These data implicated that the expression of cGKI is restricted to a subpopulation of somatostatin secreting D-cells.
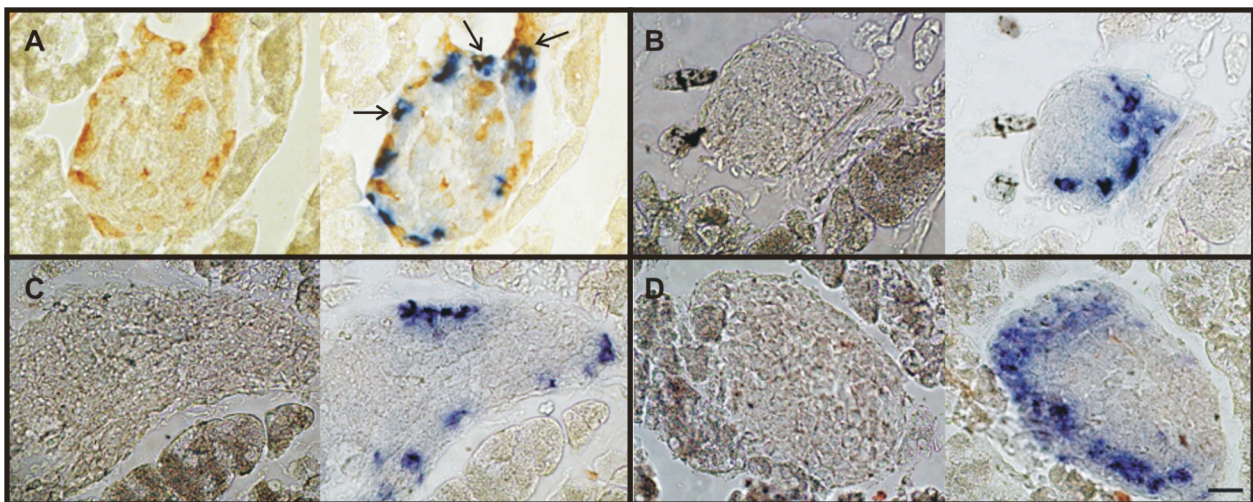

Fig. 19: Successive stainings for cGKI and somatostatin in pancreatic islets of Langerhans by standard immunohistochemical methods. Brown staining (left part of all pictures) indicated the expression of cGKI. Blue staining (right part of all pictures) demonstrates the expression of somatostatin in control (A), cGKI$^{-/-}$ (B), cGKIα (C), and cGKIβ (D) rescue mice. Please note the co-localization of cGKI and somatostatin in a subset of D-cells only in the control islets (black arrow). Scale bar, 20 μm.

Next, high-resolution immunofluorescence experiments were performed by the use of specific antibodies to detect cGKI and the A-cell marker glucagon. These analysis demonstrated co-localization of cGKI and glucagon in all A-cells of control animals (Fig. 20A). Again, the cGKI protein was not detected in cGKI deficient islets of cGKI$^{-/-}$, cGKIα, and cGKIβ rescue mice.

However, in all three genotypes a clear tendency of diminished A-cell glucagon expression was detectable. Together, these data reveal that cGKI is mainly expressed in A-cells of pancreatic islets, and thus, might play a functional role in glucagon release.
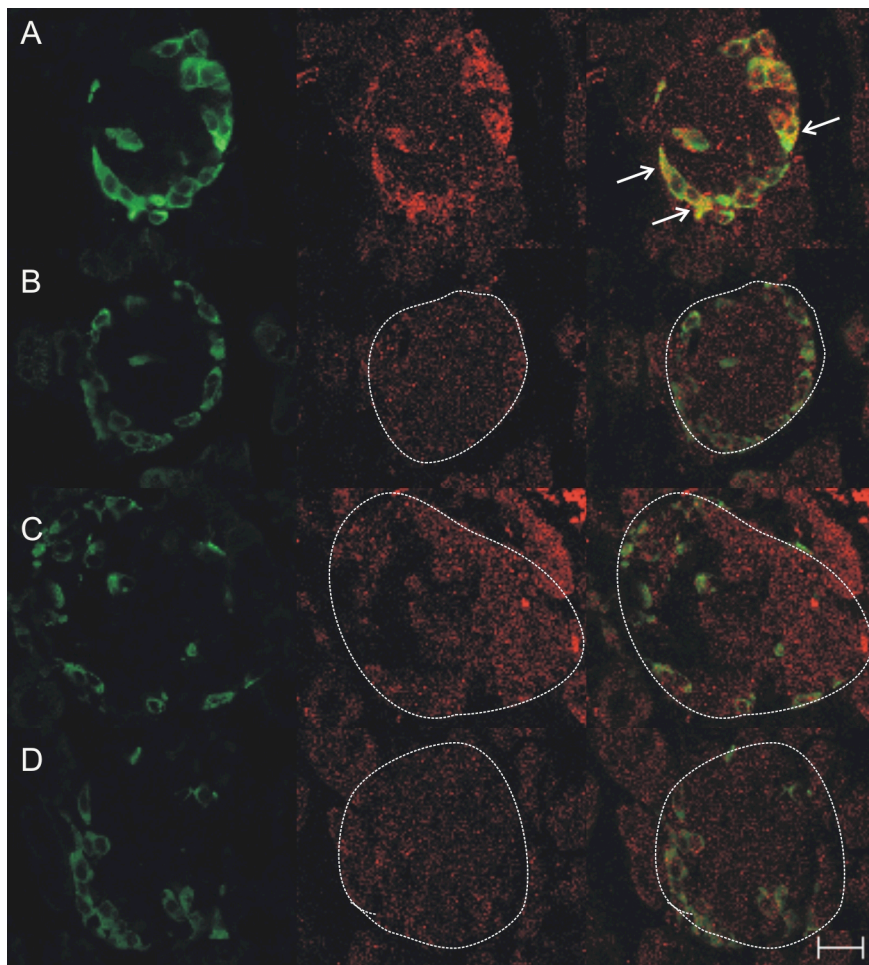

Fig. 20: Immunofluorescence double stainings for cGKI and glucagon in pancreatic islets of Langerhans. Green staining indicates glucagon, red staining cGKI. Co-staining was only detectable in islets of control mice (A) (arrows) whereas in cGKI$^{-/-}$ (B), cGKIα (C) and cGKIβ (D) rescue animals only the diminished signal for glucagon was detectable. For better illustration a white line was introduced to indicate the islets perimeter. Scale bars, 20 µm.

To analyze the specific role of cGKI on glucagon secretion, the cGKI islet knockout animals are an ideal model system, because cGKI$^{-/-}$, as well as cGKIα and cGKIβ rescue animals did not express cGKI in pancreatic islets and therefore are functionally cGKI islet knockout mice that allow a loss-of function analysis of cGKI in A-cells.

3.3.1 Expression of cGKI isoforms in pancreatic islets

The cGKI type Iα and the cGKI type Iβ are two isoforms of the cGKI protein. To specify the isoform expression of cGKI in islets, western blot, RT-PCR and immunohistochemistry analysis were carried out. Immunoblot analysis indicated the exclusive expression of the Iα isoform in control islets, whereas the Iβ isoform was completely absent from islet protein homogenates (Fig. 21).
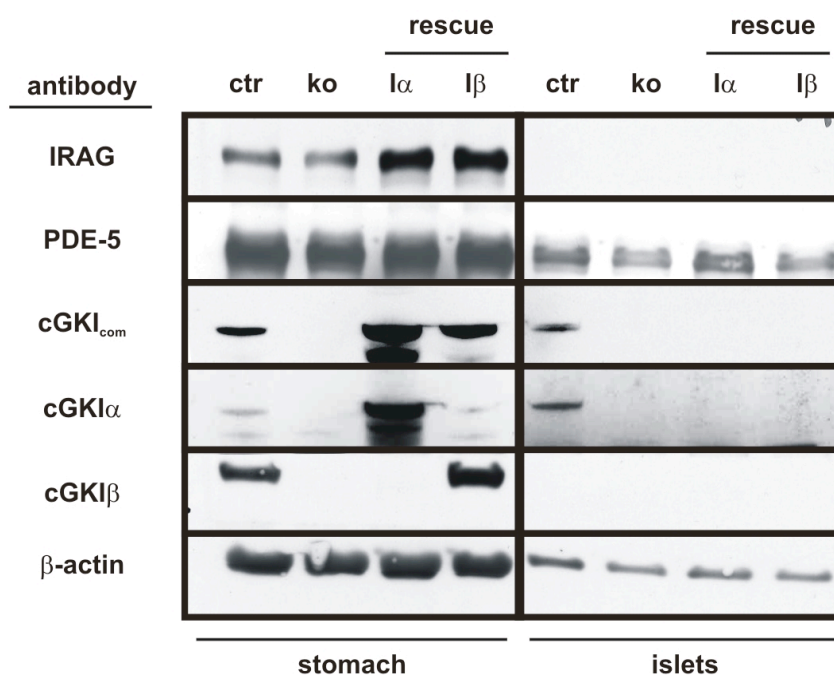
Fig. 21: Western blot analysis of cGKI isoforms and cGKI target proteins in pancreatic islets. By using isoform specific antibodies to detect the respective proteins in islet homogenates only the cGKIα isoform was found to be expressed in control lysates (ctr). Neither, the Iα nor the Iβ isoform was expressed in pancreatic islets of cGKI$^{-/-}$ (ko), cGKIα (Iα) and cGKIβ (Iβ) rescue animals. The specific cGKIβ target protein IRAG was absent from islet protein homogenates of all four genotypoes. In all genotypes, PDE-5 expression was demonstrated by the use of specific PDE-5 antibodies. As controls for the cGKI isoforms as well as for IRAG expression and PDE-5, protein lysates of control (ctr), cGKI$^{-/-}$ (ko), cGKIα (Iα) and cGKIβ (Iβ) stomachs were loaded. Please note the expression of cGKIα and Iβ in the stomach of Iα and Iβ rescue mice, respectively. By detecting β-actin in the same protein homogenates equal loading of the gel was shown. cGKI$_{com}$ – antibody directing both cGKI isoforms; cGKIα – cGKIα isoform specific antibody; cGKIβ – cGKIβ isoform specific antibody.

The isoform specific expression analysis further excluded a possible contamination of platelet and/or blood vessels cGKI in islets homogenates. Both, platelets and blood vessels mainly express the cGKIβ isoform, which was not detectable in isolated islets. As expected, cGKI protein was not detectable by the use of the isoform specific antibodies in the cGKI knockout islets of cGKI$^{-/-}$, cGKIα, and cGKIβ rescue mice. Additionally, the specific cGKIβ interaction partner inositol-1,4,5-triphosphate receptor associated cGMP kinase substrate (IRAG) was not detectable in protein homogenates of pancreatic islets of all genotypes analyzed. However, another important component of the cGMP/cGKI pathway the PDE-5 was detectable in islets indicating that PDE-5 is involved in the regulation of islet cGMP-levels (Fig. 21).

In line with the immunoblot analysis (Fig. 21), immunohistochemical stainings with the cGKIα specific antibody confirmed the expression of this isoform in control islet cells that mainly localized to the mantle (Fig. 22A). In addition, semi-quantitative RT-PCR analysis using cGKIα specific primers detected the Iα mRNA in islets isolated from control animals (Fig. 22E).
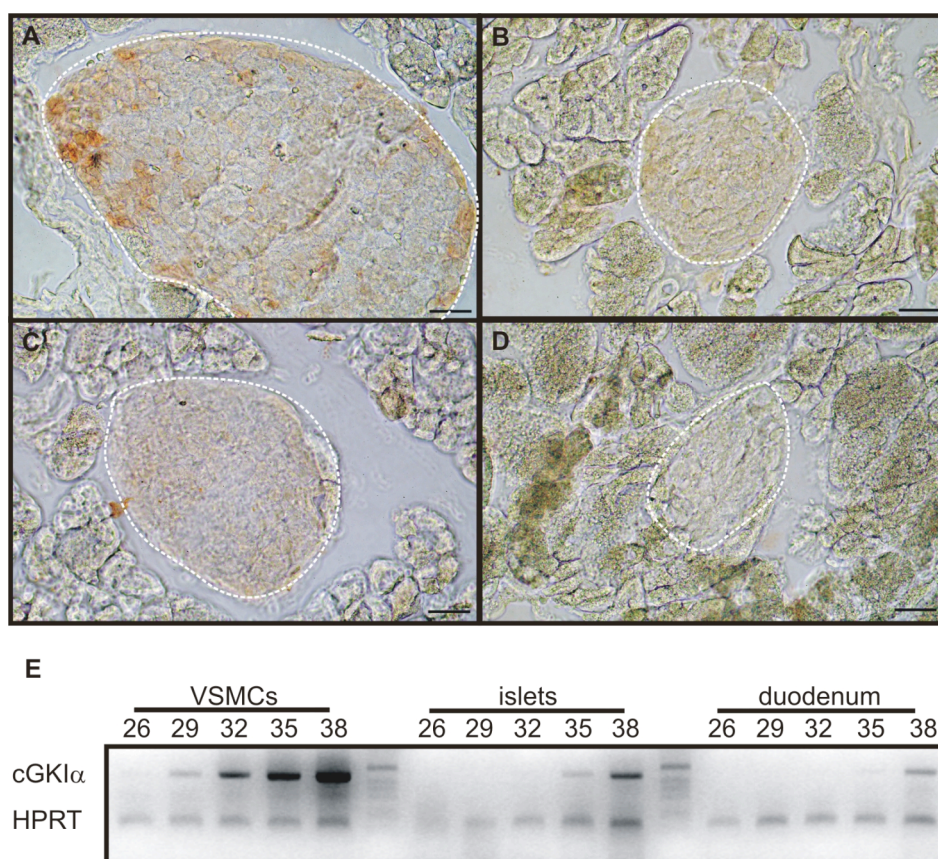
Fig. 22: Immunohistochemistry and RT-PCR analysis of cGKIα isoform in pancreatic islets. Positive staining was detectable with a cGKIα isoform specific antibody in pancreatic islets of control animals (A). Islets of cGKI$^{-/-}$ (B), cGKIα (C), and cGKIβ (D) rescue mice were unstained. For better illustration a white line was introduced to indicate the islets perimeter. Scale bars, 20 μm. (E) Semi-quantitative RT-PCR with cGKIα specific primers. Numbers indicate the number of cycles when PCR-samples were collected. As control tissue total mRNA isolated from duodenum and cultured vascular smooth muscle cells (VSMCs) from the aorta of control animals were analyzed. HPRT was co-amplified as an internal PCR-standard.

Thus, cGKIα has been shown to be the sole cGKI isoform in pancreatic islets, with its expression distribution to the periphery of the islet.

3.3.2 Analysis of a putative NO/NPs-cGMP-cGKI signaling pathway in islets

The synthesis of cGMP is catalyzed by guanylyl cyclases, which convert GTP to cGMP. This synthesis can be carried out by soluble or particular guanylyl cyclases (sGCs or pGCs). These enzymes are essential components of the NO/NPs-cGMP-cGKI signaling pathway. RT-PCR experiments on mRNA showed the expression of particular (Fig. 23), as well as of soluble guanylyl cyclases in whole islets of control animals (Fig. 24).

The pGCs are transmembrane receptors for different natriuretic peptides (NPs). NPR1 is activated by atrial (ANP), as well as by brain-type natriuretic peptide (BNP), whereas NPR2 is mainly activated by C-type natriuretic peptide. The mRNA for both natriuretic receptors was identified in control islets (Fig. 23).
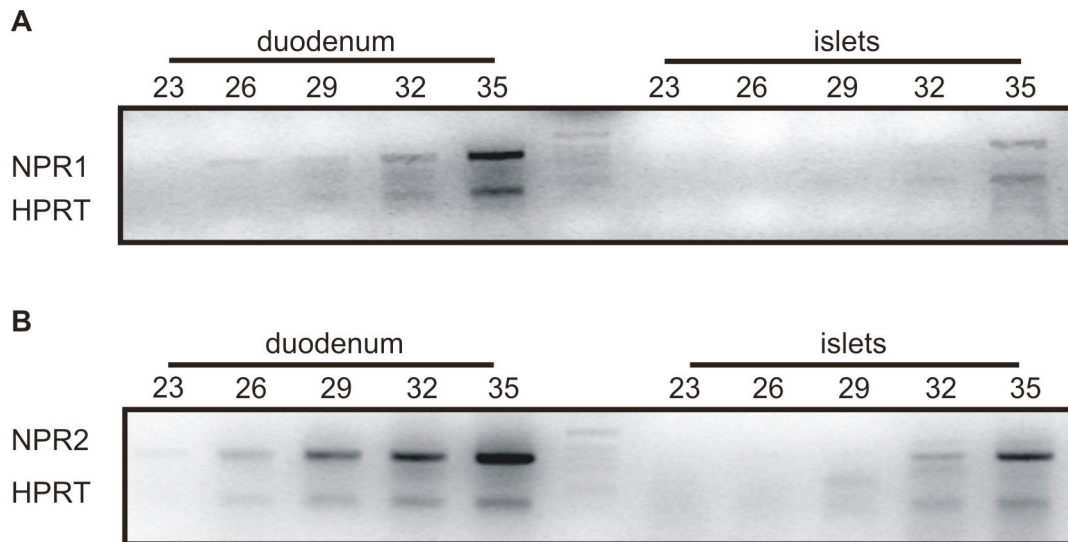
A

B

Fig. 23: Semi-quantitative RT-PCR analysis for particular guanylyl cyclases in pancreatic islets. PCR-products amplified with NPR1 (A) and NPR2 (B) specific primers from islets and duodenum are shown. The duodenal mRNA isolated from control animals was used as positive control for both primer pairs. HPRT was co-amplified as an internal standard.

The soluble guanylyl cyclases are assembled by an alpha (α_1 or α_2) and a beta (β_1) subunit. Only the heteromer can be activated by the gaseous signaling molecule NO. The beta subunit is essential for the function of the enzyme. RT-PCR analysis with specific primer pairs for the particular sGC subunits revealed that only the specific mRNA coding for the α_2 subunit was detectable together with the essential beta subunit in pancreatic islets. Thus, a functional GC protein in islets is most likely assumed by the α_2/β_1 heteromer.

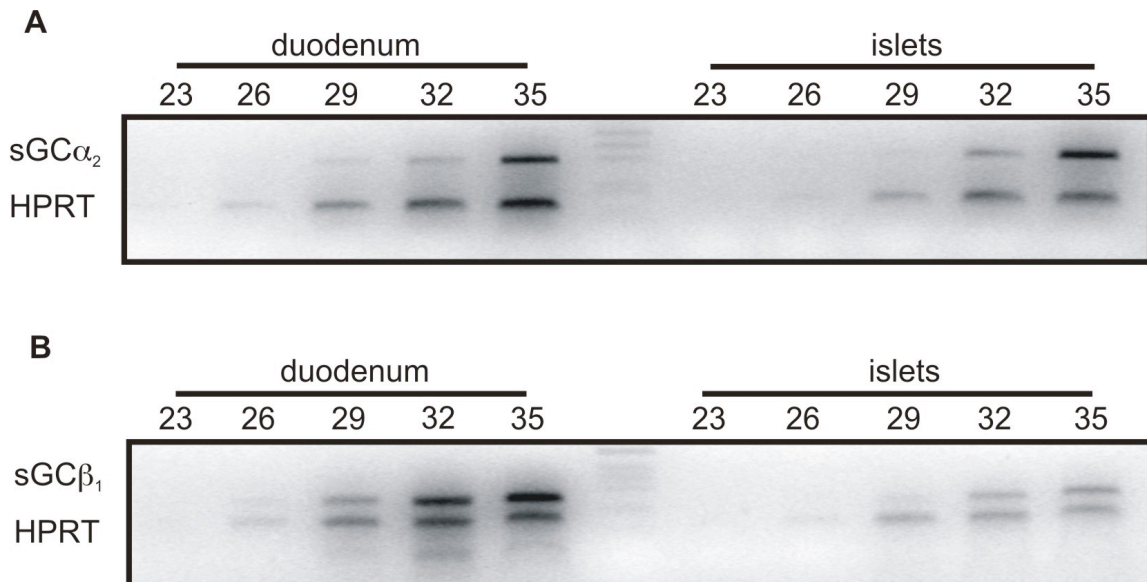**A**

B

Fig. 24: Semi-quantitative RT-PCR analysis for soluble guanylyl cyclases in pancreatic islets. PCR-products amplified with sGCα_2 (A) and sGCβ_1 (B) specific primers from islets and duodenum of control mice are shown. As positive control for both primer pairs mRNA isolated from duodenum of a control animal was used. HPRT was co-amplified as an internal standard.

Taken together, the specific mRNA transcripts for the soluble guanylyl cyclases as well as the receptors of the natriuretic peptides A, B and C were detectable indicating that the important enzymes synthesizing cGMP are present in islets. However, the RT-PCR analysis was carried out on total RNA isolated from whole islets. No details regarding the cellular localization (A-, B-, and/or D-cells) of the guanylyl cyclases can be made.

3.3.3 Glucose homeostasis in cGKI deficient mice

3.3.3.1 Glucose homeostasis after fasting

So far, the basal characterization of various transgenic animals, which lack cGKI in islets, suggests a possible involvement of the kinase on glucose homeostasis and/or glucagon release. To investigate the role of cGKI on these essential regulatory processes, *in vivo* experiments were performed. Blood glucose levels of control and cGKI$^{-/-}$, cGKIα, and cGKIβ rescue animals were determined after 12 h fasting. The cGKIα and cGKIβ rescue mice and their respective control animals analyzed were between 15 to 30 weeks old. Because of the significantly reduced life expectancy of the conventional cGKI knockouts the cGKI$^{-/-}$ mice and their littermates were already analyzed prior to adulthood at 6 to 8 weeks after birth.
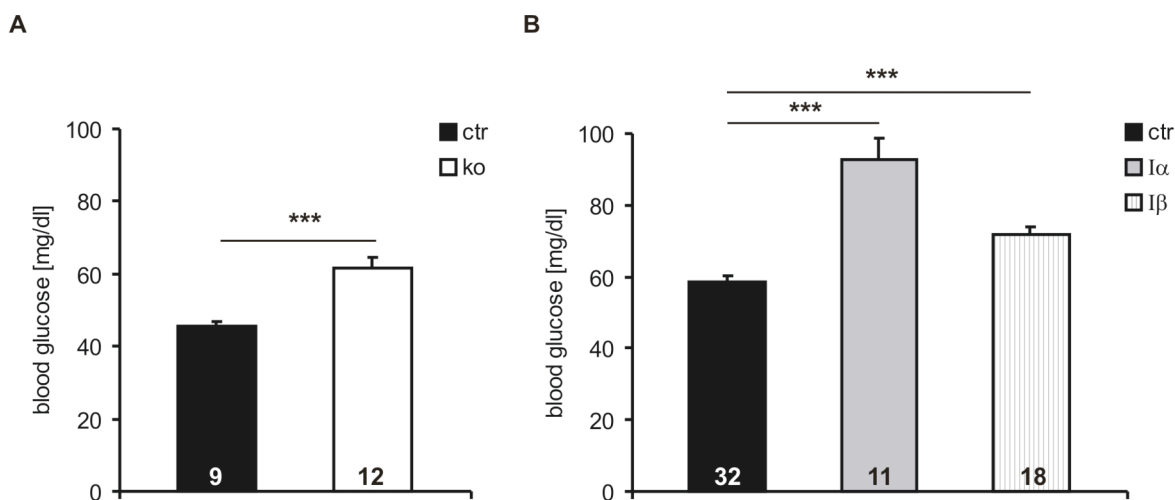
Fig. 25: Basal blood glucose levels of mice lacking cGKI in islets increased after 12 h fasting. (A) Basal blood glucose levels determined from 6-8 week-old cGKI$^{-/-}$ mice and their littermate controls. (B) Basal blood glucose levels measured in 15-30 weeks old cGKIα, cGKIβ and control animals. (***; $p < 0.001$)

As shown in figure 25 all three genotypes lacking islet cGKI had significantly increased basal blood glucose levels in comparison to their littermate controls. In detail, the cGKI$^{-/-}$ mice had significantly higher basal fasting blood glucose levels (61.4 ± 2.9 mg/dl (n=12)) compared to control animals (45.5 ± 1.5 mg/dl (n=9)). The basal blood glucose levels of cGKIβ (71.8 ± 2.3 mg/dl (n=18)) rescue mice were lower than those of cGKIα (92.7 ± 5.9 mg/dl (n = 11)) rescue mice, but still significantly higher than those of their littermate controls (ctr 58.6 ± 1.6 mg/dl (n=32)).

Since, the cGKI knockout mice display hereditary abnormalities of smooth muscle cells and various organ systems, which contribute to their poor overall health status and result in premature death in particular, the cGKIα rescue mice were used to investigate *in vivo* functions of islet cGKI. Consistently with the increased basal blood glucose levels, serum glucagon levels of cGKIα rescue mice were significantly elevated compared to control mice (ctr 15.2 ± 1.8 pM (n = 20); cGKIα 22.3 ± 3.6 pM (n=8)) (Fig. 26A). Basal serum insulin levels did not differ between the control and cGKIα rescue animals (ctr 34.6 ± 4.6 pM (n=23); cGKIα 32.1 ± 6.1 pM (n=8)) (Fig. 26B).
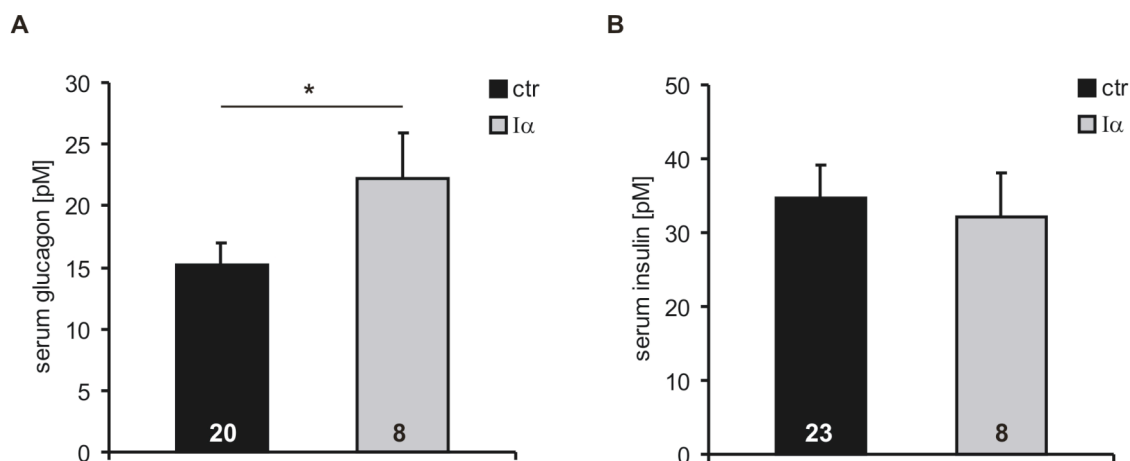

Fig. 26: Fasting serum glucagon and insulin levels of cGKIα. (A) Basal glucagon, and insulin levels after 12 h fasting from control and cGKIα rescue animals. In line with the elevated basal blood glucose levels (shown in Fig. 25), the mean serum glucagon levels were significantly increased in cGKIα rescue animals. (B) The analysis of serum insulin revealed no differences between cGKIα rescue mice compared to littermate controls. (*; $p < 0.05$; ***; $p < 0.001$)

These findings emphasize that islet cGKI is involved in glucagon secretion from pancreatic A-cells, whereas it plays no obvious role for the insulin secretion of pancreatic B-cells.

3.3.3.2 Insulin tolerance test

Glucose homeostasis is balanced between the periphral insulin sensitivity and the ability of A-cells secret glucagon as a response to hypoglycemia (Takahashi et al., 2005). To test the involvement of cGKI in peripheral insulin sensitivity, hypoglycemia was induced by lowering the blood glucose levels by the intra peritoneal application of insulin. Therefore, the 12 h fasted cGKIα rescue animals received 0.5 mU insulin intra peritoneal (i.p.) per gram body weight (Fig. 27). Although cGKIα rescue mice had initially elevated basal blood glucose levels, the dosage of 0.5 mU insulin lowered the blood glucose levels in these animals to the same level as in littermate controls 60 minutes after i.p. application (ctr 35.3 ± 4.2 mg/dl (n=8); cGKIα 33.9 ± 2.8 mg/dl (n=8)). Similar to control animals, the cGKIα mice, which lack cGKI in islets, were able to counter regulate the decrease of blood glucose levels to physiological levels (ctr 68.8 ± 4.6 (n=8); cGKIα 72.1 ± 5.1 mg/dl (n=8)) within 180 minutes after insulin challenge.
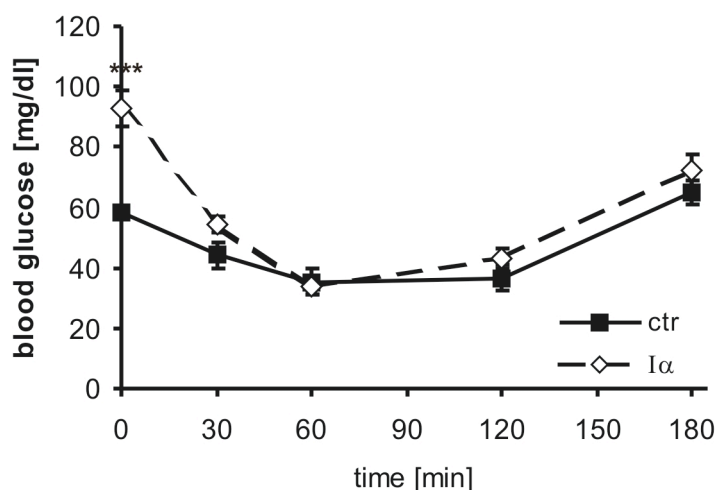
Fig. 27: Insulin tolerance test. 0.5 mU/g insulin were injected intra peritoneal after 12 h fasting. Blood glucose levels were decreased to 35.3 ± 4.2 in control (ctr) and 33.9 ± 2.8 mg/dl in cGKIα (Iα) rescue animals. Both genotypes were able to counter-regulate the decrease of blood glucose during 180 minutes in the same manner (for both genotypes n=8). (***; $p < 0.001$).

These data suggest that cGKIα rescue animals do not have a disturbed glucose handling after exogenous insulin treatment.

3.3.3.3 Glucose tolerance test

To investigate the possibility of an insulin resistance, and to identify a potential pre-diabetes, an oral glucose tolerance test was performed (Alberti and Zimmet, 1998). Therefore, glucose homeostasis was investigated by oral glucose challenges (20 mg/g body weight). During the first 15 minutes after glucose application, both, control and cGKIα rescue animals showed an increase in blood glucose levels (ctr 210.5 ± 14.8 mg/dl (n=8); cGKIα 243.4 ± 23 mg/dl (n=8)) (Fig. 28A). In control animals blood glucose levels continued to increase for another 15 minutes, whereas blood sugar levels of cGKIα rescue mice remained at constant levels (ctr 313.9 ± 11.9 mg/dl (n=8); cGKIα 233.1 ± 21.1 mg/dl (n=8)). In control animals the counter regulation was first measurable another 30 minutes later (ctr 248.5 ± 19.8 mg/dl (n=8)), when blood glucose levels of cGKIα mice continued to decline (cGKIα 141 ± 10.7 mg/dl (n=8)). 120 minutes after glucose treatment no differences were detectable between both genotypes (ctr 126.3 ± 5.5 mg/dl (n=8); cGKIα 116.5 ± 8.3 mg/dl (n=8)). Glucose tolerance was significantly better in cGKIα rescue animals compared to control littermates as shown by a faster glucose clearance in course of the investigated 120 min time period following the oral application of glucose. Serum glucagon concentrations were also monitored during glucose challenge. As shown in detail (Fig. 28A) cGKIα rescue animals had higher basal serum glucagon levels (22.3 ± 3.6 pM (n=8)) compared to littermate controls (15.2 ± 1.8 pM (n=20)). This difference was still significant in the first fifteen minutes after the glucose treatment (ctr 13.3 ± 1.6 pM (n=8-5); cGKIα 20.8 ± 1.8 pM (n=8-7)). During the time course of the

experiment glucagon levels of controls and cGKIα rescue animals converged at comparable levels. However, there was still a clear tendency to augmented glucagon levels in cGKIα rescue animals.

No significant differences between control and cGKIα rescue mice were detected in terms of serum insulin levels (Fig. 28C). However, 15 minutes after glucose application glucose-stimulated serum insulin concentrations were raised to higher maximal levels in genetically modified cGKIα rescue animals, but this tendency did not reach statistic significance (ctr 68.5 ± 12.2 pM (n=11); cGKIα 84 ± 19 pM (n=8)).

The serum leptin concentrations were also investigated during glucose challenge in control and cGKIα rescue mice (Fig. 28D). Leptin is synthesized and secreted mainly from adipocytes (Taylor et al., 1999). The leptin concentration increased during the tolerance test in control animals as expected with the maximum leptin level detectable 120 minutes after glucose treatment (ctr 195.02 ± 38 pM (n=8)). The leptin level of cGKIα rescue mice was significantly lower at the beginning (ctr 93.5 ± 24.7 pM (n=17); cGKIα 14.1 ± 2.6 pM (n=9)) and did not increase during the glucose challenge (cGKIα 35.5 ± 10.1 pM (n=8)) compared to control animals.
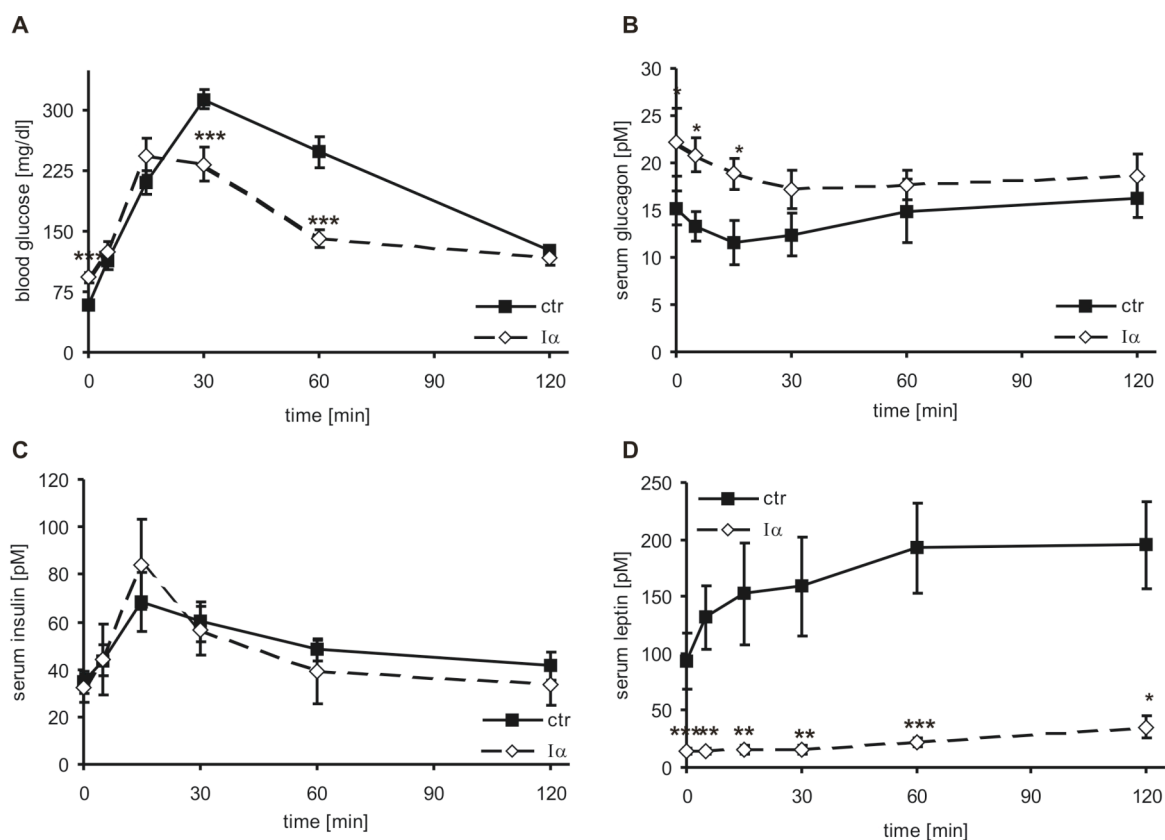
Fig. 28: Oral glucose tolerance test in control and cGKIα rescue mice. The time courses of (A) blood glucose, (B) serum glucagon, (C) serum insulin and (D) serum leptin are shown for control (■) and cGKIα rescue (◇) mice. (*; p < 0.05; **; p < 0.01; ***; p < 0.001); (n=6-11);

The presented *in vivo* data demonstrated that cGKI animals that lack cGKI in islets have chronically increased levels of basal serum glucagon. These elevated levels are most likely due to

increased secretion of glucagon from pancreatic A-cells. Therefore, it was proposed that the ablation of cGKI in A-cells resulted in an anomalous glucagon release. To test this hypothesis further hormone secretion experiments on isolated islets were carried out.

3.3.4 *In vitro* glucagon secretion experiments

Pancreatic islets *in vivo* receive multiple neuronal inputs from e.g. parasympathetic nerves (Gromada et al., 2007). Since cGKI is also expressed in various neuronal tissues, its ablation (in cGKI$^{-/-}$ and cGKIα and Iβ rescue animals) might affect pancreatic hormone release *in vivo* independent from the hormone secreting islet cells. Therefore, additional experiments were performed *in vitro* on isolated islets to directly assess the role of islet cGKI on glucagon secretion. Since cGKI$^{-/-}$ mice showed the same fasting phenotype as the cGKIα rescue mice, islets isolated from cGKI$^{-/-}$ animals were compared to their littermate controls.

Under (unphysiological) low glucose conditions (1 mM) pancreatic A-cells of control animals released glucagon by an average secretion rate of 4.6 ± 0.7 pg/islet/h (n=18) (Fig. 29). In contrast to control islets, cGKI deficient islets released significantly less glucagon (1.9 ± 0.2 pg/islet/h (n=16)) in the presence of 1 mM glucose. As expected, in control islets glucagon secretion was suppressed after exposure to 6 mM and 20 mM glucose to 2.7 ± 0.7 pg/islet/h (n=7) and 1.6 ± 0.2 pg/islet/h (n=7), whereas islets that lack cGKI actually increased their glucagon release rates to 4.7 ± 0.9 pg/islet/h (n=12) and 2.6 ± 0.2 pg/islet/h (n=7) (Fig. 29).
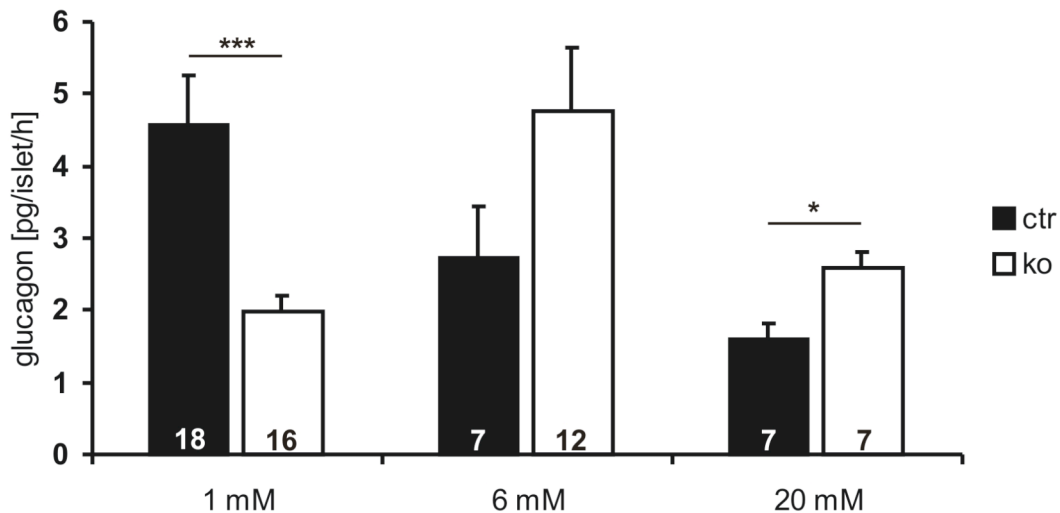
Fig. 29: Glucagon secretion of isolated islets. Glucagon release from isolated control islets was suppressed by 41% at 6 mM and 66% at 20 mM compared to 1 mM glucose (black bars). In contrast, glucagon release from isolated cGKI$^{-/-}$ islets (open bars) was low at 1 mM glucose compared to control islets and increased in an unusual mode at 6 mM and 20 mM. (***, $p < 0.001$; *, $p < 0.05$).

These data underline the direct role of A-cell cGKI on the regulation of glucagon secretion. Taken together, the deletion of cGKI in pancreatic islet cells leads to an abnormal glucagon release. Under physiological conditions (6 mM and 20 mM glucose) cGKI deficient islets show increased rather than decreased glucagon releasing rates. However, the mean glucagon content was not different between control and cGKI$^{-/-}$ islets (ctr 3.2 ± 0.1 ng/iselt (n = 12); cGKI$^{-/-}$ 3.4 ± 0.1 ng/islet (n = 14)).

4 Discussion

4.1 Expression analysis and putative function of the sodium channel $Na_V1.7$ in pancreatic islets

Glucagon secretion from pancreatic A-cells plays a major role for the counter regulation of hypoglycaemia, whereas hyperglycaemia inhibits glucagon release. The mechanisms regulating the release are incompletely understood and currently the source of much debate (Gromada et al., 2007). In addition, it has to be noted that TTX-sensitive sodium channels were detected in A-, B-, and D-cells respectively (Gopel et al., 2000b; Leung et al., 2005). In recent studies analyzing TTX-sensitive sodium channels in pancreatic glucagon-secreting A-cells, sodium channels were proposed to be involved in the secretion of glucagon (Gopel et al., 2000b; MacDonald et al., 2007). Previous analysis of TTX acting on glucagon secretion via TTX-sensitive sodium channels showed that TTX was an inhibitor of glucagon release at low glucose conditions (1 mM) (Gopel et al., 2000b). Furthermore, it was shown that TTX inhibits the spontaneous electrical activity of glucagon-secreting A-cells exposed to 0.5 mM glucose (MacDonald et al., 2007). Some evidence for the putative genetic basis of sodium channel isoforms expressed in islets comes from the analysis of single cell RT-PCR and RT-PCR performed on mRNA isolated from whole islets (Vignali et al., 2006). In fact, it has been shown that the TTX-sensitive sodium channels $Na_V1.3$ and $Na_V1.7$ were expressed in isolated pancreatic islets. But the distribution of $Na_V1.7$ and/or $Na_V1.3$ in A-, B-, and/or D-cells remained unclear (Vignali et al., 2006). In the present study the expression pattern and function of $Na_V1.7$ in pancreatic islets was investigated.

In order to analyze the specific role of the sodium channel isoforms on glucagon secretion, a conditional deletion of the $Na_V1.7$ isoform was generated by the use of the Cre-loxP recombination system in murine A-cells (Herrera, 2000) and termed $Na_V1.7^{Acko}$. In agreement to the earlier report (Vignali et al., 2006) $Na_V1.7$ expression was detectable in control animals. In the tissue-specific $Na_V1.7^{Acko}$ mutants $Na_V1.7$ protein was no more detectable. Interestingly, even $Na_V1.7$ mRNA was no more identified in islets of the $Na_V1.7^{Acko}$ mice indicating that already the mRNA was degraded immediately after transcription or produced in small amounts that were not detectable by the RT-PCR approach chosen. The *in vitro* analysis demonstrated that the deletion of $Na_V1.7$ in pancreatic A-cells led to an increase in glucagon secretion at high glucose conditions (20 mM). The mean glucagon releasing rate at high glucose levels was indeed comparable to that measured under low glucose conditions (1 mM). However, at low glucose levels the deletion of $Na_V1.7$ had no effect on the glucagon secretion compared to control animals. These results are in contrast to other data showing the inhibition of glucagon secretion in the presence of TTX at low glucose conditions (Barg et al., 2000). These authors postulated that sodium channels in A-cells act as pacemaker channels to activate calcium channels, which in turn triggers hormone release from islet A-cells.

The conflicting data might be explained by the expression of another TTX sensitive sodium channel isoform in pancreatic A-cells responsible for glucagon release at low glucose conditions. Previous data showed that $Na_V1.1$, $Na_V1.3$ and $Na_V1.6$ are expressed in whole pancreatic islets, and, in addition, $Na_V1.3$ was detected in single-islet cells (Vignali et al., 2006). Furthermore, immunostainings with $Na_V1.3$ specific antibodies revealed the expression of $Na_V1.3$ in a comparable manner to that of $Na_V1.7$ (data not shown). Very recently a floxed $Na_V1.3$ mouse line was generated (Nassar et al., 2006). Using the Cre/loxP system these animals could provide further insight into the sodium channel dependent hormone release in islets. In addition, although $Na_V1.7$ was deleted in conditional A-cell specific knockout mice the steady state inactivation patterns of the positive sodium channel isoform were still present in 1 out of 13 cells. Thus it remained possible that some A-cells still expressed a functional channel that was not detected in the $Na_V1.7^{Acko}$ mice. At least two explanations for this finding are possible. First, a subpopulation of pancreatic A-cells is equipped with more than one TTX-sensitive sodium channel isoform, which in turn could be involved in glucagon release at low glucose conditions. Second, the recombination efficiency of the Cre-recombinase under control of the glucagon promotor is less than 100%. The incomplete recombination, thus knockout of a gene of interest in a given tissue is a known limitation of the Cre/loxP system, has already been shown for many Cre lines and floxed genes. Indeed, a previous study showed that less than 100% of A-cells showed recombination by the use of the Gluc-Cre mice (Quoix et al., 2007). Furthermore, it has to be considered that A-, B- and D-cells express TTX-sensitive sodium channel isoforms (Gopel et al., 2000a; Gopel et al., 2000b). It is well established that both insulin and somatostatin act directly as negative regulators of glucagon release (Gromada et al., 2007; Ravier and Rutter, 2005). In particular somatostatin is an important regulator at basal glucose levels, (Brunicardi et al., 2001; Strowski et al., 2006). Due to the fact that A-cell activity is strongly influence by paracrine mechanisms from B- and D-cells TTX effects on glucagon secretion could also be a consequence of these paracrine effects (Franklin et al., 2005; Unger, 1985; Yoshimoto et al., 1999).

Although, the $Na_V1.7$ deletion was associated with disturbances of glucagon secretion *in vitro*, this phenotype had no influence on blood glucose levels *in vivo*. Differences in control and knockout mice were neither detectable after 12 h fasting nor during glucose challenge. Again, a possible explanation might be that $Na_V1.7$ was not deleted in 100% of the islet A-cells. In addition, it has to be considered that $Na_V1.7$ is not expressed in ever A-cell. Thus some A-cells are still functional. It is known that the dysfunction of B-cells during diabetes type-1 has to affect more than 80% of the cells until a phenotype is detectable. Thus, a subset of functional A-cells might be sufficient to mask the defect in the A-cell line. In addition, glucose homeostasis is an important mechanism also regulated by other glucagon independent mechanisms, which might compensate for the dysfunction of A-cells. In consequence, although glucagon release from pancreatic A-cells are disturbed *in vitro*, other control mechanisms are activated *in vivo* to keep the blood glucose levels

in balance. The present study rather shows that $Na_V1.7$ is a negative regulator of glucagon release at high glucose conditions and does not act as a pacemaker at low glucose conditions.

4.2 Expression pattern of cGKI and related compounds in pancreatic islets of Langerhans

The production of NO in pancreatic islets of Langerhans was shown in previous studies (Alm et al., 1999; Lajoix et al., 2001), whereas its function was discussed controversially (Panagiotidis et al., 1992; Schmidt et al., 1992). Indeed, it was suggested that endogenous NO positively stimulates glucagon secretion, which was efficiently suppressed by the use of NOS inhibitors (Akesson et al., 1996). In general, NO stimulates cGMP synthesis by activating sGCs (Koesling et al., 2004). Furthermore, cGMP is known to bind to and activate cGKI in many cells (Hofmann et al., 2000). In the present study the cell specific expression of cGKI in pancreatic islets of Langerhans was analyzed in detail. An established conventional cGKI knockout mouse line (Pfeifer et al., 1998) and recently generated cGKIα and cGKIβ rescue mice, which lack cGKI in non-smooth muscle cells (Weber et al., 2007), were analyzed in comparison to control animals. All gene-targeted cGKI animals lacked the expression of cGKI protein in pancreatic islets, which made them a valuable tool to study the functional consequences in cGKI deficient islets. In detail, insulin-secreting B-cells were negative for cGKI expression. However, the cGKI protein was expressed in glucagon-secreting A-cells and in a subpopulation of somatostatin-secreting D-cells. Interestingly, only the cGKIα isoform was detectable, whereas the cGKIβ isoform could not be identified in pancreatic islets. In line with this finding, IRAG the common interaction partner of cGKIβ (Ammendola et al., 2001) was not found in pancreatic islets. In addition, the lack of cGKIβ in protein homogenates from pancreatic islets excludes the contamination of islet protein homogenates with platelets, which mainly express the cGKIβ isoform (Antl et al., 2007). Islet cells release their hormones directly to the blood, thus A-, B- and D-cells are surrounded by blood vessels that pass through the islets (Cabrera et al., 2006). Interestingly, cGKIα and cGKIβ rescue mice expressing cGKI under the control of the smooth muscle promotor SM22α (Weber et al., 2007) did not express cGKI in the small islet capillaries indicating that these vessels lack a smooth muscle cell layer or cGKI is not reconstituted in the respective cells. However, the data confirmed the expression of cGKI in larger blood vessels (Geiselhoringer et al., 2004; Lukowski et al., 2008) of the exocrine pancreas of cGKI rescue mice. As stated earlier, cGKI was not detected in islets of cGKIα and cGKIβ rescue mice.

The second messenger cGMP can be generated by cytoplasmatic sGCs and membrane-localized pGCs (Garbers and Lowe, 1994; Koesling et al., 2004). The transcripts for both enzymes were identified by RT-PCR in islets of Langerhans. Of the sGCs two isoforms are known, which are composed of a $\alpha_1\beta_1$ or a $\alpha_2\beta_1$ heterodimer (Koesling et al., 2004). Recently it was shown that mice, which lack the β_1 subunit, express neither the α_1 nor the α_2 subunit indicating the β_1 subunit is

essential to form a functional enzyme (Friebe et al., 2007). Furthermore, the $\alpha_1\beta_1$ and $\alpha_2\beta_1$ heterodimers differ in their tissue-specific distributions (Koesling et al., 2004). The $\alpha_1\beta_1$ isoform has a broad distribution, e.g. lung, vascular smooth muscle cells, and platelets (Browner et al., 2004; Gambaryan et al., 2008; Koesling et al., 1988), whereas the $\alpha_2\beta_1$ heterodimer is mainly restricted to the brain, placenta and uterus (Budworth et al., 1999; Mergia et al., 2003). In the present study RT-PCR analysis revealed that the β_1 and the α_2 subunit are present in pancreatic islets. Therefore, the molecular basis for a functional heterodimer, which can produce cGMP, is fulfilled.

Regarding the pGCs, the mRNA information for the natriuretic peptide receptors 1 and 2 were detectable in the islets of Langerhans. This suggests that receptors for the natriuretic peptides (ANP, BNP, and CNP) exist in the endocrine pancreas. This aspect was already shown in previous studies, investigating the effects of ANP on islet hormone secretion (Verspohl and Ammon, 1989; Verspohl and Bernemann, 1996). These authors proposed that ANP does not influence insulin secretion (Verspohl and Ammon, 1989), but has an inhibitory effect on glucagon secretion in isolated rat islets (Verspohl and Bernemann, 1996).

PDE-5 hydrolyze cGMP, thus regulates cGMP levels within a cell (Kass et al., 2007). Immunoblot analysis revealed the expression of PDE-5 in islets of Langerhans. Importantly, the detection of the GCs and PDE-5 together in pancreatic islets indicates that synthesis and hydrolyzation of cGMP can be carried out within islets underlining that the NO/NP-cGMP-cGKI signaling pathway is of importance for e.g. islet function and hormone release.

4.3   Role of α-cell cGKI for glucose homeostasis

So far, only very few data indicated that cGMP levels and/or cGKI were important for islet function (Henningsson et al., 2000; Mori et al., 2001). In the present study control animals were compared to gene-targeted cGKI animals, which lack islet cGKI to determine the role of cGKI expressed in glucagon-secreting A-cells. The deletion of islet cGKI in mice was associated with increased fasting blood glucose levels. Due to the fact that all gene-targeted cGKI mutants showed similar results in blood glucose levels, it was reasonable to focus on the cGKIα rescue mice for further *in vivo* investigations. The increased blood glucose levels matched well with the fact that cGKI mutant mice had increased serum glucagon, but normal serum insulin levels. This suggests that cGKI is involved in glucagon release from pancreatic A-cells. In general, glucagon secreted from A-cells facilitates the glycogen breakdown and gluconeogenesis in the liver by binding to specific glucagon receptors (Kanno et al., 2002), which in turn leads to increased blood glucose levels. Thus, the loss of cGKIα in pancreatic A-cells intensifies the fasting state with increased glucagon secretion and enhanced blood glucose levels. The blood glucose levels (~ 5.0 mM) detected in cGKIα rescue mice were not high enough to induce reactive insulin release. This is in line with previous reports, which show that glucose-induced insulin secretion requires more than

5 mM glucose in mice (MacDonald et al., 2007).

The cGKIα rescue mice and control animals show a similar response during the exogenous insulin challenge, whereas the glucose tolerance test was improved in the mutant mice. The improved glucose tolerance test in the cGKIα rescue mice might be induced by secondary islet-independent effects, which were not caused by the deletion of cGKI in the endocrine pancreas. In line with these hypothesis cGKIα rescue mice have significantly lower serum leptin levels than control animals. Leptin is an adipose derived hormone, and secreted in order to reduce food intake and to signal satiety (Morioka et al., 2007; Myers, 2004; Szanto and Kahn, 2000; Zhao et al., 2000). Indeed, cGKIα rescue animals have a reduced body weight compared to control animals (Weber et al., 2007). This phenotype is probably accompanied with a lower relative fat mass, since the animals are not smaller than their littermates (data not shown). Therefore, cGKI could even be involved in leptin synthesis/secretion, which has not been further investigated. Glucagon release is also under hypothalamic control (Evans et al., 2004; Miki et al., 2001). Adrenaline increases glucagon secretion via adrenoreceptors localized in the plasma membrane of murine A-cells (Liu et al., 2004; Vieira et al., 2004). Previous studies revealed the expression of cGKI in the hypothalamus (Feil et al., 2005a; Feil et al., 2005b). Consequently, the increased glucagon release could be as well influenced by the lack of cGKI in the hypothalamus.

However, glucagon secretion experiments on isolated islets of cGKI knockout mice revealed that glucagon release is disturbed in the mutant mice at low, basal, and high glucose conditions compared to control animals. These experiments were performed in the absence of any extra-islet stimuli (e.g. nervous control, leptin, adrenalin), excluding an influence of possible secondary effects (please see above) of the cGKI deletion *in vivo*. Therefore, the effects were due to the loss of cGKI in the islets themselves. Nevertheless, it is possible that secondary effects intensify the islet specific phenotype caused by the deletion cGKI *in vivo*.

Both the *in vivo* and the *in vitro* findings together establish the relevance of the cGMP/cGKI-signaling pathway in pancreatic A-cell. Previous studies investigating islet function by the use of NO-donors, L-arginine, and/or NO inhibitors revealed that islet NO mostly increased glucagon secretion, which is in disagreement with the results shown in this study (Akesson et al., 1996; Aring et al., 1999; Henningsson et al., 2000; Henningsson et al., 2002; Schmidt et al., 1992). However, these pharmacological approaches might be different from the analysis of genetic mouse models. It has to be noted that most of the previous investigations showed as well controversial consequences for the role of NO on insulin secretion. Hormone release from B-cells was stimulated (Akesson et al., 1996; Schmidt et al., 1992; Spinas et al., 1998), not affected (Jones et al., 1992) or inhibited (Akesson et al., 1996; Aring et al., 1999; Henningsson et al., 2002). In addition, NOS were detected both in A- and B-cells (Henningsson et al., 2000; Henningsson et al., 2002; Lajoix et al., 2001; Panagiotidis et al., 1992; Salehi et al., 2008). Therefore, effects on

glucagon release can result from NO derived from A- and/or B-cells, as well as from insulin secreted upon B-cell exocytosis. Thus, modified paracrine signaling might affect glucagon secretion, since insulin and somatostatin themselves act as negative regulators of glucagon secretion (MacDonald et al., 2007; Ravier and Rutter, 2005). However, islet NO production was shown to increase cGMP levels in islets at basal and high glucose conditions (Henningsson et al., 2000), which in turn could induce activation of cGKI. Therefore, it is possible that NO inhibits glucagon release via the cGMP/cGKI signaling pathway directly in A-cells. Indeed, in all these previous studies NO influenced all pancreatic islet cells, whereas in cGKI mutant mice the direct effect of this protein was studied in A-cells. Furthermore, not only the NO/cGMP pathway activates cGKI, cGMP accumulation can also be induced via NPs. Recent studies have shown that ANP inhibited glucagon secretion without affecting insulin secretion (Verspohl and Ammon, 1989; Verspohl and Bernemann, 1996). In line with the presented data, this indicates that cGKI acts as a negative regulator of glucagon secretion.

Taken together, this study demonstrates for the first time the expression of cGKIα in glucagon secreting A-cells, and its inhibitory effect on glucagon secretion. However, secondary effects caused by the lack of cGKI in other tissues could intensify the findings of e.g. the *in vivo* phenotypes. Importantly, the *in vitro* investigations on isolated islets underlined the direct involvement of A-cell cGKI affecting glucagon release. As mentioned above, glucagon secretion is triggered by an increase of cytoplasmatic $[Ca^{2+}]_i$. As reported for many physiological processes, such as platelet activation, vascular tone, and neuronal plasticity (Hofmann, 2005), it is conceivable that cGKI expressed in pancreatic A-cells also might be a negative regulator of $[Ca^{2+}]_i$, which, in general, triggers glucagon release (Ashcroft and Rorsman, 2004; MacDonald et al., 2007). Thus, cGKI might regulate the decrease in $[Ca^{2+}]_i$ via the regulation of functional important ion channels. For example, cGKI could exert the functional regulation of K_{ATP}-channels as already shown in transfected cell-lines (Chai and Lin, 2008) or phosphorylate L-type voltage gated Ca^{2+}-channels (Yang et al., 2007).

5 Conclusion

In conclusion, the *in vitro* data presented here showed that both the sodium channel isoform $Na_V1.7$ and the serine/threonine-specific protein kinase cGKI are inhibitors of glucagon secretion at high glucose levels. Low glucose (3 to 5 mM) induces glucagon release from pancreatic A-cells, which is triggered by the closure of K_{ATP}-channels and the activation of Ca^{2+}-channels. The consequentially increase of intracellular calcium concentration $[Ca^{2+}]_i$ leads to glucagon secretion, which is intensified by the deletion of islet $cGKI\alpha$ in A-cells. Physiologically, at high glucose conditions hormone release from islet A-cells is reduced by mechanisms not clearly identified. The present study shows, that $Na_V1.7$ and cGKI are involved in this inhibitory process, since the deletion of the particular protein rather increases than suppresses glucagon secretion at high glucose conditions. The exact signaling mechanisms have to be elucidated. Indeed, for the first time, the presented data supports the concept of a NO/NP-cGMP-cGKI signaling pathway via the $cGKI\alpha$ isoform in murine islets. Hence, both $Na_V1.7$ and $cGKI\alpha$ are essential regulators of glucose homeostasis.
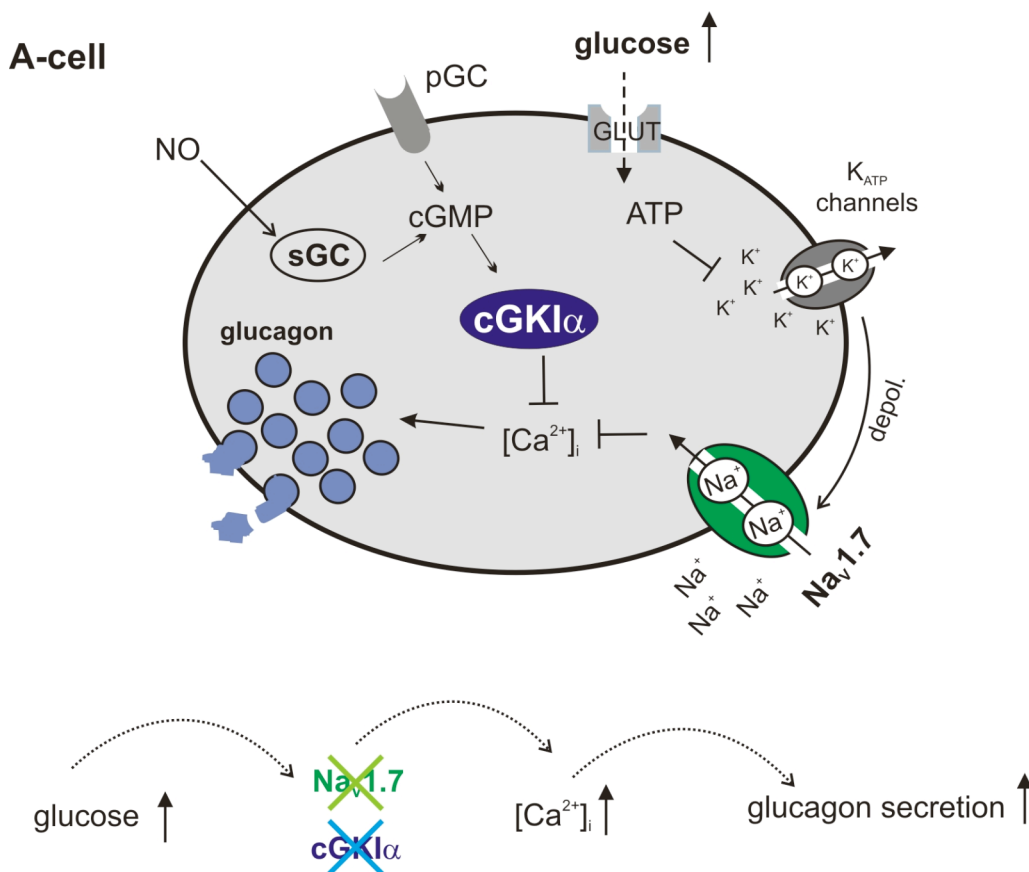
Fig. 30: Schematic illustration summarizing the conclusion. GLUT – glucose transporter; Na^+ - sodium ion; K^+ - potassium ion; $[Ca^{2+}]_i$ – intracellular calcium concentration; K_{ATP}-channel – ATP dependent potassium channel; $Na_V1.7$ – voltage-dependent sodium channel isoform 1.7; $cGKI\alpha$ – $I\alpha$ isoform of the cGMP-dependent protein kinase G; sGC – soluble guanylyl cyclases; pGC – particular guanylyl cyclases; cGMP – cyclic guanosine-3', 5'-monophosphate; depol. - depolarization.

6 Zusammenfassung

Die Langerhansschen Inselzellen sind Zellagglomerate im endokrinen Teil des Pankreas. Sie erkennen Schwankungen des Blutzuckerspiegels und regulieren diesen bei Abweichungen durch die gezielte Freisetzung der Hormone Insulin bzw. Glukagon. B-Zellen sezernieren Insulin im hyperglykämischen Zustand, um den Blutzucker zu senken. Im Gegensatz dazu schütten A-Zellen bei Hypoglykämie Glukagon aus, das den Abbau von Glycogen in der Leber stoppt und gleichzeitig die Freisetzung von Glukose fördert. Die exakten Mechanismen, die zur Sekretion von Glukagon führen, sind noch weitestgehend ungeklärt. Generell geht man davon aus, dass eine Aktivierung von Kalziumkanälen, ein Einstrom von Kalzium, und somit ein Anstieg der intrazellulären Kalziumkonzentration zur Ausschüttung von Glukagon aus den A-Zellen führt. Neben Kalziumkanälen spielen auch Natriumkanäle eine wichtige Rolle bei diesem Sekretionsprozess. Die Expression von Natriumkanälen in den A-Zellen wurde bereits dargestellt. Mit dieser Arbeit konnte erstmals gezeigt werden, dass in den A-Zellen die $Na_V1.7$-Isoform der Natriumkanäle exprimiert wird. Um die genaue Funktion des $Na_V1.7$ in diesen Zellen feststellen zu können, wurden mit Hilfe des Cre-loxP Rekombinationssystems A-Zell-spezifische $Na_V1.7$ Knockoutmäuse ($Na_V1.7^{Acko}$) generiert. *In vitro* entfiel durch die Deletion des $Na_V1.7$ die physiologische Hemmung der Glukagonfreisetzung bei hohen Blutzuckerwerten.

Des Weiteren wurde im Rahmen dieser Arbeit die Rolle der Iα Isoform der cGMP abhängigen Proteinkinase G vom Typ I (cGKIα) an der Glukagonsekretion untersucht. Die cGKIα wird überwiegend in den A-Zellen der Inseln exprimiert. Die Analyse von unterscheidlichen cGKIα defizienten Mäusen, denen unter anderem die cGKI in den Inseln fehlt, zeigte ebenfalls eine gestörte Glukagonfreisetzung bei Hochglukose: wiederum war die Glukagonausschüttung bei diesen Bedingungen verstärkt statt inhibiert. Eine erhöhte Glukagonsekretion war bereits bei basalen Glukosekonzentrationen zu beobachten. Zusätzlich hatten diese Mäuse eine verbesserte Glukoseverwertung nach oraler Applikation, sowie erhöhte Nüchternblutzucker- und Serumglukagonwerte.

Insgesamt zeigen die in dieser Arbeit erhobenen Daten, dass sowohl der $Na_V1.7$ als auch die cGKI als negative Regulatoren an der Glukagonsekretion beteiligt sind.

7 Appendix

7.1 *Primer Sequences*

7.1.1 Oligonucleotides

Primer	Sequence	Product
HPRT	5' – gta atg atc agt caa cgg ggg ac – 3' 5' – tgg tta agg ttg caa gct tgc tgg – 3'	175 bp
$Na_V1.7\_B$	5' – gat aag gca act tcc gac g – 3' 5' – gat ccc tgt gaa gac cag g – 3'	ctr: 398 bp ko: - bp
$Na_V1.7\_C$	5' – ctg agg aca tgc tga atg ac – 3' 5' – ctt gca gtt ctc cgt tga tc – 3'	ctr: 686 bp ko: 273 bp
$Na_V1.7\_D$	5' – gat aag gca act tcc gac g – 3' 5' – ctg cat gcc gac cac ggc – 3'	ctr: 698 bp ko: 285 bp
NRP-B	5' – agc cat gcc ctc tat gc – 3' 5' – ata tgc tgg tac cac ctt cc – 3'	364 bp
NRP-A	5' – agg cgc ttg tgc tct atg – 3' 5' – tat cct gcc cat cgt ctc – 3'	357 bp
Prkg1_alpha	5' – gga agt tca cta aat ccg aga g – 3' 5' – tga gga ttt cat cag gaa gg – 3'	425 bp
$sGC\alpha_2$	5' – aga tgc tcc tat gca gac c – 3' 5' – cat cag agt acc ttc agg aag c – 3'	303 bp
$sGC\beta_1$	5' – agc cct tac acc ttc tgc – 3' 5' – cac tca gt ttc tcc aca tcc – 3'	251 bp

7.1.2 Genotyping PCR primers

Mouse line	Primer	Sequence		Product
R26R	VL15 VL16 VL17	5' – gcg aag agt ttg tcc tca acc – 3' 5' – gga gcg gga gaa atg gat atg – 3' 5' – aaa gtc gct ctg agt tgt tat – 3'	VL16 + VL17 VL15 + VL17	ctr: 550 bp ko: 300 bp
floxed $Na_V1.7$	VL18 VL20	5' – cag aga ttt ctg cat tag aat ttg ttc – 3' 5' – gtt cct ctc ttt gaa tgc tgg gca – 3'	VL18 + VL20 VL18 + VL20	ctr: 317 bp ko: 395 bp
GlucCre	VL21 VL22	5' – gct gcc acg acc aag tga cag caa tg – 3' 5' – gta gtt att cgg atc atc agc tac ac – 3'		401 bp
cGKI ko	RF125 RF53 RF118	5' – gtc aag tga cca cta tg – 3' 5' – cct ggc tgt vgat ttc act cca – 3' 5' – aaa tta ctt gtc aaa ttc ttg – 3'	RF53 + RF125 RF53 + RF118	ctr: 284 bp ko: 250 bp

SMIα ko	RF67	5' – ctc aga gtg gaa ggc ctg ctt – 3'	RF67 + SW16	ctr: 292 bp
	SW12	5' – cgc aag ggt tact ca cca ca – 3'	RF67 + SW12	ko: 150 bp
	SW16	5' – cct cct tga gca tga gaa tct tg – 3'		
SMIβ ko	RF67	5' – ctc aga gtg gaa ggc ctg ctt – 3'	RF67 + SW16	ctr: 292 bp
	SW8	5' – cgc aag ggt tac tca cca ca – 3'	RF67 + SW8	ko: 195 bp
	SW16	5' – cct cct tga gca tga gaa tct tg – 3'		

7.2 Antibodies

7.2.1 Primary antibodies

antibody	origin	application (dilution)	references
glucagon	monoclonal mouse	immunohistochemistry (1:2000)	Sigma
insulin	polyclonal guinea pig	immunohistochemistry (1:2500)	DAKO
somatostatin	polyclonal rabbit	immunohistochemistry (1:1000) western blot (1:200)	Santa Cruz
somatostatin	monoclonal rat	immunohistochemistry (1:500)	Chemicon
cGKI	polyclonal rabbit	immunohistochemistry (1:50) western blot (1:200)	Prof. Dr. F. Hofmann (München)
cGKIα	polyclonal rabbit	immunohistochemistry (1:50) western blot (1:500)	Prof. Dr. F. Hofmann (München)
cGKIβ	polyclonal rabbit	western blot (1:500)	Prof. Dr. F. Hofmann (München)
PDE5	polyclonal rabbit	western blot (1:500)	Prof. Dr. J. Beavo (Washington)
β-actin	polyclonal rabbit	western blot (1:10 000)	Abcam
IRAG	polyclonal rabbit	western blot (1:500)	Prof. Dr. Franz Hofmann (München)

7.2.2 Secondary antibodies

antibody	origin	application (dilution)	references
biotinylated-anti-rabbit	goat	immunohistochemistry (1:200)	Vector Laboratories
biotinylated-anti-guinea pig	goat	immunohistochemistry (1:200)	Vector Laboratories
biotinylated-anti-rat	goat	immunohistochemistry (1:200)	Vector Laboratories
Cy3-conjugated-anti-guinea-pig	goat	immunohistochemistry (1:500)	DAKO
Cy2-conjugated-anti-rabbit	goat	immunohistochemistry (1:50)	DAKO
FITC-conjugated-anti-mouse	goat	immunohistochemistry (1:500)	DAKO
Cy3-conjugated-anti-rabbit	goat	immunohistochemistry (1:500)	DAKO
anti-rabbit-HRP	goat	western blot (1:2000)	Cell signalling

8 References

Ahren, B. 2000. Autonomic regulation of islet hormone secretion--implications for health and disease. *Diabetologia*. 43:393-410.

Akesson, B., H. Mosen, G. Panagiotidis, and I. Lundquist. 1996. Interaction of the islet nitric oxide system with L-arginine-induced secretion of insulin and glucagon in mice. *Br J Pharmacol*. 119:758-64.

Alberti, K.G., and P.Z. Zimmet. 1998. Definition, diagnosis and classification of diabetes mellitus and its complications. Part 1: diagnosis and classification of diabetes mellitus provisional report of a WHO consultation. *Diabet Med*. 15:539-53.

Alm, P., P. Ekstrom, R. Henningsson, and I. Lundquist. 1999. Morphological evidence for the existence of nitric oxide and carbon monoxide pathways in the rat islets of Langerhans: an immunocytochemical and confocal microscopical study. *Diabetologia*. 42:978-86.

Ammendola, A., A. Geiselhoringer, F. Hofmann, and J. Schlossmann. 2001. Molecular determinants of the interaction between the inositol 1,4,5-trisphosphate receptor-associated cGMP kinase substrate (IRAG) and cGMP kinase Ibeta. *J Biol Chem*. 276:24153-9.

Antl, M., M.L. von Bruhl, C. Eiglsperger, M. Werner, I. Konrad, T. Kocher, M. Wilm, F. Hofmann, S. Massberg, and J. Schlossmann. 2007. IRAG mediates NO/cGMP-dependent inhibition of platelet aggregation and thrombus formation. *Blood*. 109:552-9.

Aring, B. kesson, and I. Lundquist. 1999. Influence of nitric oxide modulators on cholinergically stimulated hormone release from mouse islets. *J Physiol*. 515 (Pt 2):463-73.

Ashcroft, F., and P. Rorsman. 2004. Type 2 diabetes mellitus: not quite exciting enough? *Hum Mol Genet*. 13 Spec No 1:R21-31.

Baetens, D., F. Malaisse-Lagae, A. Perrelet, and L. Orci. 1979. Endocrine pancreas: three-dimensional reconstruction shows two types of islets of langerhans. *Science*. 206:1323-5.

Barg, S., J. Galvanovskis, S.O. Gopel, P. Rorsman, and L. Eliasson. 2000. Tight coupling between electrical activity and exocytosis in mouse glucagon-secreting alpha-cells. *Diabetes*. 49:1500-10.

Broglio, F., C. Gottero, A. Benso, F. Prodam, M. Volante, S. Destefanis, C. Gauna, G. Muccioli, M. Papotti, A.J. van der Lely, and E. Ghigo. 2003. Ghrelin and the endocrine pancreas. *Endocrine*. 22:19-24.

Browner, N.C., N.B. Dey, K.D. Bloch, and T.M. Lincoln. 2004. Regulation of cGMP-dependent protein kinase expression by soluble guanylyl cyclase in vascular smooth muscle cells. *J Biol Chem*. 279:46631-6.

Brunicardi, F.C., R. Kleinman, S. Moldovan, T.H. Nguyen, P.C. Watt, J. Walsh, and R. Gingerich. 2001. Immunoneutralization of somatostatin, insulin, and glucagon causes alterations in islet cell secretion in the isolated perfused human pancreas. *Pancreas*. 23:302-8.

Budworth, J., S. Meillerais, I. Charles, and K. Powell. 1999. Tissue distribution of the human soluble guanylate cyclases. *Biochem Biophys Res Commun*. 263:696-701.

Cabrera, O., D.M. Berman, N.S. Kenyon, C. Ricordi, P.O. Berggren, and A. Caicedo. 2006. The unique cytoarchitecture of human pancreatic islets has implications for islet cell function. *Proc Natl Acad Sci U S A*. 103:2334-9.

Campbell, S.C., H. Richardson, W.F. Ferris, C.S. Butler, and W.M. Macfarlane. 2007. Nitric oxide stimulates insulin gene transcription in pancreatic beta-cells. *Biochem Biophys Res Commun*. 353:1011-6.

Catterall, W.A. 2000. From ionic currents to molecular mechanisms: the structure and function of voltage-gated sodium channels. *Neuron*. 26:13-25.

References

Catterall, W.A., S. Cestele, V. Yarov-Yarovoy, F.H. Yu, K. Konoki, and T. Scheuer. 2007. Voltage-gated ion channels and gating modifier toxins. *Toxicon*. 49:124-41.

Catterall, W.A., A.L. Goldin, and S.G. Waxman. 2005. International Union of Pharmacology. XLVII. Nomenclature and structure-function relationships of voltage-gated sodium channels. *Pharmacol Rev*. 57:397-409.

Chai, Y., and Y. Lin. 2008. Dual regulation of the ATP-sensitive potassium channel by activation of cGMP-dependent protein kinase. *Plügers Archiv European Journal of Physiology*.

Chanrion, B., C. Mannoury la Cour, F. Bertaso, M. Lerner-Natoli, M. Freissmuth, M.J. Millan, J. Bockaert, and P. Marin. 2007. Physical interaction between the serotonin transporter and neuronal nitric oxide synthase underlies reciprocal modulation of their activity. *Proc Natl Acad Sci U S A*. 104:8119-24.

Cherubini, E., J.L. Gaiarsa, and Y. Ben-Ari. 1991. GABA: an excitatory transmitter in early postnatal life. *Trends Neurosci*. 14:515-9.

Corbett, J.A., J.L. Wang, T.P. Misko, W. Zhao, W.F. Hickey, and M.L. McDaniel. 1993. Nitric oxide mediates IL-1 beta-induced islet dysfunction and destruction: prevention by dexamethasone. *Autoimmunity*. 15:145-53.

Cox, J.J., F. Reimann, A.K. Nicholas, G. Thornton, E. Roberts, K. Springell, G. Karbani, H. Jafri, J. Mannan, Y. Raashid, L. Al-Gazali, H. Hamamy, E.M. Valente, S. Gorman, R. Williams, D.P. McHale, J.N. Wood, F.M. Gribble, and C.G. Woods. 2006. An SCN9A channelopathy causes congenital inability to experience pain. *Nature*. 444:894-8.

Cummins, T.R., S.D. Dib-Hajj, and S.G. Waxman. 2004. Electrophysiological properties of mutant Nav1.7 sodium channels in a painful inherited neuropathy. *J Neurosci*. 24:8232-6.

de Vente, J., E. Asan, S. Gambaryan, M. Markerink-van Ittersum, H. Axer, K. Gallatz, S.M. Lohmann, and M. Palkovits. 2001. Localization of cGMP-dependent protein kinase type II in rat brain. *Neuroscience*. 108:27-49.

Djouhri, L., R. Newton, S.R. Levinson, C.M. Berry, B. Carruthers, and S.N. Lawson. 2003. Sensory and electrophysiological properties of guinea-pig sensory neurones expressing Nav 1.7 (PN1) Na+ channel alpha subunit protein. *J Physiol*. 546:565-76.

Eizirik, D.L., and D. Pavlovic. 1997. Is there a role for nitric oxide in beta-cell dysfunction and damage in IDDM? *Diabetes Metab Rev*. 13:293-307.

el-Husseini, A.E., C. Bladen, and S.R. Vincent. 1995. Molecular characterization of a type II cyclic GMP-dependent protein kinase expressed in the rat brain. *J Neurochem*. 64:2814-7.

Elayat, A.A., M.M. el-Naggar, and M. Tahir. 1995. An immunocytochemical and morphometric study of the rat pancreatic islets. *J Anat*. 186 (Pt 3):629-37.

Evans, M.L., R.J. McCrimmon, D.E. Flanagan, T. Keshavarz, X. Fan, E.C. McNay, R.J. Jacob, and R.S. Sherwin. 2004. Hypothalamic ATP-sensitive K + channels play a key role in sensing hypoglycemia and triggering counterregulatory epinephrine and glucagon responses. *Diabetes*. 53:2542-51.

Feil, R., F. Hofmann, and T. Kleppisch. 2005a. Function of cGMP-dependent protein kinases in the nervous system. *Rev Neurosci*. 16:23-41.

Feil, S., P. Zimmermann, A. Knorn, S. Brummer, J. Schlossmann, F. Hofmann, and R. Feil. 2005b. Distribution of cGMP-dependent protein kinase type I and its isoforms in the mouse brain and retina. *Neuroscience*. 135:863-8.

Felts, P.A., S. Yokoyama, S. Dib-Hajj, J.A. Black, and S.G. Waxman. 1997. Sodium channel alpha-subunit mRNAs I, II, III, NaG, Na6 and hNE (PN1): different expression patterns in developing rat nervous system. *Brain Res Mol Brain Res*. 45:71-82.

Fertleman, C.R., M.D. Baker, K.A. Parker, S. Moffatt, F.V. Elmslie, B. Abrahamsen, J. Ostman, N. Klugbauer, J.N. Wood, R.M. Gardiner, and M. Rees. 2006. SCN9A mutations in

paroxysmal extreme pain disorder: allelic variants underlie distinct channel defects and phenotypes. *Neuron*. 52:767-74.

Fertleman, C.R., C.D. Ferrie, J. Aicardi, N.A. Bednarek, O. Eeg-Olofsson, F.V. Elmslie, D.A. Griesemer, F. Goutieres, M. Kirkpatrick, I.N. Malmros, M. Pollitzer, M. Rossiter, E. Roulet-Perez, R. Schubert, V.V. Smith, H. Testard, V. Wong, and J.B. Stephenson. 2007. Paroxysmal extreme pain disorder (previously familial rectal pain syndrome). *Neurology*. 69:586-95.

Foller, M., S. Feil, K. Ghoreschi, S. Koka, A. Gerling, M. Thunemann, F. Hofmann, B. Schuler, J. Vogel, B. Pichler, R.S. Kasinathan, J.P. Nicolay, S.M. Huber, F. Lang, and R. Feil. 2008. Anemia and splenomegaly in cGKI-deficient mice. *Proc Natl Acad Sci U S A*. 105:6771-6.

Franklin, I., J. Gromada, A. Gjinovci, S. Theander, and C.B. Wollheim. 2005. Beta-cell secretory products activate alpha-cell ATP-dependent potassium channels to inhibit glucagon release. *Diabetes*. 54:1808-15.

Friebe, A., E. Mergia, O. Dangel, A. Lange, and D. Koesling. 2007. Fatal gastrointestinal obstruction and hypertension in mice lacking nitric oxide-sensitive guanylyl cyclase. *Proc Natl Acad Sci U S A*. 104:7699-704.

Gambaryan, S., J. Geiger, U.R. Schwarz, E. Butt, A. Begonja, A. Obergfell, and U. Walter. 2004. Potent inhibition of human platelets by cGMP analogs independent of cGMP-dependent protein kinase. *Blood*. 103:2593-600.

Gambaryan, S., A. Kobsar, S. Hartmann, I. Birschmann, P.J. Kuhlencordt, W. Muller-Esterl, S.M. Lohmann, and U. Walter. 2008. NO-synthase-/NO-independent regulation of human and murine platelet soluble guanylyl cyclase activity. *J Thromb Haemost*.

Garbers, D.L., and D.G. Lowe. 1994. Guanylyl cyclase receptors. *J Biol Chem*. 269:30741-4.

Geiselhoringer, A., M. Gaisa, F. Hofmann, and J. Schlossmann. 2004. Distribution of IRAG and cGKI-isoforms in murine tissues. *FEBS Lett*. 575:19-22.

Gopel, S., T. Kanno, S. Barg, J. Galvanovskis, and P. Rorsman. 1999. Voltage-gated and resting membrane currents recorded from B-cells in intact mouse pancreatic islets. *J Physiol*. 521 Pt 3:717-28.

Gopel, S., Q. Zhang, L. Eliasson, X.S. Ma, J. Galvanovskis, T. Kanno, A. Salehi, and P. Rorsman. 2004. Capacitance measurements of exocytosis in mouse pancreatic alpha-, beta- and delta-cells within intact islets of Langerhans. *J Physiol*. 556:711-26.

Gopel, S.O., T. Kanno, S. Barg, and P. Rorsman. 2000a. Patch-clamp characterisation of somatostatin-secreting -cells in intact mouse pancreatic islets. *J Physiol*. 528:497-507.

Gopel, S.O., T. Kanno, S. Barg, X.G. Weng, J. Gromada, and P. Rorsman. 2000b. Regulation of glucagon release in mouse -cells by KATP channels and inactivation of TTX-sensitive Na+ channels. *J Physiol*. 528:509-20.

Green, D.J., A. Maiorana, G. O'Driscoll, and R. Taylor. 2004. Effect of exercise training on endothelium-derived nitric oxide function in humans. *J Physiol*. 561:1-25.

Gromada, J., I. Franklin, and C.B. Wollheim. 2007. Alpha-cells of the endocrine pancreas: 35 years of research but the enigma remains. *Endocr Rev*. 28:84-116.

Gromada, J., X. Ma, M. Hoy, K. Bokvist, A. Salehi, P.O. Berggren, and P. Rorsman. 2004. ATP-sensitive K+ channel-dependent regulation of glucagon release and electrical activity by glucose in wild-type and SUR1-/- mouse alpha-cells. *Diabetes*. 53 Suppl 3:S181-9.

Henningsson, R., P. Alm, E. Lindstrom, and I. Lundquist. 2000. Chronic blockade of NO synthase paradoxically increases islet NO production and modulates islet hormone release. *Am J Physiol Endocrinol Metab*. 279:E95-E107.

Henningsson, R., A. Salehi, and I. Lundquist. 2002. Role of nitric oxide synthase isoforms in glucose-stimulated insulin release. *Am J Physiol Cell Physiol*. 283:C296-304.

Herrera, P.L. 2000. Adult insulin- and glucagon-producing cells differentiate from two independent cell lineages. *Development*. 127:2317-22.

Herrera, P.L. 2002. Defining the cell lineages of the islets of Langerhans using transgenic mice. *Int J Dev Biol*. 46:97-103.

Hofmann, F. 2005. The biology of cyclic GMP-dependent protein kinases. *J Biol Chem*. 280:1-4.

Hofmann, F., A. Ammendola, and J. Schlossmann. 2000. Rising behind NO: cGMP-dependent protein kinases. *J Cell Sci*. 113 (Pt 10):1671-6.

Jones, P.M., S.J. Persaud, T. Bjaaland, J.D. Pearson, and S.L. Howell. 1992. Nitric oxide is not involved in the initiation of insulin secretion from rat islets of Langerhans. *Diabetologia*. 35:1020-7.

Kanno, T., S.O. Gopel, P. Rorsman, and M. Wakui. 2002. Cellular function in multicellular system for hormone-secretion: electrophysiological aspect of studies on alpha-, beta- and delta-cells of the pancreatic islet. *Neurosci Res*. 42:79-90.

Kass, D.A., E. Takimoto, T. Nagayama, and H.C. Champion. 2007. Phosphodiesterase regulation of nitric oxide signaling. *Cardiovasc Res*. 75:303-14.

Kaupp, U.B., and R. Seifert. 2002. Cyclic nucleotide-gated ion channels. *Physiol Rev*. 82:769-824.

Keilbach, A., P. Ruth, and F. Hofmann. 1992. Detection of cGMP dependent protein kinase isozymes by specific antibodies. *Eur J Biochem*. 208:467-73.

Kleppisch, T. 1999. Langzeitpotenzierung im Hippocampus: Die funktionelle Rolle von zyklischem Guanosinmonophosphat und der Zyklo-Guanosinmonophosphat-abhängigen Proteinkinase. *Habilitationsschrift*.

Kleppisch, T., A. Pfeifer, P. Klatt, P. Ruth, A. Montkowski, R. Fassler, and F. Hofmann. 1999. Long-term potentiation in the hippocampal CA1 region of mice lacking cGMP-dependent kinases is normal and susceptible to inhibition of nitric oxide synthase. *J Neurosci*. 19:48-55.

Koesling, D., J. Herz, H. Gausepohl, F. Niroomand, K.D. Hinsch, A. Mulsch, E. Bohme, G. Schultz, and R. Frank. 1988. The primary structure of the 70 kDa subunit of bovine soluble guanylate cyclase. *FEBS Lett*. 239:29-34.

Koesling, D., M. Russwurm, E. Mergia, F. Mullershausen, and A. Friebe. 2004. Nitric oxide-sensitive guanylyl cyclase: structure and regulation. *Neurochem Int*. 45:813-9.

Krumenacker, J.S., K.A. Hanafy, and F. Murad. 2004. Regulation of nitric oxide and soluble guanylyl cyclase. *Brain Res Bull*. 62:505-15.

Lajoix, A.D., H. Reggio, T. Chardes, S. Peraldi-Roux, F. Tribillac, M. Roye, S. Dietz, C. Broca, M. Manteghetti, G. Ribes, C.B. Wollheim, and R. Gross. 2001. A neuronal isoform of nitric oxide synthase expressed in pancreatic beta-cells controls insulin secretion. *Diabetes*. 50:1311-23.

Lakso, M., B. Sauer, B. Mosinger, Jr., E.J. Lee, R.W. Manning, S.H. Yu, K.L. Mulder, and H. Westphal. 1992. Targeted oncogene activation by site-specific recombination in transgenic mice. *Proc Natl Acad Sci U S A*. 89:6232-6.

Landgraf, W., P. Ruth, A. Keilbach, B. May, A. Welling, and F. Hofmann. 1992. Cyclic GMP-dependent protein kinase and smooth muscle relaxation. *J Cardiovasc Pharmacol*. 20 Suppl 1:S18-22.

Leung, Y.M., I. Ahmed, L. Sheu, R.G. Tsushima, N.E. Diamant, and H.Y. Gaisano. 2006. Two populations of pancreatic islet alpha-cells displaying distinct Ca2+ channel properties. *Biochem Biophys Res Commun*. 345:340-4.

Leung, Y.M., I. Ahmed, L. Sheu, R.G. Tsushima, N.E. Diamant, M. Hara, and H.Y. Gaisano. 2005. Electrophysiological characterization of pancreatic islet cells in the mouse insulin promoter-green fluorescent protein mouse. *Endocrinology*. 146:4766-75.

Liu, Y.J., E. Vieira, and E. Gylfe. 2004. A store-operated mechanism determines the activity of the electrically excitable glucagon-secreting pancreatic alpha-cell. *Cell Calcium*. 35:357-65.

Lohmann, S.M., A.B. Vaandrager, A. Smolenski, U. Walter, and H.R. De Jonge. 1997. Distinct and specific functions of cGMP-dependent protein kinases. *Trends Biochem Sci*. 22:307-12.

Lukowski, R., S. Weber, P. Weinmeister, S. Feil, and R. Feil. 2005. Cre/loxP-vermittelte konditionale Mutagenese des cGMP-Signalwegs in der Maus. *BIOspektrum*:287-290.

Lukowski, R., P. Weinmeister, D. Bernhard, S. Feil, M. Gotthardt, J. Herz, S. Massberg, A. Zernecke, C. Weber, F. Hofmann, and R. Feil. 2008. Role of smooth muscle cGMP/cGKI signaling in murine vascular restenosis. *Arterioscler Thromb Vasc Biol*. 28:1244-50.

MacDonald, P.E., Y.Z. De Marinis, R. Ramracheya, A. Salehi, X. Ma, P.R. Johnson, R. Cox, L. Eliasson, and P. Rorsman. 2007. A K ATP channel-dependent pathway within alpha cells regulates glucagon release from both rodent and human islets of Langerhans. *PLoS Biol*. 5:e143.

MacDonald, P.E., J.W. Joseph, and P. Rorsman. 2005. Glucose-sensing mechanisms in pancreatic beta-cells. *Philos Trans R Soc Lond B Biol Sci*. 360:2211-25.

Massberg, S., M. Sausbier, P. Klatt, M. Bauer, A. Pfeifer, W. Siess, R. Fassler, P. Ruth, F. Krombach, and F. Hofmann. 1999. Increased adhesion and aggregation of platelets lacking cyclic guanosine 3',5'-monophosphate kinase I. *J Exp Med*. 189:1255-64.

Mergia, E., M. Russwurm, G. Zoidl, and D. Koesling. 2003. Major occurrence of the new alpha2beta1 isoform of NO-sensitive guanylyl cyclase in brain. *Cell Signal*. 15:189-95.

Miki, T., B. Liss, K. Minami, T. Shiuchi, A. Saraya, Y. Kashima, M. Horiuchi, F. Ashcroft, Y. Minokoshi, J. Roeper, and S. Seino. 2001. ATP-sensitive K+ channels in the hypothalamus are essential for the maintenance of glucose homeostasis. *Nat Neurosci*. 4:507-12.

Mori, T., Y. Murakami, K. Koshimura, K. Hamaguchi, and Y. Kato. 2001. Involvement of cyclic guanosine 3',5'-monophosphate in nitric oxide-induced glucagon secretion from pancreatic alpha cells. *Metabolism*. 50:703-7.

Morioka, T., E. Asilmaz, J. Hu, J.F. Dishinger, A.J. Kurpad, C.F. Elias, H. Li, J.K. Elmquist, R.T. Kennedy, and R.N. Kulkarni. 2007. Disruption of leptin receptor expression in the pancreas directly affects beta cell growth and function in mice. *J Clin Invest*. 117:2860-8.

Myers, M.G., Jr. 2004. Leptin receptor signaling and the regulation of mammalian physiology. *Recent Prog Horm Res*. 59:287-304.

Nagy, A. 2000. Cre recombinase: the universal reagent for genome tailoring. *Genesis*. 26:99-109.

Nassar, M.A., M.D. Baker, A. Levato, R. Ingram, G. Mallucci, S.B. McMahon, and J.N. Wood. 2006. Nerve injury induces robust allodynia and ectopic discharges in Nav1.3 null mutant mice. *Mol Pain*. 2:33.

Nassar, M.A., L.C. Stirling, G. Forlani, M.D. Baker, E.A. Matthews, A.H. Dickenson, and J.N. Wood. 2004. Nociceptor-specific gene deletion reveals a major role for Nav1.7 (PN1) in acute and inflammatory pain. *Proc Natl Acad Sci U S A*. 101:12706-11.

Nathan, C., and Q.W. Xie. 1994. Nitric oxide synthases: roles, tolls, and controls. *Cell*. 78:915-8.

Ny, L., A. Pfeifer, A. Aszodi, M. Ahmad, P. Alm, P. Hedlund, R. Fassler, and K.E. Andersson. 2000. Impaired relaxation of stomach smooth muscle in mice lacking cyclic GMP-dependent protein kinase I. *Br J Pharmacol*. 129:395-401.

Orban, P.C., D. Chui, and J.D. Marth. 1992. Tissue- and site-specific DNA recombination in transgenic mice. *Proc Natl Acad Sci U S A*. 89:6861-5.

Panagiotidis, G., P. Alm, and I. Lundquist. 1992. Inhibition of islet nitric oxide synthase increases arginine-induced insulin release. *Eur J Pharmacol*. 229:277-8.

Parker, J.C., M.A. VanVolkenburg, R.J. Ketchum, K.L. Brayman, and K.M. Andrews. 1995. Cyclic

AMP phosphodiesterases of human and rat islets of Langerhans: contributions of types III and IV to the modulation of insulin secretion. *Biochem Biophys Res Commun*. 217:916-23.

Persson, K., R.K. Pandita, A. Aszodi, M. Ahmad, A. Pfeifer, R. Fassler, and K.E. Andersson. 2000. Functional characteristics of urinary tract smooth muscles in mice lacking cGMP protein kinase type I. *Am J Physiol Regul Integr Comp Physiol*. 279:R1112-20.

Pfeifer, A., P. Klatt, S. Massberg, L. Ny, M. Sausbier, C. Hirneiss, G.X. Wang, M. Korth, A. Aszodi, K.E. Andersson, F. Krombach, A. Mayerhofer, P. Ruth, R. Fassler, and F. Hofmann. 1998. Defective smooth muscle regulation in cGMP kinase I-deficient mice. *Embo J*. 17:3045-51.

Quoix, N., R. Cheng-Xue, Y. Guiot, P.L. Herrera, J.C. Henquin, and P. Gilon. 2007. The GluCre-ROSA26EYFP mouse: a new model for easy identification of living pancreatic alpha-cells. *FEBS Lett*. 581:4235-40.

Rastaldo, R., P. Pagliaro, S. Cappello, C. Penna, D. Mancardi, N. Westerhof, and G. Losano. 2007. Nitric oxide and cardiac function. *Life Sci*. 81:779-93.

Ravier, M.A., and G.A. Rutter. 2005. Glucose or insulin, but not zinc ions, inhibit glucagon secretion from mouse pancreatic alpha-cells. *Diabetes*. 54:1789-97.

Rorsman, P., P.O. Berggren, K. Bokvist, H. Ericson, H. Mohler, C.G. Ostenson, and P.A. Smith. 1989. Glucose-inhibition of glucagon secretion involves activation of GABAA-receptor chloride channels. *Nature*. 341:233-6.

Rybalkin, S.D., C. Yan, K.E. Bornfeldt, and J.A. Beavo. 2003. Cyclic GMP phosphodiesterases and regulation of smooth muscle function. *Circ Res*. 93:280-91.

Salehi, A., S. Meidute Abaraviciene, J. Jimenez-Feltstrom, C.G. Ostenson, S. Efendic, and I. Lundquist. 2008. Excessive islet NO generation in type 2 diabetic GK rats coincides with abnormal hormone secretion and is counteracted by GLP-1. *PLoS ONE*. 3:e2165.

Sandler, S., D.L. Eizirik, C. Svensson, E. Strandell, M. Welsh, and N. Welsh. 1991. Biochemical and molecular actions of interleukin-1 on pancreatic beta-cells. *Autoimmunity*. 10:241-53.

Sangameswaran, L., L.M. Fish, B.D. Koch, D.K. Rabert, S.G. Delgado, M. Ilnicka, L.B. Jakeman, S. Novakovic, K. Wong, P. Sze, E. Tzoumaka, G.R. Stewart, R.C. Herman, H. Chan, R.M. Eglen, and J.C. Hunter. 1997. A novel tetrodotoxin-sensitive, voltage-gated sodium channel expressed in rat and human dorsal root ganglia. *J Biol Chem*. 272:14805-9.

Sauer, B., and N. Henderson. 1988. Site-specific DNA recombination in mammalian cells by the Cre recombinase of bacteriophage P1. *Proc Natl Acad Sci U S A*. 85:5166-70.

Schmidt, H.H., T.D. Warner, K. Ishii, H. Sheng, and F. Murad. 1992. Insulin secretion from pancreatic B cells caused by L-arginine-derived nitrogen oxides. *Science*. 255:721-3.

Schuit, F.C., M.P. Derde, and D.G. Pipeleers. 1989. Sensitivity of rat pancreatic A and B cells to somatostatin. *Diabetologia*. 32:207-12.

Schulla, V., E. Renstrom, R. Feil, S. Feil, I. Franklin, A. Gjinovci, X.J. Jing, D. Laux, I. Lundquist, M.A. Magnuson, S. Obermuller, C.S. Olofsson, A. Salehi, A. Wendt, N. Klugbauer, C.B. Wollheim, P. Rorsman, and F. Hofmann. 2003. Impaired insulin secretion and glucose tolerance in beta cell-selective Ca(v)1.2 Ca2+ channel null mice. *Embo J*. 22:3844-54.

Soriano, P. 1999. Generalized lacZ expression with the ROSA26 Cre reporter strain. *Nat Genet*. 21:70-1.

Spinas, G.A., R. Laffranchi, I. Francoys, I. David, C. Richter, and M. Reinecke. 1998. The early phase of glucose-stimulated insulin secretion requires nitric oxide. *Diabetologia*. 41:292-9.

Strowski, M.Z., D.E. Cashen, E.T. Birzin, L. Yang, V. Singh, T.M. Jacks, K.W. Nowak, S.P. Rohrer, A.A. Patchett, R.G. Smith, and J.M. Schaeffer. 2006. Antidiabetic activity of a highly potent and selective nonpeptide somatostatin receptor subtype-2 agonist. *Endocrinology*. 147:4664-73.

Szanto, I., and C.R. Kahn. 2000. Selective interaction between leptin and insulin signaling

pathways in a hepatic cell line. *Proc Natl Acad Sci U S A*. 97:2355-60.

Takahashi, E., M. Ito, N. Miyamoto, T. Nagasu, M. Ino, and I. Tanaka. 2005. Increased glucose tolerance in N-type Ca2+ channel alpha(1B)-subunit gene-deficient mice. *Int J Mol Med*. 15:937-44.

Taylor, A.E., J. Hubbard, and E.J. Anderson. 1999. Impact of binge eating on metabolic and leptin dynamics in normal young women. *J Clin Endocrinol Metab*. 84:428-34.

Tripathi, P., L. Kashyap, and V. Singh. 2007. The role of nitric oxide in inflammatory reactions. *FEMS Immunol Med Microbiol*. 51:443-52.

Unger, R.H. 1971. Glucagon physiology and pathophysiology. *N Engl J Med*. 285:443-9.

Unger, R.H. 1985. Glucagon physiology and pathophysiology in the light of new advances. *Diabetologia*. 28:574-8.

Verspohl, E.J., and H.P. Ammon. 1989. Atrial natriuretic peptide (ANP) acts via specific binding sites on cGMP system of rat pancreatic islets without affecting insulin release. *Naunyn Schmiedebergs Arch Pharmacol*. 339:348-53.

Verspohl, E.J., and I.K. Bernemann. 1996. Atrial natriuretic peptide (ANP)-induced inhibition of glucagon secretion: mechanism of action in isolated rat pancreatic islets. *Peptides*. 17:1023-9.

Vieira, E., Y.J. Liu, and E. Gylfe. 2004. Involvement of alpha1 and beta-adrenoceptors in adrenaline stimulation of the glucagon-secreting mouse alpha-cell. *Naunyn Schmiedebergs Arch Pharmacol*. 369:179-83.

Vignali, S., V. Leiss, R. Karl, F. Hofmann, and A. Welling. 2006. Characterization of voltage-dependent sodium and calcium channels in mouse pancreatic A- and B-cells. *J Physiol*. 572:691-706.

Walz, H.A., N. Wierup, J. Vikman, V.C. Manganiello, E. Degerman, L. Eliasson, and L.S. Holst. 2007. Beta-cell PDE3B regulates Ca2+-stimulated exocytosis of insulin. *Cell Signal*. 19:1505-13.

Waxman, S.G. 2006. Neurobiology: a channel sets the gain on pain. *Nature*. 444:831-2.

Waxman, S.G. 2007. Nav1.7, its mutations, and the syndromes that they cause. *Neurology*. 69:505-7.

Weber, S., D. Bernhard, R. Lukowski, P. Weinmeister, R. Worner, J.W. Wegener, N. Valtcheva, S. Feil, J. Schlossmann, F. Hofmann, and R. Feil. 2007. Rescue of cGMP kinase I knockout mice by smooth muscle specific expression of either isozyme. *Circ Res*. 101:1096-103.

Werner, C., G. Raivich, M. Cowen, T. Strekalova, I. Sillaber, J.T. Buters, R. Spanagel, and F. Hofmann. 2004. Importance of NO/cGMP signalling via cGMP-dependent protein kinase II for controlling emotionality and neurobehavioural effects of alcohol. *Eur J Neurosci*. 20:3498-506.

Werner, C.G., V. Godfrey, R.R. Arnold, G.L. Featherstone, D. Bender, J. Schlossmann, M. Schiemann, F. Hofmann, and K.B. Pryzwansky. 2005. Neutrophil dysfunction in guanosine 3',5'-cyclic monophosphate-dependent protein kinase I-deficient mice. *J Immunol*. 175:1919-29.

Wierup, N., H. Svensson, H. Mulder, and F. Sundler. 2002. The ghrelin cell: a novel developmentally regulated islet cell in the human pancreas. *Regul Pept*. 107:63-9.

Wink, D.A., K.M. Miranda, and M.G. Espey. 2000. Effects of oxidative and nitrosative stress in cytotoxicity. *Semin Perinatol*. 24:20-3.

Yang, L., G. Liu, S.I. Zakharov, A.M. Bellinger, M. Mongillo, and S.O. Marx. 2007. Protein kinase G phosphorylates Cav1.2 alpha1c and beta2 subunits. *Circ Res*. 101:465-74.

Yang, Y., Y. Wang, S. Li, Z. Xu, H. Li, L. Ma, J. Fan, D. Bu, B. Liu, Z. Fan, G. Wu, J. Jin, B. Ding,

X. Zhu, and Y. Shen. 2004. Mutations in SCN9A, encoding a sodium channel alpha subunit, in patients with primary erythermalgia. *J Med Genet*. 41:171-4.

Yoshimoto, Y., Y. Fukuyama, Y. Horio, A. Inanobe, M. Gotoh, and Y. Kurachi. 1999. Somatostatin induces hyperpolarization in pancreatic islet alpha cells by activating a G protein-gated K+ channel. *FEBS Lett*. 444:265-9.

Yu, F.H., and W.A. Catterall. 2004. The VGL-chanome: a protein superfamily specialized for electrical signaling and ionic homeostasis. *Sci STKE*. 2004:re15.

Zhao, A.Z., M.M. Shinohara, D. Huang, M. Shimizu, H. Eldar-Finkelman, E.G. Krebs, J.A. Beavo, and K.E. Bornfeldt. 2000. Leptin induces insulin-like signaling that antagonizes cAMP elevation by glucagon in hepatocytes. *J Biol Chem*. 275:11348-54.

VI. Publications

Journal articles:

Leiss, V., Weinmeister, P., Welling, A., Hofmann, F., Lukowski, R. (2008). Cyclic GMP kinase I modulates glucagon release. *Diabetes*. (submitted)

Vignali S., **Leiss, V.**, Karl, R., Hofmann, F., Welling, A. (2006). Characterization of voltage-dependent sodium and calcium channels in mouse pancreatic A- and B-cells. *J Physiol*. 572:691-706.

Abstracts:

Leiss, V., Weinmeister, P., Hofmann, F., Welling, A., Lukowski, R. (2008). Analyzing the possible roles of endogenous cGKI in pancreatic islet cells on glucose homeostasis. *49. Frühjahrstagung der DGPT*. (Mainz, Germany)

Welling, A., **Leiss, V.**, Auer, V., Hofmann, F. (2008). Pancreatic A-cell $Na_V1.7$ sodium channel is involved in glucagon release in mice. *49. Frühjahrstagung der DGPT*. (Mainz, Germany)

Leiss, V., Auer, V., Vignali, S., Lukowski, R., Zhang, Q., Rorsman, P., Hofmann, F., Welling, A. (2007). Role of sodium and calcium channels on glucagon secretion in mice. *48. Frühjahrstagung der DGPT*. (Mainz, Germany)

Auer, V., **Leiss, V.**, Vignali, S., Hofmann, A., Welling, A. (2007). Deletion of the $Na_V1.7$ sodium channel in pancreatic A- and B-cells of mice. *48. Frühjahrstagung der DGPT*. (Mainz, Germany)

Vignali, S., **Leiss, V.**, Auer, V., Hofmann, F., Welling, A. (2006). B- and A-cells of murine pancreatic islets express different sodium and clacium channels. *47. Frühjahrstagung der DGPT*. (Mainz, Germany)

Vignali, S., **Leiss, V.**, Auer, V., Hofmann, F., Welling, A. (2006). B- and A-cells of murine pancreatic islets express different sodium and clacium channels. *85. Jahrestagung der Deutschen Physiologischen Gesellschaft*. (München, Germany)

Vignali, S., **Leiss, V.**, Karl, R., Hofmann, F., Weling, A. (2005). Electrophysiological, pharmacological and molecular analysis of sodium and calcium channels in pancreatic islet cells of the mouse. *8. Insel-Workshop*. (Goslar, Germany)

Leiss, V., Vignali, S., Karl, R., Hofmann, F., Welling, A. (2005). Identification of different HVA calcium channel subtypes in pancreatic islet cells of the mouse. *46. Frühjahrstagung der DGPT*. (Mainz, Germany)

Vignali, S., **Leiss, V.**, Karl, R., Hofmann, F., Welling, A. (2005). Analysis of sodium and LVA calcium channels in pancreatic islet cells of the mouse. *46. Frühjahrstagung der DGPT*. (Mainz, Germany)

VII. Acknowledgments

VIII. Curriculum Vitae

Persönliche Daten

Name	Veronika Leiss
Titel:	Dipl. Biol. univ.
Geburtsort, -datum:	München, 27. Juni 1981
Familienstand	ledig
Nationalität	deutsch
Anschrift	Montgelasstr. 33
	81679 München
	Tel.: 0176 20676562
	e-mail: v.leiss@gmx.de

Ausbildung

seit 03/2005	Promotion am Institut für Pharmakologie und Toxikologie der Technischen Universität München mit dem Titel *„Regulation of Glucagon Secretion"* (Prof. Dr. F. Hofmann, PD. Dr. A. Welling)
08/2006 – 09/2006	Wissenschaftlicher Forschungsaufenthalt im Rahmen eines Kooperationsforschungsprojektes am Oxford Centre of Diabetes, Endocrinology and Metabolism, University of Oxford, Oxford, Großbritannien (Prof. Dr. P. Rorsman)
05/2004 – 02/2005	Diplomarbeit am Institut für Pharmakologie und Toxikologie der Technischen Universität München mit dem Titel *„Molekularbiologische und elektro-physiologische Charakterisierung von High-voltage-aktivierten Kalziumkanälen in Langerhans-Inselzellen der Maus"* (Prof. Dr. F. Hofmann, PD. Dr. A. Welling)
10/2000-02/2005	Studium der Biologie an der Technischen Universität München (1,4)
	Hauptfach: Genetik
	Nebenfächer: Biochemie, Pharmakologie und Toxikologie

Schule

2000	Abitur am Michaeli-Gymnasium in München (2,1)